*The Canadian Mineralogist*
Vol. 38, pp. 471-510 (2000)

# GRENVILLIAN METAMORPHISM OF MONOCYCLIC ROCKS, GEORGIAN BAY, ONTARIO, CANADA: IMPLICATIONS FOR CONVERGENCE HISTORY*

NATASHA WODICKA[1], JOHN W.F. KETCHUM[2] AND REBECCA A. JAMIESON

*Department of Earth Sciences, Dalhousie University, Halifax, Nova Scotia B3H 3J5, Canada*

## ABSTRACT

The Parry Sound and Shawanaga domains of the Central Gneiss Belt along Georgian Bay, Ontario, contain monocyclic rocks that originated at or near the southeastern margin of Laurentia between *ca.* 1450 and 1120 Ma. Their deformation and metamorphism are entirely attributable to Grenvillian orogenesis. Metamorphic assemblages, fabrics, and P–T–t paths from these rocks therefore provide important constraints on Grenvillian thermal and tectonic history. Rocks in the interior and basal Parry Sound assemblages of the northern Parry Sound domain were metamorphosed to granulite-facies conditions during an early phase of Grenvillian tectonism, *i.e.*, at *ca.* 1161 and 1163 Ma, respectively. The most likely setting for high-P – high-T granulite-facies metamorphism in the interior Parry Sound assemblage was at or near the base of crust that was underplated by voluminous mafic magma. In contrast, heat advected from anorthosite could account for intermediate-P granulite-facies metamorphism in the basal Parry Sound assemblage. In the upper part of the basal Parry Sound assemblage, retrogression from the granulite to upper-amphibolite facies likely occurred in response to thrust emplacement of the interior Parry Sound assemblage onto this part of the basal Parry Sound assemblage at *ca.* 1159 Ma. In the lower part of the basal Parry Sound assemblage, thrust deformation and re-equilibration at lower-amphibolite-facies conditions took place at *ca.* 1120 Ma. In the southern Parry Sound domain, a highly attenuated sequence of quartzites and mafic rocks, deposited some time after 1140–1120 Ma, was affected by upper-amphibolite-facies metamorphism before or at 1080 Ma. Northwest of and structurally below the Parry Sound domain, rocks in the Shawanaga domain were affected by eclogite-facies metamorphism at *ca.* 1090–1085 Ma, suggesting deep burial or partial subduction of the Laurentian margin beneath the Central Metasedimentary Belt at this time. Widespread upper-amphibolite-facies metamorphism after *ca.* 1080 Ma was associated with a major phase of northwest-directed thrusting and crustal thickening. Sillimanite-grade conditions in the Shawanaga domain were maintained until at least *ca.* 1020 Ma, the time of major extensional deformation. Data on metamorphic grade and age are consistent with progressive northwest-directed juxtaposition of lithotectonic assemblages metamorphosed at progressively later times, and may thus record progressive or multistage convergence at the southeastern margin of Laurentia. Evidence for multiple phases of Grenvillian high-grade metamorphism in the Parry Sound and Shawanaga domains suggests that construction and interpretation of P–T–t paths from these rocks require careful assessment of timing and overprinting relationships. Derived P–T–t paths suggest that exhumation of interior Parry Sound granulites resulted from thrusting soon after peak metamorphism, whereas those for rocks of the Shawanaga domain suggest that exhumation was likely associated with both thrusting and extension.

*Keywords*: Grenville Province, monocyclic rocks, granulite, amphibolite, retrogression, P–T–t paths, overprinting effects, convergence history, Georgian Bay, Ontario.

## SOMMAIRE

Les domaines de Parry Sound et Shawanaga de la Ceinture gneissique centrale le long de la baie Georgienne, en Ontario, contiennent des roches monocycliques qui ont pris naissance à (ou près de) la marge sud-est de Laurentia entre environ 1450 et 1120 Ma. Leur métamorphisme et déformation sont dûs entièrement à l'orogenèse grenvillienne. Ainsi, les assemblages métamorphiques, les textures et les trajectoires P–T–t provenant de ces roches permettent d'établir des contraintes importantes quant à l'histoire thermique et tectonique grenvillienne. Dans la région nord du domaine de Parry Sound, les roches provenant de l'intérieur et de la base des assemblages de Parry Sound ont été métamorphisées au faciès granulite pendant une phase précoce du tectonisme grenvillien, soit vers 1161 et 1163 Ma, respectivement. Le milieu le plus probable pour le métamorphisme du faciès granulite de pression et température élevées à l'intérieur de l'assemblage de Parry Sound était à (ou près de) la base de la croûte sous-plaquée par des venues volumineuses de magma mafique. D'autre part, la chaleur émise durant la mise en place d'une anorthosite pourrait être la cause du métamorphisme au faciès granulite de pression intermédiaire à la base de l'assemblage de Parry Sound. Dans la partie supérieure de la base de l'assemblage de Parry Sound, la rétrogression du faciès granulite au faciès

* Geological Survey of Canada contribution number 1998069. LITHOPROBE contribution number 957.

[1] *Present address*: Geological Survey of Canada, 601 Booth Street, Ottawa, Ontario K1A 0E8, Canada. *E-mail address*: nwodicka@nrcan.gc.ca

[2] *Present address*: Jack Satterly Geochronology Laboratory, Royal Ontario Museum, 100 Queen's Park, Toronto, Ontario M5S 2C6, Canada.

amphibolite supérieur était probablement en réponse au chevauchement de l'intérieur de l'assemblage de Parry Sound sur la base de l'assemblage de Parry Sound à environ 1159 Ma. Dans la partie inférieure de l'assemblage de Parry Sound, la déformation associée au chevauchement et le ré-équilibrage au faciès amphibolite inférieur ont eu lieu vers 1120 Ma. Dans la région sud du domaine de Parry Sound, une séquence très attenuée de quartzites et de roches mafiques, déposée peu de temps après 1140–1120 Ma, a subi un métamorphisme au faciès amphibolite supérieur avant ou vers 1080 Ma. Au nord-ouest du domaine de Parry Sound, les roches du domaine de Shawanaga qui occupent un niveau structural inférieur ont subi un métamorphisme au faciès éclogite vers 1090–1085 Ma, ce qui concorderait avec l'enfouissement ou la subduction partielle de la marge laurentienne sous la Ceinture métasedimentaire centrale. Le métamorphisme de grande étendue au faciès amphibolite supérieur postérieur à 1080 Ma résulterait d'une phase majeure de chevauchement vers le nord-ouest et d'un épaississement de la croûte. Les conditions au grade de sillimanite dans le domaine de Shawanaga ont été maintenues jusqu'à environ 1020 Ma, l'âge de la déformation majeure associée à l'extension. Les données métamorphiques et géochronologiques sont compatibles avec la juxtaposition progressive de direction nord-ouest d'unités lithotectoniques métamorphisées à des périodes progressivement plus tardives, et documentent une convergence progressive ou en multiples stades à la marge sud-est de Laurentia. Vue l'existence de phases multiples de métamorphisme grenvillien de degré élevé dans les domaines de Parry Sound et Shawanaga, la construction et l'interprétation des trajectoires P–T–t pour ces roches requièrent une évaluation consciencieuse des relations de temps et de superposition. D'après les trajectoires P–T–t dérivées, l'exhumation de l'intérieur du domaine de Parry Sound résulterait du chevauchement qui a eu lieu peu après l'apogée du métamorphisme, tandis que celles pour les roches du domaine de Shawanaga indiquent une exhumation probablement associée au chevauchement et à l'extension.

*Mots-clés:* Province du Grenville, roches monocycliques, granulite, amphibolite, rétrogression, trajectoires P–T–t, effets de superposition, histoire de convergence, baie Georgienne, Ontario.

## Introduction

Important advances have been made in understanding the relationships between tectonics and metamorphism within orogenic belts through the use of quantitative pressure – temperature – time (P–T–t) data (*e.g.*, Spear *et al.* 1984, Selverstone *et al.* 1984) and the application of one- and two-dimensional thermal-kinematic models (*e.g.*, Oxburgh & Turcotte 1974, England & Richardson 1977, England & Thompson 1984, Ruppel & Hodges 1994, Huerta *et al.* 1998). However, interactions between thermal and tectonic processes, and their consequences for regional metamorphism, remain poorly understood (Jamieson *et al.* 1998). In ancient orogenic belts, these problems are compounded by difficulties associated with the construction and interpretation of P–T–t paths, especially in high-grade rocks (*e.g.*, Jamieson 1988, Frost & Chacko 1989, Vernon 1996), and difficulties in understanding exhumed crustal sections, which are typically overprinted by later effects, in terms of fundamental metamorphic processes.

The deeply eroded Grenville orogen of the Canadian Shield offers an excellent opportunity to examine the metamorphic and structural evolution of the lower continental crust during the development of a collisional orogen of Himalayan proportions (*e.g.*, Dewey & Burke 1973, Windley 1986). As a result of late- to post-Grenvillian extensional and erosional unroofing, middle to deep levels of crust are exposed throughout most of the Grenville orogen, as shown by the prevalence of granulite- and upper-amphibolite-facies rocks (*e.g.*, Davidson 1986, Rivers *et al.* 1989, Anovitz & Essene 1990). In the Ontario segment of the Grenville orogen, metamorphic and geochronological studies have provided thermobarometric and thermochronological constraints on pre-Grenvillian (>1190 Ma) and Grenvillian (*ca.* 1190–980 Ma) metamorphism. Some authors have presented P–T–t paths that have been interpreted in terms of Grenvillian thermal and tectonic processes (*e.g.*, Anovitz & Chase 1990, Tuccillo *et al.* 1990, Jamieson *et al.* 1995). However, the well-documented superposition of multiple pre-Grenvillian and Grenvillian high-grade metamorphic and tectonic events in many parts of the Grenville orogen (*e.g.*, Jamieson *et al.* 1992, Tuccillo *et al.* 1992, Ketchum *et al.* 1994, Culshaw *et al.* 1997) means that constructing and interpreting P–T–t paths from these rocks requires careful assessment of timing and overprinting relationships, and the degree to which maximum P–T estimates really reflect peak P–T conditions (*e.g.*, Frost & Chacko 1989, Frost *et al.* 1998, Pattison 1998). Only then can the metamorphic data provide quantitative constraints on the tectonic processes operating during the Grenvillian orogenesis.

In this paper, we report metamorphic data from the Parry Sound and Shawanaga domains along the well-exposed eastern shore of Georgian Bay (Figs. 1, 2, and 3). This region contains rocks that were affected only by Grenvillian metamorphism, and therefore potentially provides the best opportunity to study links between metamorphic and tectonic processes during Grenvillian orogenesis. Our metamorphic data, combined with data on timing of metamorphism, are consistent with the progressive northwest-directed juxtaposition of lithotectonic assemblages metamorphosed at progressively later times. However, we also show that derivation of tectonically meaningful P–T–t paths for these high-grade rocks is limited by variable overprinting and partial re-equilibration of mineral assemblages, fabrics, and thermobarometers. The extent of overprinting can be linked to strain, fluid access, and high-temperature residence time.

## Geological Setting

### *Regional framework*

In the southeastern Canadian Shield (Fig. 1), the Grenville orogen is widely regarded as a Himalayan-scale, deeply eroded, convergent orogen developed as a result of collision between the SE-facing Laurentian margin and arc assemblages and continental terranes lying to the southeast (*e.g.*, Rivers *et al.* 1989, Easton 1992, McLelland *et al.* 1996). The Ontario segment of the Grenville orogen comprises (Fig. 1; Wynne-Edwards 1972): (1) the Grenville Front Tectonic Zone, which marks the northwestern boundary of the orogen, (2) the Central Gneiss Belt (CGB), which consists largely of reworked high-grade rocks (pre-1400 Ma) of

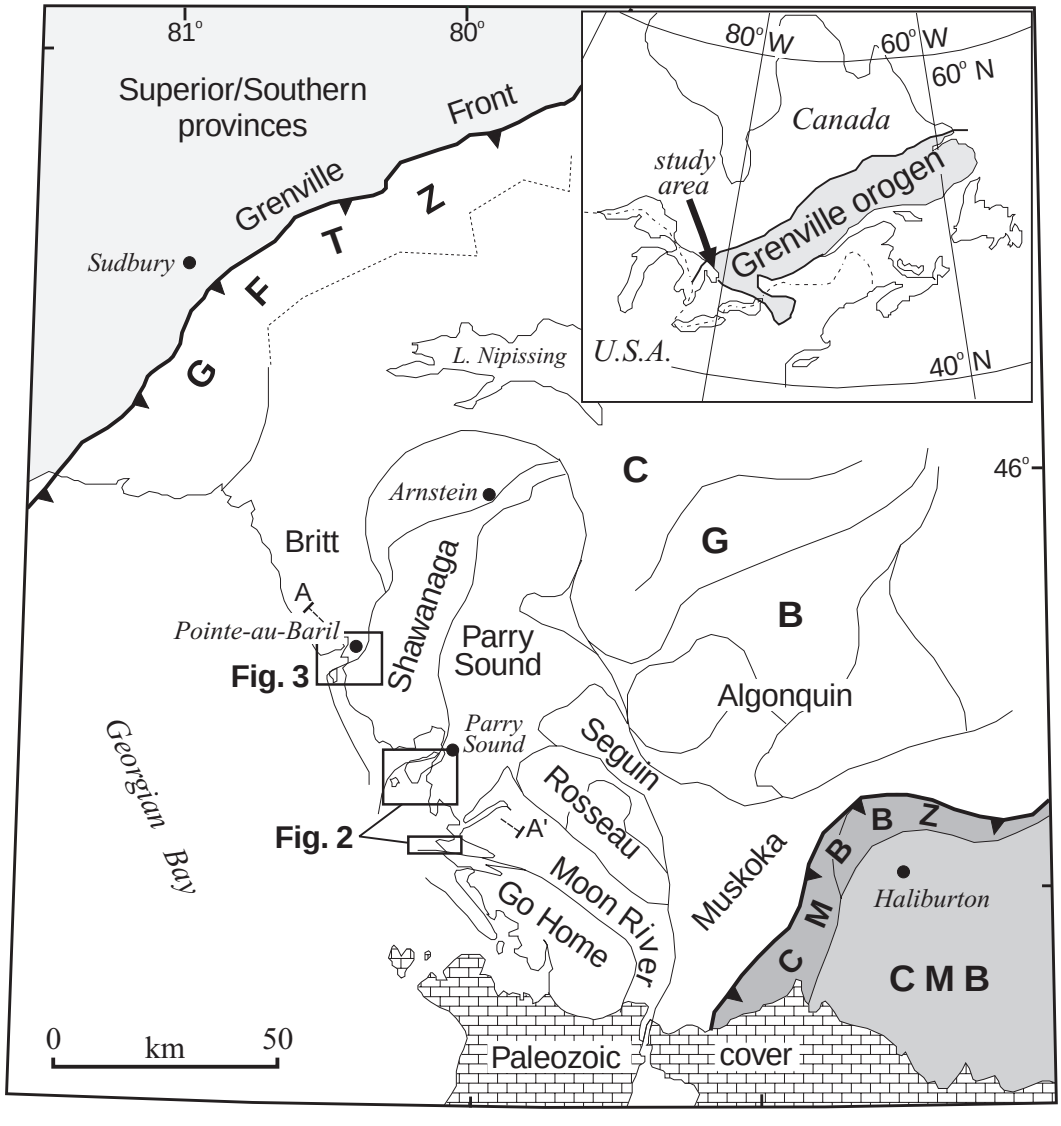


FIG. 1. Location of study area and lithotectonic domains within the Central Gneiss Belt (CGB), Ontario segment of the Grenville orogen. GFTZ: Grenville Front Tectonic Zone, CMBBZ: Central Metasedimentary Belt boundary thrust zone, CMB: Central Metasedimentary Belt. Heavy barbed lines indicate major thrust boundaries. Thin lines represent domain boundaries after Davidson (1984) and Davidson & van Breemen (1988), with minor modifications by Culshaw *et al.* (1997). Geology of the Parry Sound and Pointe-au-Baril areas is shown in Figures 2 and 3, respectively. Inset map shows location of study area in Grenville orogen of the southeastern Canadian Shield.

the Laurentian craton and younger supracrustal sequences deposited on its margin, and (3) the Central Metasedimentary Belt (CMB) interpreted as a post-1400 Ma composite system of magmatic arcs and marginal basins (*e.g.*, Windley 1989, Easton 1992, Davidson 1995), accreted to or accumulated on the Laurentian

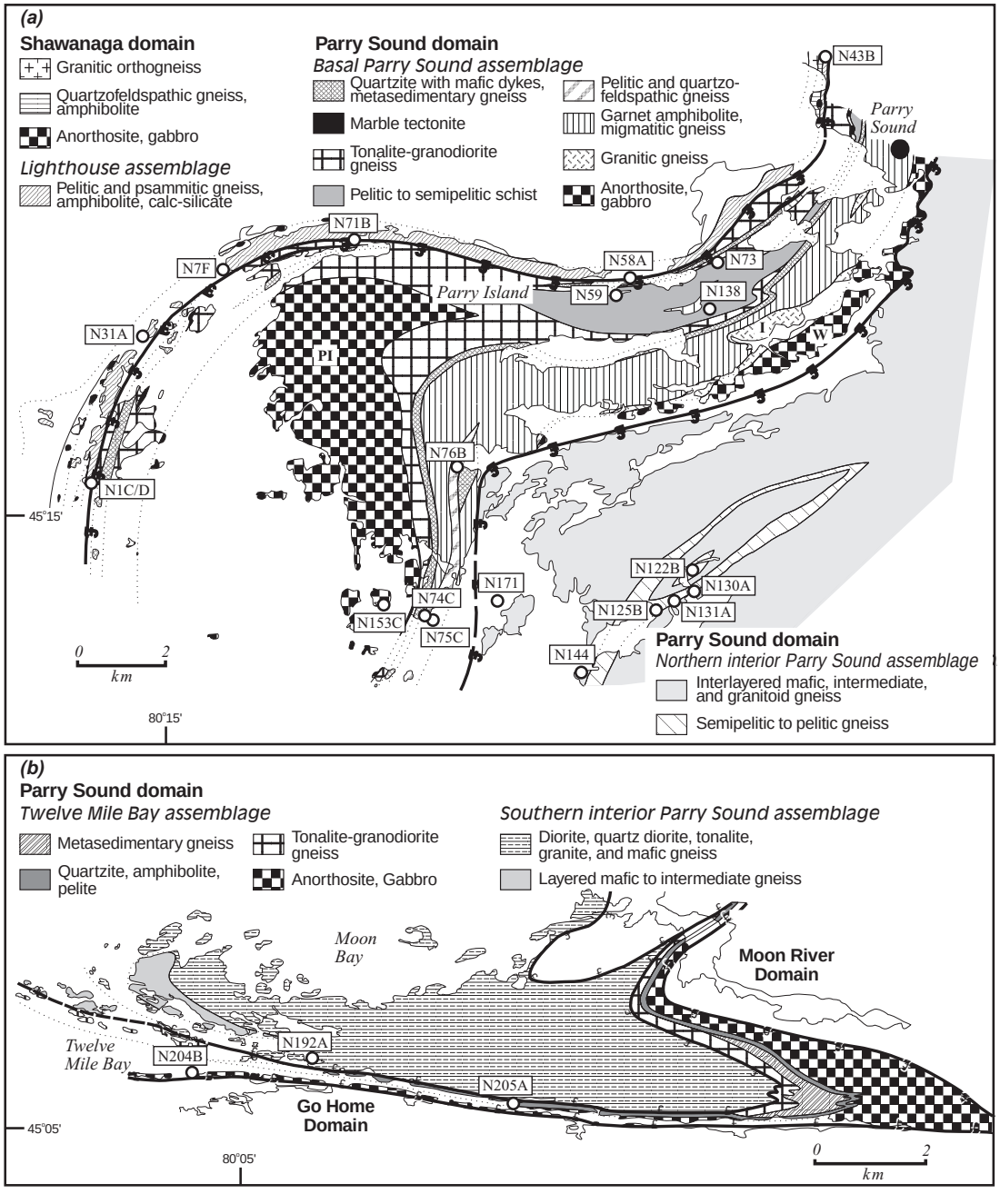


FIG. 2. Geological map of (a) the northern Parry Sound and southern Shawanaga domains, and (b) the southern Parry Sound domain along Georgian Bay (after Davidson 1984, Culshaw *et al.* 1989, 1994, Wodicka 1994). The boundaries of the Lighthouse assemblage differ slightly from those of the Lighthouse gneiss association of Culshaw *et al.* (1989; their Fig. 2). PI: Parry Island anorthosite, W: Whitestone anorthosite, I: Isabella Island granitic gneiss. Location of samples used for thermobarometry is shown.

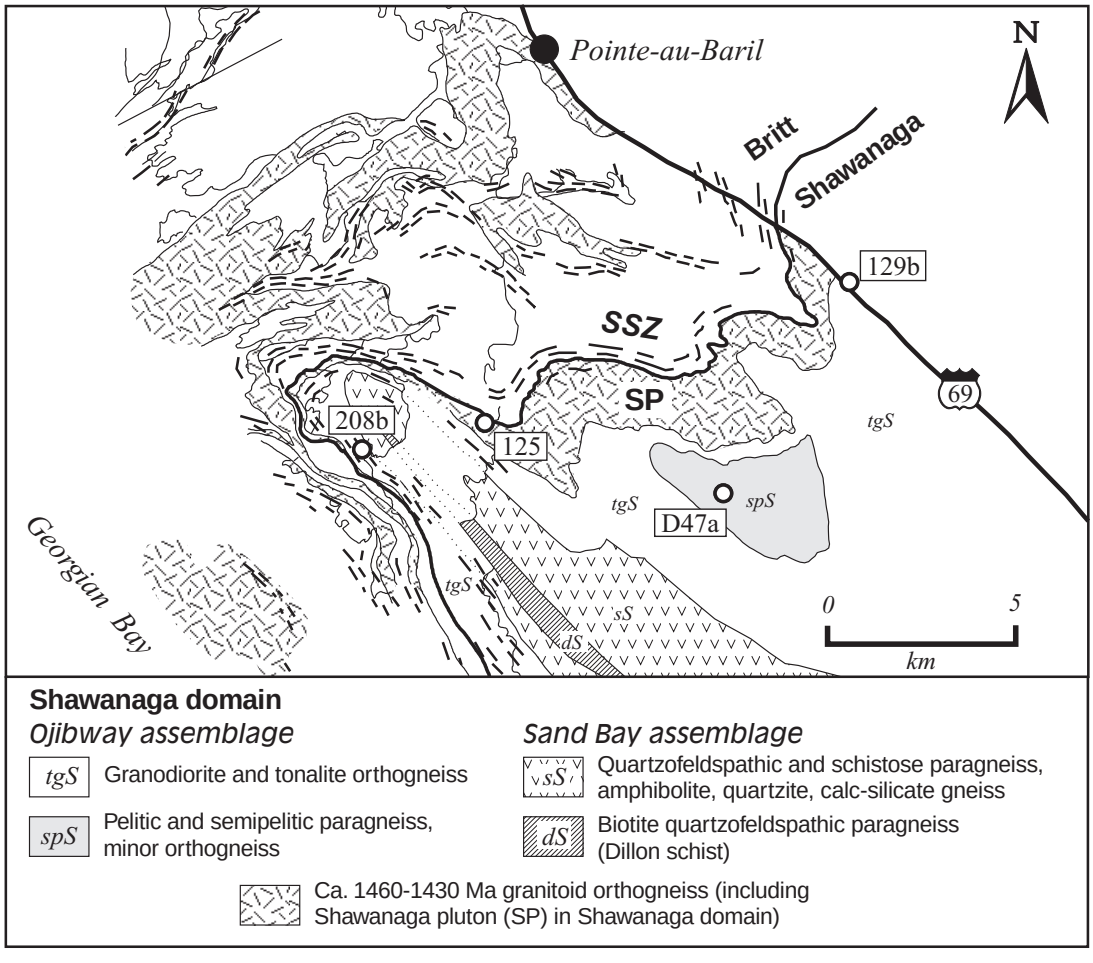


FIG. 3. Geological map of the Shawanaga domain in the vicinity of Pointe-au-Baril (after Culshaw *et al.* 1994, Ketchum 1995). Lithological contacts are folded by regional-scale NNW-trending folds. Dashes indicate extensional shear zones. SP: Shawanaga pluton, SSZ: Shawanaga shear zone. Location of samples used for thermobarometry is shown.

margin during more than 300 m.y. of tectonic activity. The CMB overlies the CGB along the crustal-scale Central Metasedimentary Belt boundary thrust zone (Fig. 1; Hanmer & McEachern 1992).

Contractional deformation that culminated in continent–continent collision led to the progressive juxtaposition, internal imbrication, and northwestward translation of Mesoproterozoic allochthonous assemblages of the CGB and CMB, and reworking of Paleo- and Mesoproterozoic parautochthonous units of the CGB (*e.g.*, Rivers *et al.* 1989, Easton 1992, Jamieson *et al.* 1992, Davidson 1995, Culshaw *et al.* 1997). Thrust displacement began as early as *ca.* 1190 Ma (McEachern & van Breemen 1993) and ended at *ca.* 980 Ma along the Grenville Front Tectonic Zone (*e.g.*, Haggart *et al.* 1993, Krogh 1994). During and following the later stages of convergence, much of the Ontario segment of the Grenville orogen underwent extension (*e.g.*, Carlson *et al.* 1990, Culshaw *et al.* 1994, Jamieson *et al.* 1995, Busch & van der Pluijm 1996, Busch *et al.* 1996, Ketchum *et al.* 1998). Whereas the CGB appears to have extended by distributed, subhorizontal ductile flow in an extremely weak lower crust (Culshaw *et al.* 1997), narrow, steeply dipping, late- to post-orogenic extensional faults characterize the CMB (Carlson *et al.* 1990, Busch & van der Pluijm 1996, Busch *et al.* 1996).

Contrasts in geological, metamorphic, and structural histories have been used to distinguish a number of lithotectonic units in the CGB (Davidson & Morgan 1981, Davidson *et al.* 1982, Culshaw *et al.* 1983, 1988,

1989, 1990, 1994). A NW–SE cross-section of the CGB and its bounding shear zones shows a crustal-scale duplex with contrasting structural styles in the upper and lower levels of the crust (Fig. 4a; Culshaw *et al.* 1997). Relatively thick parautochthonous units (*i.e.*, Grenville Front Tectonic Zone and the Britt domain) and transported allochthonous elements of the Laurentian craton (*i.e.*, lower Go Home, southern Rosseau, and Algonquin domains; Ketchum 1995) characterize the lower and intermediate structural levels, respectively. In contrast, thin allochthonous sheets that originated near the Laurentian margin (*i.e.*, Shawanaga and upper Go Home domains) and as part of the CMB (*i.e.*, Parry Sound domain) occupy higher structural levels. The Parry Sound domain, with its presumed CMB parentage (Wodicka *et al.* 1996), is now structurally overlain by lithotectonic units that have Laurentian affinities (*i.e.*, Moon River and Muskoka domains). The Moon River domain is interpreted to have been emplaced onto the Parry Sound domain along an out-of-sequence ductile thrust zone (Culshaw *et al.* 1997). The allochthonous rocks of the CGB are separated from the underlying parautochthonous units by a regional *décollement*, the Shawanaga shear zone (Fig. 4b; Culshaw *et al.* 1994, Ketchum 1995).

Most of the tectonic boundaries shown in Figure 4 are interpreted to have originated as NW-directed thrusts, but many of them have been partly or pervasively overprinted by SE-directed extensional fabrics (see below; *e.g.*, Culshaw *et al.* 1994, Jamieson *et al.*

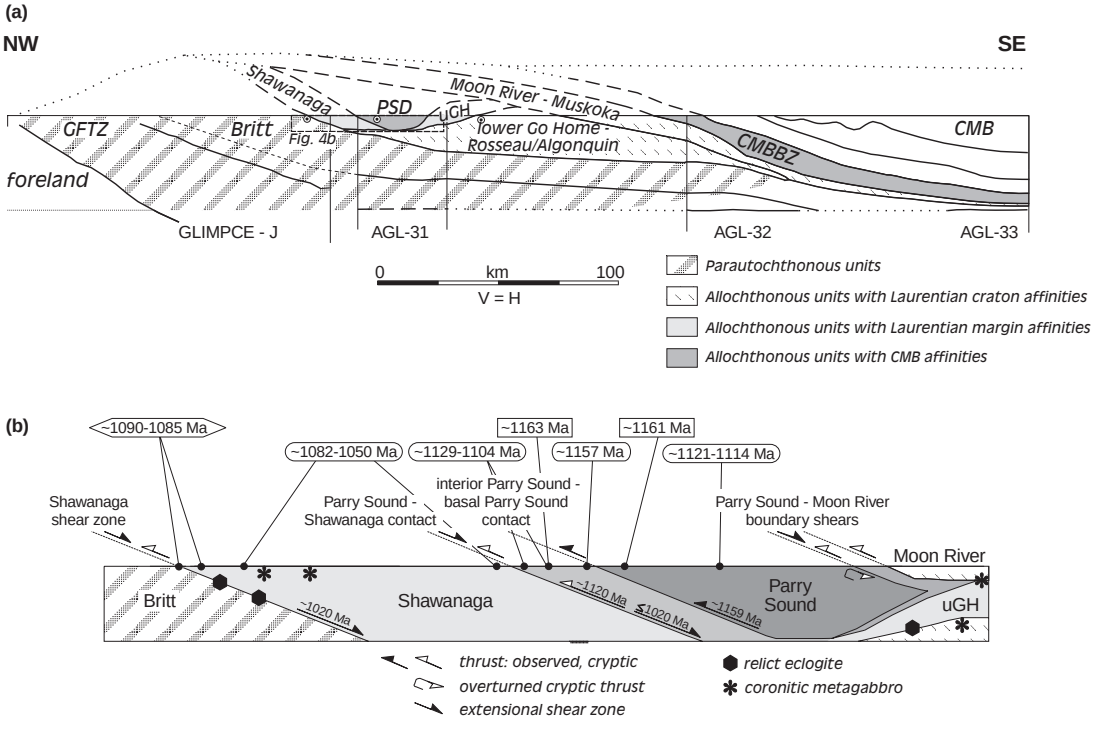


FIG. 4. (a) Crustal-scale cross-section extending from the Grenville Front to the CMB (Fig. 1), based on geological and structural data and seismic reflection profiles (AGL–31, 32, 33 and GLIMPSE–J; Green *et al.* 1988, White *et al.* 1994; *cf.* Culshaw *et al.* 1997). Abbreviations: PSD: Parry Sound domain, uGH: upper Go Home domain, GFTZ, CMBBZ, and CMB as in Figure 1; foreland corresponds to Southern and Superior Provinces in Figure 1. Circles with dots indicate NE-trending lineation. Details of the construction techniques are given by Culshaw *et al.* (1997). (b) Schematic cross-section along A–A' of Figure 1 (after Culshaw *et al.* 1997) showing (1) approximate time of thrusting and extension as determined by U–Pb and $^{40}Ar/^{39}Ar$ geochronology for the basal Parry Sound boundary shears and Shawanaga shear zone, (2) distribution of relict eclogite and coronitic metagabbro in allochthonous units, and (3) U–Pb data for granulite-facies metamorphism (boxes with square edges), eclogite-facies metamorphism (lozenge-shaped boxes), and amphibolite-facies metamorphism (boxes with rounded edges) in the study area. Solid lines represent the boundaries between lithotectonic units shown in Figure 1. Arrows show shear sense (normal and thrust), and hooked arrow represents an inferred folded thrust. References for age dates are given in the text.

1995). The superposition of late orogenic extension on the ductile thrust belt is considered to be responsible for the subhorizontal structural attitude and NW-trending folds dominant along Georgian Bay (Culshaw *et al.* 1994).

In this paper, we focus on allochthonous monocyclic rocks of the Parry Sound and Shawanaga domains, which preserve no evidence for pre-Grenvillian orogenesis (*e.g.*, Wodicka 1994, Ketchum 1995, Culshaw *et al.* 1997). Their metamorphic mineral assemblages are considered to be entirely of Grenvillian age. Thus, these rocks provide the best available constraints on the thermal and tectonic evolution of this part of the Grenville orogen. The following section summarizes the most important features of these allochthonous domains.

Throughout this paper, we use the term "monocyclic" for units affected only by Grenvillian orogenesis (*e.g.*, Rivers *et al.* 1989). The term "allochthonous" is used to describe any far-travelled unit, whether or not it is inferred to have originally formed part of Laurentia (*e.g.*, Rivers *et al.* 1989, Culshaw *et al.* 1997, Ketchum & Davidson 2000). The term "Grenvillian orogenesis" is used here for events (tectonic, metamorphic, and plutonic) within the range *ca.* 1190 to 980 Ma (*e.g.*, Rivers *et al.* 1989, Rivers 1997).

### *The Parry Sound domain*

Geological and geochronological data suggest that the Parry Sound domain (Davidson & Morgan 1981) comprises at least three distinctive lithotectonic assemblages. From highest to lowest structural level, these include the: (1) interior Parry Sound, (2) basal Parry Sound, and (3) Twelve Mile Bay assemblages (Fig. 2; Culshaw *et al.* 1989, 1994, Wodicka 1994, Wodicka *et al.* 1996). The interior Parry Sound assemblage (Culshaw *et al.* 1994) consists of *ca.* 1400–1300 Ma (van Breemen *et al.* 1986, Wodicka *et al.* 1996) granulite-facies metaplutonic rocks ranging from gabbro to granite, with subordinate metasupracrustal rocks including pelitic gneiss, calc-silicate, and marble (Culshaw *et al.* 1989, Wodicka 1994). The upper part of the basal Parry Sound assemblage (Culshaw *et al.* 1994) consists of the Whitestone anorthosite (1350 ± 50 Ma; van Breemen *et al.* 1986) intruded by the 1383 ± 14 Ma Isabella Island granitic gneiss (Wodicka *et al.* 1996), garnet amphibolite of probable igneous origin, and minor pelitic and quartzofeldspathic gneiss. The lower part of the assemblage comprises *ca.* 1400–1330 Ma tonalitic to granodioritic orthogneiss, the Parry Island anorthosite intruded at 1163 ± 3 Ma, and post-*ca.* 1436 Ma quartzite interlayered with pelitic and semipelitic gneiss and schist, quartzofeldspathic gneiss, amphibolite, and marble (Wodicka *et al.* 1996). In contrast to the uppermost units, these rocks are cut by variably deformed and metamorphosed mafic dykes emplaced at some time between 1163 and 1151 Ma (Wodicka *et al.* 1996), suggesting that the basal Parry Sound assemblage could be composite (Wodicka 1994, Wodicka *et al.* 1996). The Twelve Mile Bay assemblage (Wodicka *et al.* 1996), which structurally underlies the interior Parry Sound assemblage in the south (Fig. 2b), comprises a thin sequence of supracrustal rocks (quartzite, pelitic gneiss, and amphibolite) in tectonic contact with tonalitic to granodioritic orthogneiss and anorthosite cut by mafic dykes. These rocks resemble those of the basal Parry Sound assemblage, but the quartzite is younger (deposited after *ca.* 1140–1120 Ma; Wodicka *et al.* 1996).

The Parry Sound domain has clear lithological and age affinities with rocks of the Central Metasedimentary Belt boundary thrust zone and eastern CMB (Wodicka *et al.* 1996). It is now completely detached from its presumed southeastern source, implying at least 100 km of displacement of the allochthon (Fig. 4a). Field evidence and U–Pb geochronology suggest that the different lithotectonic elements of the Parry Sound domain were assembled early in the convergence history prior to their final emplacement onto the Laurentian craton (Wodicka *et al.* 1996, Culshaw *et al.* 1997).

### *The Shawanaga domain*

The Shawanaga domain (Ketchum 1995), which structurally underlies the Parry Sound domain, can be divided into four lithotectonic assemblages (Figs. 2a and 3; Culshaw *et al.* 1988, 1989, 1994, 1997). In descending structural order, these are the (1) Lighthouse assemblage, (2) Sand Bay assemblage, (3) Ojibway assemblage, and (4) Shawanaga pluton. The uppermost Lighthouse assemblage comprises interlayered pelitic and psammitic gneiss (metagreywacke–shale), quartzofeldspathic gneiss, amphibolite, and calc-silicate (Fig. 2a). Originally interpreted as belonging to the basal Parry Sound assemblage (Culshaw *et al.* 1989, Wodicka 1994), the Lighthouse assemblage has been re-assigned to the Shawanaga domain primarily on the basis of the absence of mafic dykes, which contrasts with the overlying units of the basal Parry Sound assemblage (Culshaw & Dostal 1997). The structurally underlying Sand Bay assemblage is characterized by migmatitic quartzofeldspathic gneiss and schist, quartzite, calcareous gneiss, amphibolite, and rare marble (Fig. 3; Davidson *et al.* 1982, Culshaw *et al.* 1994). Single-crystal zircon dating of a quartz-rich paragneiss indicates deposition after *ca.* 1417 Ma (T. Krogh, unpubl. data). On the basis of field relations and geochemical data, paragneisses of the Sand Bay assemblage are interpreted to mark the opening of a Grenvillian ocean or a marginal basin landward of an Andean-type margin (Culshaw & Dostal 1997). A unit of granodioritic orthogneiss lying above this supracrustal assemblage has been dated at $1346^{+69}_{-39}$ Ma (U–Pb on zircon; van Breemen *et al.* 1986). The Ojibway assemblage is dominated by migmatitic granodioritic to tonalitic orthogneiss (1466 ± 11 Ma; T. Krogh, unpubl. data) in which

leucosomes become progressively more abundant toward the southeast, close to the contact with the Parry Sound domain. It also contains isolated concordant layers of granitic gneiss and amphibolite, as well as pelitic gneiss, which occurs as enclaves in orthogneiss and in a large exposure of supracrustal rock (Fig. 3) previously mapped as a tectonic window of the Britt domain (Culshaw *et al.* 1994). The lowermost Shawanaga pluton, a granitic to granodioritic orthogneiss, forms an elongate body between the parautochthonous Britt domain and the Ojibway assemblage (Fig. 3). Dated at *ca.* 1460 Ma (T. Krogh, unpubl. data), this pluton is similar in age to both the Britt domain and the Ojibway granitoid orthogneisses. The monocyclic rocks of the Shawanaga domain are interpreted to represent the remnants of an active, post-1450 Ma Laurentian margin (Culshaw & Dostal 1997, Culshaw *et al.* 1997).

In the Shawanaga domain, rare layers of garnet-bearing amphibolite interpreted as mafic dykes are confined to the Sand Bay assemblage (Ketchum 1995, Culshaw & Dostal 1997). These dykes are texturally distinct from mafic dykes in both the underlying Britt and overlying Parry Sound domains, and may represent syn-volcanic intrusions (Culshaw & Dostal 1997). Minor mafic intrusions in the Ojibway assemblage and Shawanaga pluton include small podiform bodies of metagabbro, and garnet–clinopyroxene-rich rocks interpreted as retrograded eclogites (Fig. 4b; Davidson 1990, 1991). The metagabbro bodies belong to the *ca.* 1170–1150 Ma (Davidson & van Breemen 1988, van Breemen & Davidson 1990, Heaman & LeCheminant 1993) coronitic olivine metagabbro suite that occurs throughout the CGB, with the exception of the Parry Sound and Britt domains (*e.g.*, Grant 1987, Davidson 1991). Though similar in age, the coronitic metagabbros do not have the same chemical or physical attributes as the 1163–1151 Ma mafic dykes of the basal Parry Sound assemblage (N. Wodicka, unpubl. data, A. Davidson, pers. commun., 1998).

### *Structure*

Rocks throughout the Parry Sound and Shawanaga domains were deformed by penetrative ductile flow during the Grenvillian orogeny. Lithological boundaries are generally parallel to the dominant fabric, a gneissic foliation (dominantly $S \geq L$), with a shallow to locally steep, southeast-dipping enveloping surface associated with a southeast-plunging lineation. Although locally overprinted by extensional shear in high-strain zones (see below), the dominant gneissic fabric in both the Parry Sound and Shawanaga domains formed during northwest-directed thrusting, as suggested by sparse kinematic indicators and extension lineations (*e.g.*, Davidson 1984, Culshaw *et al.* 1994, Wodicka 1994, Ketchum 1995). In the basal Parry Sound assemblage, a northeast-trending lineation is preserved within the Parry Island anorthosite and paragneisses in an adjacent low-strain area (Fig. 4a; Gower 1992, Wodicka 1994). Locally, deformed 1163–1151 Ma mafic dykes, which themselves carry a northeast-plunging lineation, cut at a moderate angle the orogen-parallel fabric in the *ca.* 1163 Ma Parry Island anorthosite. Orogen-parallel deformation in the basal Parry Sound assemblage thus appears to have been broadly coeval with emplacement of the Parry Island anorthosite and mafic dykes (Wodicka 1994).

Boundaries separating lithotectonic assemblages are distinguished by the presence of kinematic indicators, localized zones of high strain, truncation of structures in adjacent rocks, and contrasts in tectonostratigraphy (Culshaw *et al.* 1994, 1997, Wodicka 1994, Ketchum 1995). The interior Parry Sound – basal Parry Sound contact is a thrust-sense shear zone that coincides with a sharp lithological break (Fig. 4b). The lower boundary of the basal Parry Sound assemblage, *i.e.*, the Parry Sound – Shawanaga contact, is interpreted as a cryptic thrust that is overprinted by a discrete extensional shear zone developed within thick, older tectonites (Culshaw *et al.* 1994, 1997, Wodicka 1994). Geochronological data suggest that displacements along the thrusts were not contemporaneous. The thrust separating the basal Parry Sound assemblage from the overlying interior Parry Sound assemblage has been dated at *ca.* 1159 Ma (van Breemen *et al.* 1986). Though not dated directly, thrust displacement along the Parry Sound – Shawanaga contact probably occurred, at least in part, at *ca.* 1120 Ma (Wodicka 1994).

The allochthonous Shawanaga domain is separated from the parautochthonous Britt domain by the shallowly to moderately dipping upper-amphibolite-facies Shawanaga shear zone (Ketchum 1995). The shear zone coincides with an important seismic reflector that dips gently beneath the Parry Sound domain (White *et al.* 1994). It displays dominantly top–to-the-southeast extensional kinematic indicators, but there is evidence that the extensional shear zone reactivated an older thrust with opposite vergence (Culshaw *et al.* 1994, Ketchum 1995, Ketchum *et al.* 1998). Geochronological constraints indicate that major extensional displacement along the Shawanaga shear zone occurred at *ca.* 1020 Ma (Ketchum *et al.* 1998).

Large, recumbent, nappe-like folds in the Shawanaga domain (Culshaw *et al.* 1989, 1994) and isolated, reclined folds in the interior Parry Sound assemblage (Culshaw *et al.* 1989), and possibly also in the basal Parry Sound assemblage (Gower 1992), are interpreted to have formed during thrust-related deformation (Culshaw *et al.* 1994, 1997). Extension-related deformation produced regional-scale, upright, north-northwest-trending folds with subhorizontal enveloping surfaces in both the Shawanaga domain and its footwall (Britt domain) (Fig. 3; *e.g.*, Culshaw *et al.* 1994, 1997).

## PETROGRAPHIC RELATIONS

The mineralogical and textural characteristics of monocyclic rocks from the Parry Sound and Shawanaga domains are outlined below and in Tables 1 and 2. Abbreviations for mineral names are mainly after Kretz (1983).

### *The Parry Sound domain*

Mineral assemblages in the Parry Sound domain document conditions ranging from lower amphibolite to granulite facies (Fig. 5). In the *interior Parry Sound assemblage*, metamorphism generally occurred in the granulite facies (Anovitz & Essene 1990), although ret-

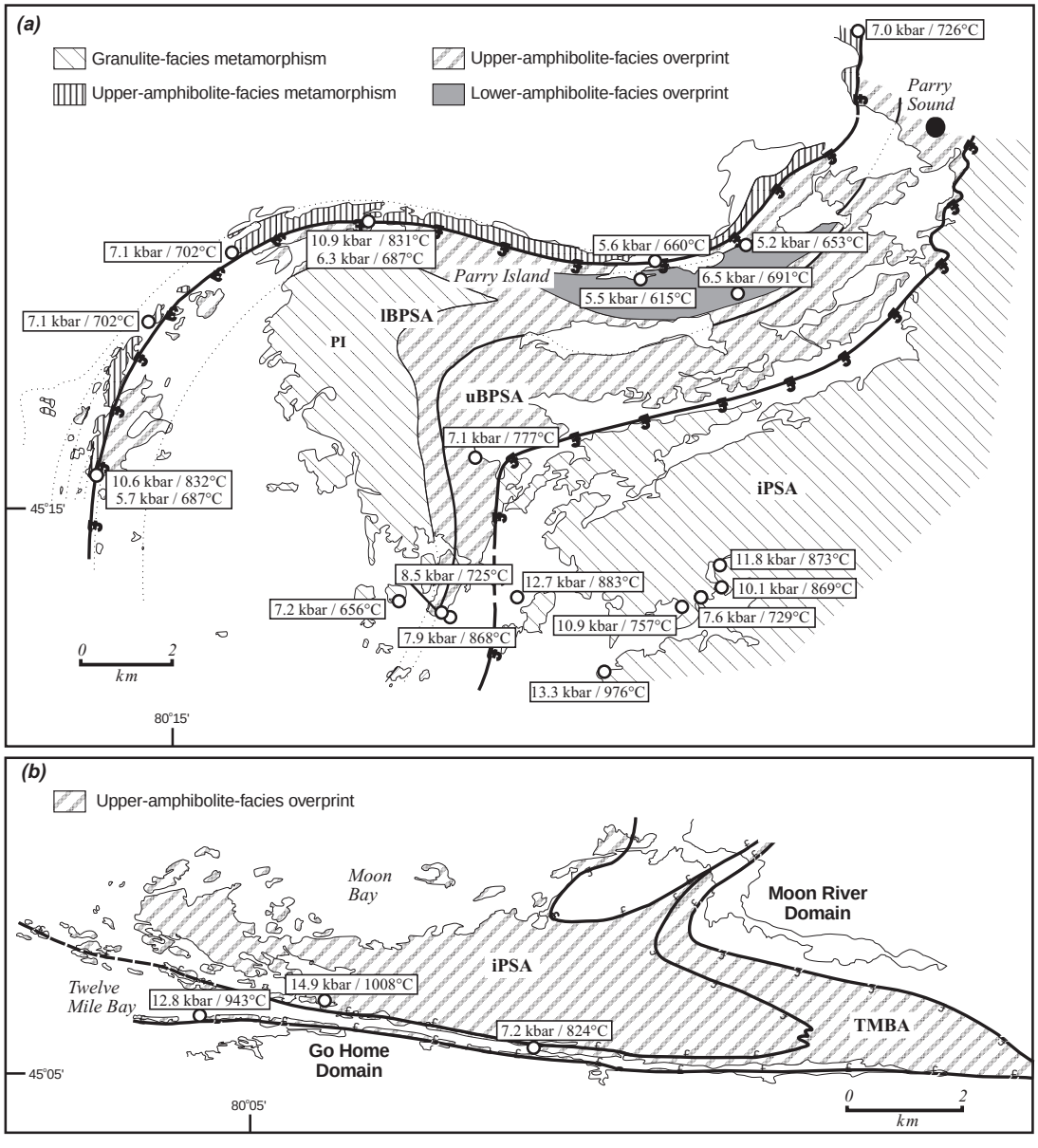


FIG. 5. Simplified geological map of the Parry Sound and southern Shawanaga domains showing (1) the distribution of granulite- and amphibolite-facies domains, and (2) P–T results across the study area. lBPSA: lower part of the basal Parry Sound assemblage, uBPSA: upper part of the basal Parry Sound assemblage, iPSA: interior Parry Sound assemblage, TMBA: Twelve Mile Bay assemblage.

TABLE 1. MINERAL ASSEMBLAGES AND TEXTURAL RELATIONS IN PARRY SOUND DOMAIN ROCKS

| Unit | Lithology | Mineralogy | Texture |
|---|---|---|---|
| Northern interior Parry Sound assemblage | Pelitic granulite | *peak:* Sil - Grt - Bt - Qtz ± Kfs ± Pl ± Spl ± Opx ± Rt ± Ilm<br>*pb:* Grt (Qtz - Sil - Bt - Spl - Rt), Kfs (Qtz - Bt), Opx (Grt), Spl (Bt - Qtz) | Thrust-related fabric; well-developed porphyroclastic texture; minor retrogression |
| | Mafic gneiss and granulite | *peak:* Hbl - Pl ± Opx ± Cpx ± Qtz ± Grt ± Bt ± Ilm<br>*pb:* Grt (Qtz - Pl - Hbl), Hbl (Pl - Qtz - Ap), Opx - Cpx (Hbl - Pl) | |
| Southern interior Parry Sound assemblage | Mafic gneiss | *retro:* Hbl - Pl ± Bt ± Ep ± Ttn [± Cpx ± Opx] | Thrust-related fabric; subequigranular granoblastic texture; extensively retrograded |
| Upper part of basal Parry Sound assemblage | Group-I pelitic gneiss | *retro:* Grt - Bt - Pl - Kfs - Qtz - Ky - Sil ± Rt ± Ilm<br>*pb:* Grt (Qtz - Bt - Zrn - Pl - Kfs - Ap - Sil), Ky | Pervasive thrust-related fabric; highly embayed garnet porphyroclasts (subidioblastic to xenoblastic) with plagioclase coronas/moats in both pelitic and mafic rocks |
| | Garnet amphibolite | *retro:* Pl - Hbl ± Grt ± Cpx ± Ttn ± Bt ± Qtz | |
| | Whitestone anorthosite | *retro:* Pl - Hbl ± Grt ± Bt ± Cpx ± Ilm ± Ttn ± Scp ± [Opx] | |
| Lower part of basal Parry Sound assemblage | Parry Island anorthosite and mafic dykes | *peak:* Opx - Hbl - Pl ± Grt ± Cpx | NE-plunging lineation defined by Opx; locally developed coronitic texture in anorthosite; well-equilibrated, granoblastic texture in mafic dykes. |
| | | *retro:* Pl - Hbl ± Scp ± Cpx ± Grt ± Bt ± Ttn ± Qtz ± Cal | Pervasive thrust-related fabric; granoblastic texture |
| | Group-II pelitic schist | *retro:* Grt - Bt - Pl - Sil - Gr - St - Qtz ± Rt ± Ilm - [Ky - Kfs - Grt]<br>*pb:* Grt (Qtz - Pl - Kfs - Sil - Rt - Ilm - Bt - Gr), Ky, Pl (Sil), St | Coarsely recrystallized and strongly retrograded; folds and crenulations with NE- and SW-plunging axes |
| | Tonalite/granodiorite gneiss | *retro:* Bt - Pl - Qtz ± Kfs ± Grt ± Hbl ± Cpx ± Ttn ± [Opx] | Pervasive thrust-related fabric; granoblastic texture |
| Twelve Mile Bay assemblage | Pelitic gneiss | *retro:* Grt - Bt - Qtz - Pl - Kfs - Sil ± Rt ± Ilm<br>*pb:* Grt (Bt - Qtz - Pl - Kfs - Sil - Zc), Kfs | Pervasive thrust-related fabric; well-equilibrated granoblastic texture |
| | Mafic gneiss | *retro:* Pl - Hbl ± Grt ± Qtz ± Bt ± Ttn [± Opx ± Cpx] | |

Notes: *'peak'* = peak mineral assemblage; *'retro'* = mineral assemblage that developed subsequent to peak metamorphism; *'pb'* = porphyroblasts. (...) indicates minerals present as inclusions in porphyroblasts and [...] indicates highly embayed and/or corroded minerals.

rogression to the amphibolite facies is extensive in the south and southeast (see below and Fig. 5; Hanmer 1984, Culshaw *et al.* 1989). Sillimanite is the ubiquitous aluminosilicate in pelitic granulites (N122b, N125b, N130a, and N131a) from the northern interior Parry Sound assemblage (Table 1), although kyanite has been reported from several localities north and east of the study area (Anovitz & Essene 1990, Davidson, pers. commun., 1990). In most pelitic granulites, porphyroclastic fabrics are prevalent (Fig. 6a): thermal peak min-

TABLE 2. MINERAL ASSEMBLAGES AND TEXTURAL RELATIONS IN SHAWANAGA DOMAIN ROCKS

| Unit | Lithology | Mineralogy | Texture |
|---|---|---|---|
| Lighthouse assemblage | Pelitic gneiss | *peak:* Grt - Ky - Kfs - Pl - Qtz - Bt ± Rt ± Ilm<br>*pb:* Grt (Qtz - Bt - Ilm - Rt - Pl - Kfs - Ms - Gr - Zrn - Ap - Py), Ky | Pervasive thrust-related fabric; garnet ranges in shape from subidioblastic to elongate grains with their long axes parallel to the foliation; late retrogression to muscovite |
| | Pelitic mylonite | *retro:* Grt - Kfs - Pl - Qtz - Ky - Sil - Bt ± Rt ± Ilm<br>*pb:* Grt (Pl - Ky - Sil), Ky, Kfs | Strong extensional fabric; fine-grained mylonitic matrix; lack of retrogression to muscovite in pelitic rocks; plagioclase coronas around garnet porphyroclasts in amphibolites |
| | Amphibolite | *retro:* Hbl - Pl ± Grt ± Bt ± Qtz ± Scp [± Cpx] | |
| Sand Bay assemblage | Paragneiss | *retro:* Qtz - Kfs - Pl - Bt - Ms - Ep ± Hbl ± Ttn ± Chl ± Rt ± Ilm | Strongly migmatitic; pervasive thrust-related fabric except in Shawanaga shear zone where extensional fabrics prevail; equigranular granoblastic texture |
| Ojibway assemblage | Tonalite/granodiorite gneiss | *retro:* Pl - Kfs - Qtz - Hbl - Bt - Ttn ± Grt ± Ep | Strongly migmatitic; pervasive thrust-related fabric except in Shawanaga shear zone where extensional fabrics prevail; mildly deformed metagabbro retains subophitic and coronitic textures, whereas intensely recrystallized coronite is reduced to amphibolite |
| | Amphibolite | *retro:* Hbl - Pl - Qtz - Bt ± Grt ± Ep | |
| | Pelitic gneiss | *retro:* Pl - Qtz - Kfs - Bt - Grt ± Ky ± Sil ± Ms ± Ilm ± Rt ± Gr<br>*pb:* Grt (Qtz - Bt - Rt), Ky (Qtz - Bt) | |
| | Coronitic metagabbro and relict eclogite | *retro:* Grt - Hbl - Pl - Cpx - Ilm - Bt [± Opx] | |

Notes: *'peak'* = peak mineral assemblage; *'retro'* = mineral assemblage that developed subsequent to peak metamorphism; *'pb'* = porphyroblasts. (...) indicates minerals present as inclusions in porphyroblasts and [...] indicates highly embayed and/or corroded minerals.

eral phases, including garnet ($Alm_{45–53}Prp_{44–51}Grs_{1–4}Sps_{1–4}$), perthite, orthopyroxene ($En_{69}Fs_{22}$), and spinel, occur as porphyroclasts wrapped by a foliation defined by aligned crystals of prismatic sillimanite, biotite, and ribbon quartz. Biotite compositions are Mg-rich ($0.19 < X_{Fe} < 0.31$, *i.e.*, phlogopite; 4–5% $TiO_2$) and are heterogeneous on the scale of a thin section. In most samples, there is no distinct correlation between Fe/(Fe + Mg) and $TiO_2$ content of the biotite with its color, morphology, or location with respect to garnet in a single section. Recrystallized plagioclase in the matrix is generally sodic ($An_{10–21}$), and there is no significant compositional variation within individual samples except N130a ($An_{2–12}$). Sillimanite is either entirely enclosed within garnet porphyroclasts or defines curved trails of inclusions that are continuous with the thrust-related fabric in the matrix. Sillimanite prisms in the matrix are aligned parallel to the extension lineation. Locally, minor retrogression led to secondary growth of biotite, and to the recrystallization of perthitic feldspar into discrete albite and K-feldspar grains.

In mafic gneiss and granulite (N144 and N171) from the northern interior Parry Sound assemblage, garnet ($Alm_{58–63}Prp_{11–12}Grs_{20–21}Sps_{5–8}$), orthopyroxene, amphibole, clinopyroxene, and plagioclase form porphyroclasts in a fine-grained matrix of plagioclase ($An_{23–27}$), quartz, amphibole (ferropargasite), orthopyroxene, clinopyroxene, biotite, and ilmenite. In strongly deformed samples, hornblende, plagioclase, and orthopyroxene porphyroclasts are recrystallized to finer-grained equivalents along their margins. The alignment of orthopyroxene, clinopyroxene, amphibole, and biotite crystals within the main foliation documents the synmetamorphic nature of the thrust-related fabric. Late alteration is restricted to minor growth of late amphibole around pyroxene, late biotite around and within the cleavage planes of hornblende, and titanite around ilmenite.

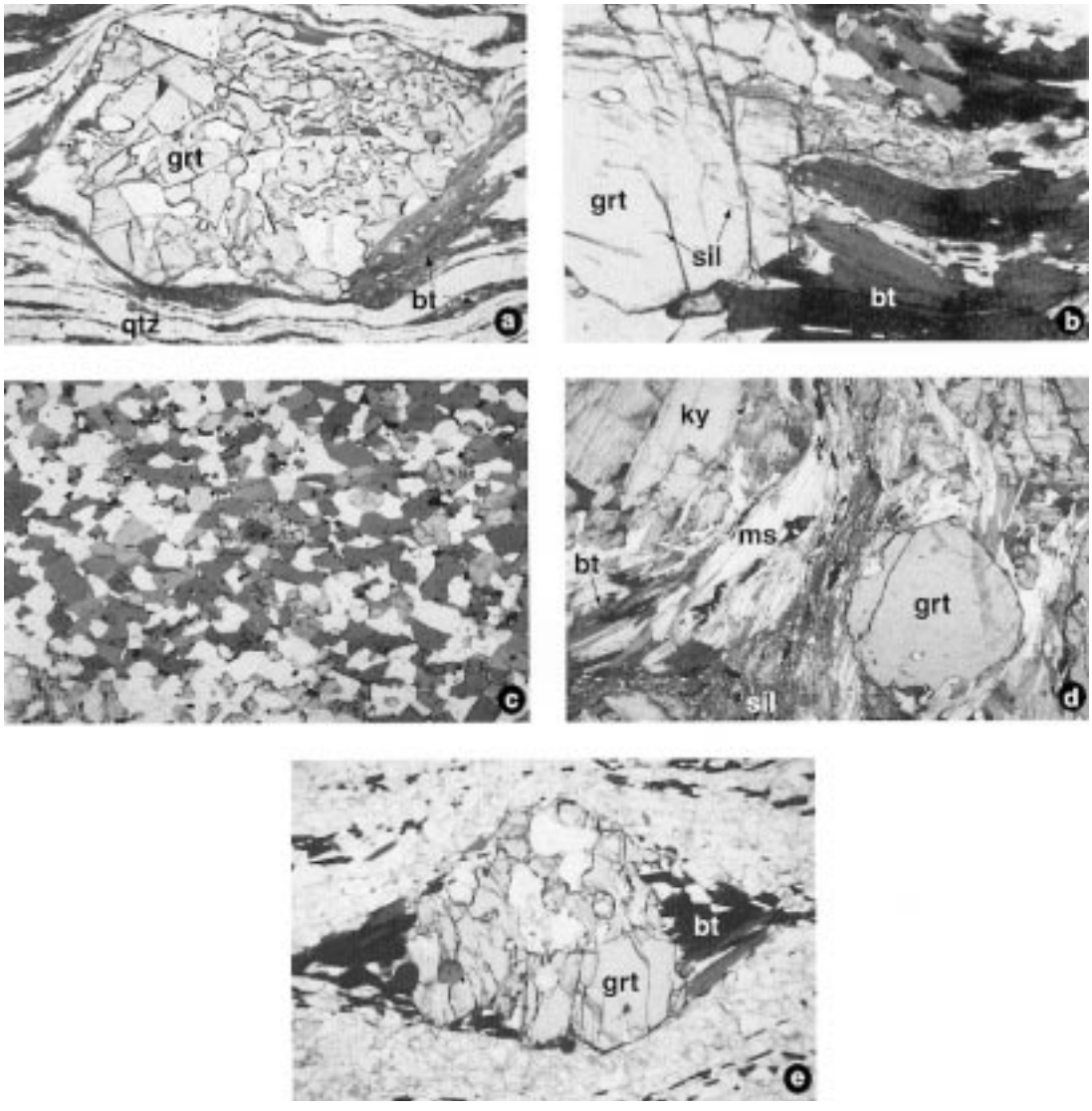


FIG. 6. Typical metamorphic textures in Parry Sound domain rocks. Numbers in square brackets indicate width of field of view. (a) Porphyroclastic texture in pelitic granulite (N130a), interior Parry Sound assemblage. Highly embayed garnet porphyroclast wrapped by mylonitic foliation defined by fine-grained biotite and ribbon quartz [5 mm]. (b) Garnet porphyroclast in a Group-I pelitic gneiss (N76b) with slightly curved trails of inclusion of sillimanite that pass continuously into the matrix foliation, upper part of the basal Parry Sound assemblage. Note resorption embayments filled with mostly biotite and some quartz [2 mm]. (c) Well-equilibrated, granoblastic texture in granulite-facies mafic dyke (N153c) containing plagioclase, orthopyroxene, hornblende, and garnet, lower part of the basal Parry Sound assemblage [7 mm]. (d) Strongly retrograded and coarsely recrystallized Group-II pelitic schist containing biotite, sillimanite, garnet, muscovite, and relict kyanite, lower part of the basal Parry Sound assemblage [2.5 mm]. (e) Embayed garnet porphyroclast in pelitic gneiss (N205a) with coarse feldspar and biotite inclusions, Twelve Mile Bay assemblage. Note pressure shadows filled with biotite and quartz [5 mm]. See text for further details.

Overall, the textural relationships outlined above for the pelitic and mafic rocks from the northern interior Parry Sound assemblage suggest that thrust-related deformation occurred under granulite-facies conditions (Table 1), which caused recrystallization of pre-existing assemblages without retrogression. Both rock types also show evidence for minor, late-stage retrogression. In some cases, retrogression of the granulite-facies rocks can be related to the emplacement of late pegmatitic dykes, as indicated by the presence of retrograde haloes adjacent to the dykes.

Rocks exposed in the southern interior Parry Sound assemblage are characterized by upper-amphibolite-facies assemblages (Fig. 5b) and are texturally distinct from rocks in the northern part of the assemblage (Table 1). In the study area, evidence for the retrograded nature of the amphibolite-facies assemblages includes (1) the presence of numerous patches of granulite-facies rocks scattered throughout the predominantly grey to black gneisses, (2) relict clinopyroxene and orthopyroxene grains rimmed by biotite ± hornblende, and (3) the presence of epidote and titanite. Field relationships indicate that extensive hydration and re-equilibration of the granulites occurred in response to fluid infiltration along the boundary of the Parry Sound and Moon River domains (Culshaw *et al.* 1997). In sample N192a, compositionally homogeneous garnet ($Alm_{64}Prp_{8}Grs_{23}Sps_{5}$) forms strikingly poikiloblastic grains, with inclusions of quartz, plagioclase, and amphibole. Amphibole (ferropargasite) and plagioclase ($An_{28}$) also occur as recrystallized grains in the matrix.

Rocks from the *upper part of the basal Parry Sound assemblage* contain mostly upper-amphibolite-facies assemblages (Table 1, Fig. 5a). However, previous petrological, compositional, and thermobarometric studies from the garnet amphibolite unit (Fig. 2a) provide evidence for an earlier granulite-facies metamorphism (Hicks 1992). Garnet amphibolites contain the assemblage Hbl + Pl + quartzofeldspathic pods ± Grt ± Cpx ± Grt ± Bt ± Ttn, whereas pelitic rocks are characterized by Grt + Ky + Sil + Kfs + Pl + Qtz + Bt + quartzofeldspathic pods ± Ilm ± Rt assemblages. The Whitestone anorthosite contains Pl + Hbl ± Grt ± Bt ± Cpx ± Ilm ± Ttn ± Scp assemblages.

Pelitic rocks from the upper part of the basal Parry Sound assemblage are texturally distinct from those from the lower part of the assemblage (Table 1) and are here referred to as *Group-I* pelitic gneisses. In these gneisses (N75c and N76b), large garnet porphyroclasts ($Alm_{70–73}Prp_{19–24}Grs_{4–5}Sps_{2–3}$) contain fine-grained inclusions in their core, and fewer but very coarse-grained inclusions in their rim. A second generation of smaller, inclusion-poor, idioblastic garnet crystals is common in the matrix. Biotite is found both as laths that define the matrix foliation ($0.52 < X_{Fe} < 0.54$; 3.5–4.0% $TiO_2$) and as coarse grains together with quartz and kyanite in the pressure shadows and resorption embayments around garnet porphyroclasts (Fig. 6b). Plagioclase occurs as granoblastic to xenoblastic matrix grains ($An_{26}$), and locally forms a thin moat around garnet. Kyanite occurs as corroded porphyroclasts aligned parallel to the main matrix foliation, whereas sillimanite defines inclusion trails in the rim of garnet that pass continuously into the matrix foliation (Fig. 6b). As indicated by its highly embayed morphology, kyanite probably ceased crystallizing prior to sillimanite.

Garnet amphibolite (N74c), spatially associated with Group-I pelitic gneiss, contains garnet ($Alm_{52}Prp_{16}Grs_{27}Sps_{5}$) typically rimmed by plagioclase coronas. The composition of the matrix plagioclase ($An_{48}$) is uniform at the thin-section scale. Clinopyroxene occurs as xenoblastic porphyroclasts, as inclusions in garnet, and as a matrix phase ($Wo_{45}En_{35}Fs_{15}$). Amphibole (magnesiopargasite) variably replaces clinopyroxene. These textural features suggest that the plagioclase – hornblende assemblage may be the consequence of the decompression–hydration reaction:

$$Pl + Hbl = Grt + Cpx + H_2O \quad (1)$$

(Hicks 1992). For consistency, all reactions are written with the higher-T assemblage on the right-hand side of the equation.

In the *lower part of the basal Parry Sound assemblage*, granulite-facies assemblages are well preserved only in the core of the mildly deformed Parry Island anorthosite and its cross-cutting mafic dykes (Table 1, Figs. 5a, 6c). Mafic dykes (N153c) contain texturally well-equilibrated orthopyroxene ($En_{61}Fs_{34}$), amphibole (magnesiopargasite), plagioclase ($An_{53}$), and garnet ($Alm_{51}Prp_{26}Grs_{20}Sps_{3}$). Peak-grade assemblages in the anorthosite are characterized by secondary orthopyroxene, clinopyroxene, hornblende ± garnet coronas around relict igneous orthopyroxene. Locally, the orogen-parallel, NE-plunging lineation in the anorthosite is defined by the alignment of orthopyroxene crystals. Toward the margin of the anorthosite body, the mafic dykes and the fabric in the anorthosite are transposed into parallelism. Anorthosite is mostly characterized by upper-amphibolite-facies Pl + Hbl ± Scp ± Cpx ± Grt ± Qtz ± Bt ± Ttn ± Cc assemblages that developed synkinematically. Pervasive, thrust-related deformation transformed the mafic dykes within the margin of the anorthosite and within the host rocks to amphibolites (Hbl + Pl ± Grt ± Cpx ± Qtz ± Bt ± Ttn). Similarly, the para- and orthogneisses flanking the anorthosite show penetratively overprinted fabrics and upper-amphibolite-facies assemblages (Fig. 5a). Pelitic gneisses are characterized by Grt + Bt + Qtz + Pl + Kfs + Ky + quartzofeldspathic pods ± Sil ± Rt ± Ilm assemblages, whereas tonalitic and granitic gneisses contain Bt + Pl + Qtz + quartzofeldspathic pods ± Kfs ± Grt ± Hbl ± Cpx ± Ttn assemblages. Rare occurrences of relict metamorphic orthopyroxene in the strongly deformed

orthogneisses suggest that the flanking gneisses share the same metamorphic history as the Parry Island anorthosite and mafic dykes. These features combine to indicate that (1) rocks in the lower part of the basal Parry Sound assemblage underwent an earlier granulite-facies metamorphism during orogen-parallel deformation, (2) growth of the upper-amphibolite-facies minerals was synchronous with thrust-related deformation, and (3) the upper-amphibolite-facies para- and orthogneisses were formerly granulite-facies rocks.

Locally, pelitic rocks from the lower part of the basal Parry Sound assemblage contain lower-amphibolite-facies assemblages. Here referred to as *Group-II* pelitic schists (N59, N73, and N138), these coarsely recrystallized rocks occur directly east of the Parry Island anorthosite (Fig. 5a). In this area, the highest-grade minerals (garnet, K-feldspar, and kyanite) are typically corroded and altered, and the new assemblage comprises garnet, plagioclase, sillimanite, staurolite, and muscovite (Fig. 6d). Locally, garnet porphyroblasts are partially rimmed by intergrowths of sillimanite and biotite. The presence of a staurolite rim around kyanite suggests the following low-temperature reaction:

$$St + Ms + Qtz = Alm + Ky + Bt + H_2O \quad (2)$$

These relationships suggest that the lower-amphibolite-facies assemblages are retrograde and formed at the expense of the upper-amphibolite-facies assemblages. In a manner analogous to pressure shadows with retrograde assemblages adjacent to porphyroblasts, the restriction of the retrograde lower-amphibolite-facies assemblages to a low-strain area adjacent to the Parry Island anorthosite suggests an origin related to a "mega-pressure-shadow" effect (Wodicka 1994). The Parry Island anorthosite is considered to have behaved as a rigid body during penetrative thrust-related deformation. Group-II rocks in the strain shadow of the anorthosite would have been shielded from maximum compressive stress by their proximity to the rigid anorthosite. Retrogression and coarse recrystallization of these rocks were most likely contemporaneous with both thrust deformation and the related upper-amphibolite-facies metamorphic overprint in the gneisses flanking the anorthosite.

The matrix foliation in Group-II pelitic schists is defined by biotite ($0.41 < X_{Fe} < 0.44$; 2–4% $TiO_2$), sillimanite, graphite, and locally kyanite. Plagioclase occurs either as a matrix phase ($An_{23–31}$) or as idioblastic porphyroblasts ($An_{33}$) that overgrow matrix crenulations. Sillimanite outlasted growth of kyanite, but is itself overprinted by muscovite in highly retrograded samples. Garnet forms several morphological populations. In samples N59 and N138, garnet ($Alm_{76–78}Prp_{14–15}Grs_6Sps_{2–3}$) occurs as porphyroblasts up to 2 cm in diameter with few to abundant inclusions in their cores that are either crystallographically oriented or define straight to curved trails of inclusions oriented at a high angle to the external foliation. In contrast, sample N73 contains a second generation of small (*ca.* 1 mm) and inclusion-free garnet grains ($Alm_{79}Prp_{14}Grs_3Sps_4$).

The *Twelve Mile Bay assemblage* is characterized by mostly upper-amphibolite-facies rocks (Fig. 5b). Pelitic gneisses (N205a) contain the assemblage Grt + Bt + Qtz + Pl + Kfs + Sil + quartzofeldspathic pods, with the notable absence of kyanite. Garnet ($Alm_{66}Prp_{26}Grs_5Sps_3$) either occurs as large, embayed poikiloblasts (Fig. 6e) or as smaller, subidioblastic, and inclusion-poor grains in the matrix. Garnet and feldspar porphyroclasts are wrapped by the matrix foliation defined by aligned prismatic to acicular sillimanite, biotite, and ribbon quartz. Compositions of the matrix biotite show a considerable variation in Fe/(Fe + Mg) ($0.40 < X_{Fe} < 0.48$). A correlation exists between a high ratio of garnet to biotite ($V_{garnet}/V_{biotite} > 1$) and a low Fe/(Fe + Mg) value in biotite.

Although most mafic rocks of the Twelve Mile Bay assemblage have been converted to amphibole, these rocks locally preserve granulite-facies assemblages (Table 1). Evidence for retrogression includes the presence of a hornblende ± biotite rim around pyroxene grains. The alignment of hornblende and biotite within the main foliation suggests that growth of these lower-temperature minerals was synchronous with deformation related to thrusting. Amphibolitic rocks (N204b) contain garnet porphyroblasts ($Alm_{53}Prp_{15}Grs_{28}Sps_4$), amphibole (ferropargasite), plagioclase ($An_{54}$) ± quartz ± biotite ± titanite. The textural features in the pelitic and mafic rocks of the Twelve Mile Bay assemblage combine to indicate upper-amphibolite-facies conditions during thrust-related deformation.

### *The Shawanaga domain*

In contrast to the Parry Sound domain, migmatitic upper-amphibolite-facies assemblages are characteristic of the Shawanaga domain (Figs. 5a, 7), although orthopyroxene is present in coronitic metagabbro and relict eclogite (Table 2). Pelitic gneiss (N7f, N31a, and N43b) from the structurally highest *Lighthouse assemblage* (Fig. 2a) contains the assemblage Grt + Ky + Kfs + Pl + Bt + quartzofeldspathic pods ± Rt ± Ilm (Table 2, Fig. 8a). Garnet ($Alm_{76–77}Prp_{13–16}Grs_{7–8}Sps_{2–3}$) forms fractured porphyroclasts with abundant, generally fine-grained inclusions in its cores that commonly define straight to weakly sigmoidal trails of inclusions oriented at a high angle to the matrix fabric. Rare inclusions in the rim are of similar size to the matrix. Plagioclase compositions are homogeneous within a given sample ($An_{28–32}$). The penetrative thrust fabric is defined by coarse quartz-aggregate ribbons, kyanite, and biotite ($0.44 < X_{Fe} < 0.46$; 3–4% $TiO_2$). These minerals are deformed around the garnet porphyroclasts. These features suggest that the high-pressure phases grew prior to or during thrust-related deformation. Leucosomes of

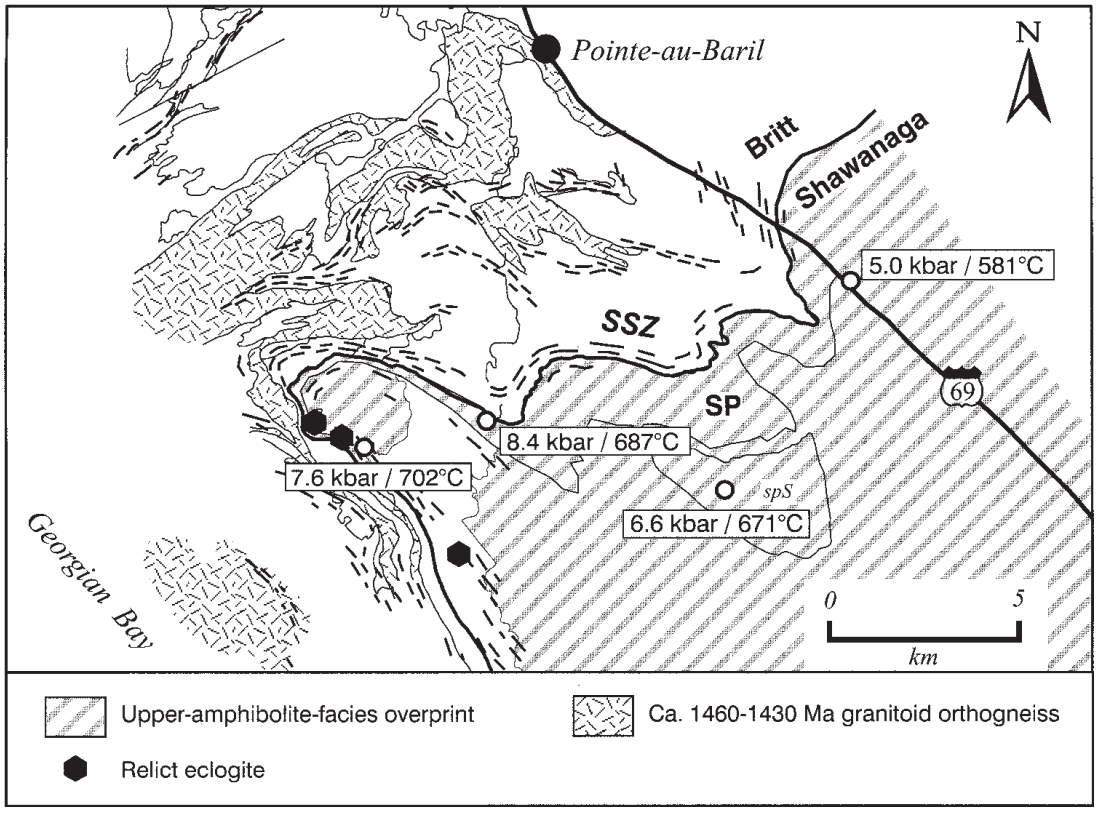


FIG. 7. Simplified geological map of the northern Shawanaga domain showing (1) the distribution of the amphibolite-facies domain and relict eclogite, and (2) P–T results across the study area. Abbreviations are as in Figure 3.

coarse-grained plagioclase + quartz + K-feldspar ± garnet are oriented parallel to the main foliation and are commonly rimmed by kyanite and biotite.

At the Parry Sound – Shawanaga contact (Figs. 2a, 4b), late extensional shearing transformed the pelitic gneisses and amphibolites of the Lighthouse assemblage into mylonites (Wodicka 1994). The pelitic mylonites (N1d, N71b, and N58a) differ from the gneisses by their finer grain-size, the presence of sillimanite, and lower modal proportions of biotite. The latter two features suggest relatively high-temperature conditions during mylonitization. Garnet, kyanite, and perthite occur as highly fractured and disaggregated (*i.e.*, kyanite) porphyroclasts in a mylonitic matrix consisting of recrystallized quartz, K-feldspar, plagioclase, sillimanite, biotite ($0.38 < X_{Fe} < 0.46$; 4–5% $TiO_2$), and rutile (Fig. 8b). Garnet is almandine–pyrope-rich ($Alm_{67–73}Prp_{21–28}Grs_5Sps_1$) with significant zoning from core to rim (from $Alm_{67}Prp_{20}Grs_9Sps_1$ to $Alm_{77}Prp_{17}Grs_5Sps_1$) detected in one sample (N71b). Coarse inclusions of plagioclase in the core of the zoned garnet are less sodic ($An_{33}$) than matrix plagioclase ($An_{26–27}$). Both kyanite and sillimanite are also present as inclusions in the rim of garnet porphyroclasts, and sillimanite locally defines inclusion trails that are continuous with the matrix foliation. The restriction of sillimanite and of garnet rims with kyanite inclusions to the pelitic mylonites suggests that these phases grew during late extensional deformation. In some places, inclusion trails in garnet cores are abruptly truncated against kyanite, which itself contains inclusion trails oriented parallel to the matrix foliation. This suggests that kyanite formed after growth of garnet cores, possibly as a result of a continuous reaction of the type:

$$Bt + Ky + Qtz = Grt + Kfs + H_2O \quad (3)$$

Kyanite along garnet margins is deformed, suggesting operation of this reaction before or during extensional shear. Ketchum (1995) observed similar relationships in pelitic rocks within the Shawanaga shear zone.

Pelitic mylonites of the Lighthouse assemblage at the Parry Sound – Shawanaga contact lack retrograde muscovite, whereas most pelitic gneisses in the immediate

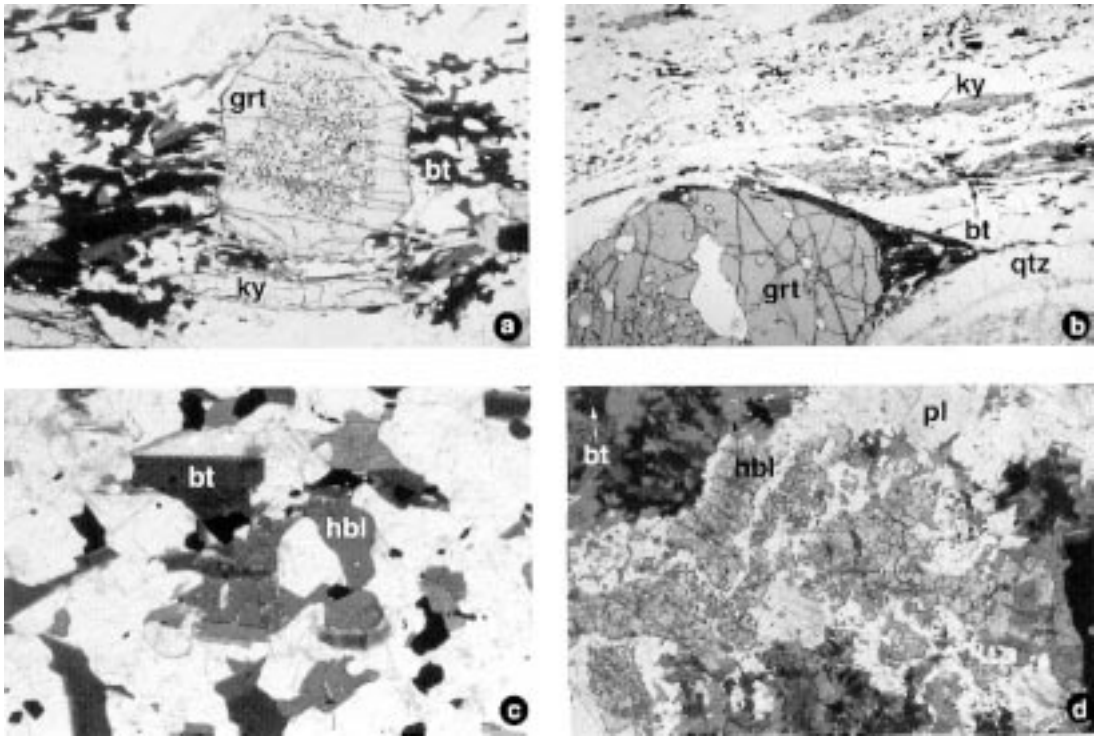


FIG. 8. Typical metamorphic textures in Shawanaga domain rocks. Numbers in square brackets indicate width of field of view. (a) Pelitic gneiss (N31a) containing garnet porphyroclast with inclusion-rich core mantled by an inclusion-free rim, Lighthouse assemblage. Note aligned kyanite in matrix [6.5 mm]. (b) Pelitic mylonite from the Parry Sound – Shawanaga contact with mylonitic foliation defined by aligned biotite, strongly disaggregated kyanite, and ribbon quartz, Lighthouse assemblage [6.5 mm]. Compare grain size and texture with those in Figure 8a. (c) Amphibole, biotite, and apatite in recrystallized, granoblastic quartzofeldspathic schist, Sand Bay assemblage [5.7 mm]. (d) Recrystallized aggregate of orthopyroxene, clinopyroxene, hornblende, and garnet in coronitic metagabbro (125), Ojibway assemblage [5.7 mm]. See text for further details.

footwall show evidence for minor retrogression of kyanite, garnet, and K-feldspar to muscovite. The coarse laths of muscovite locally form foliation "fish" with an extensional sense of shear. These features are consistent with juxtaposition of cooler basal Parry Sound hanging-wall rocks on hotter Lighthouse footwall rocks along an extensional shear zone.

Mylonitized garnet amphibolite (N1c) within the extensional shear zone contains garnet ($Alm_{58}Prp_{17}Grs_{21}Sps_4$), plagioclase, and hornblende porphyroclasts in a fine-grained mylonitic matrix consisting of recrystallized hornblende (ferropargasite) and plagioclase ($An_{34}$). Garnet porphyroclasts are highly resorbed and typically rimmed by a plagioclase corona.

Although strongly deformed by extensional shear fabrics, all lithologies of the *Sand Bay assemblage* (Fig. 3) show granoblastic polygonal textures, suggesting widespread recovery and postkinematic growth of the grains. With few exceptions, all units contain abundant leucosome hosting porphyroblasts of muscovite, magnetite, amphibole, and clinopyroxene. Paragneiss contains the assemblage Qtz + Kfs + Pl + Bt + Ms + Ep ± Hbl ± Ttn ± Chl ± Rt ± Ilm (Fig. 8c). Plagioclase ranges from fresh to strongly sericitized, with overgrowths of muscovite, calcite, and epidote. Other overgrowth relationships include muscovite on biotite, epidote on allanite, and titanite on ilmenite. In contrast to the Ojibway gneisses, muscovite and chlorite are ubiquitous in the Sand Bay gneisses. The differences in mineral assemblages and textures between the Ojibway and Sand Bay assemblages (Table 2) may be attributed to variations in composition of the bulk rocks or metamorphic fluid (or both).

In the *Ojibway assemblage* (Fig. 3), amphibolite (208b) contains the assemblage Hbl (magnesiopargasite) + Pl + Qtz + Bt ($X_{Fe}$ = 0.42; 4% $TiO_2$) ± Grt ± Ep. Garnet ($Alm_{54}Prp_{16}Grs_{22}Sps_8$) occurs as rare, embayed relics in a plagioclase-rich ($An_{49}$) matrix, sug-

gesting that garnet-consuming decompression reactions largely went to completion. In pelitic gneiss (D47a and 129b), garnet occurs as embayed porphyroblasts ($Alm_{73–79}Prp_{11–12}Grs_{4–5}Sps_{4–12}$) in a matrix of plagioclase ($An_{19–23}$), biotite ($0.55 < X_{Fe} < 0.60$; 4% $TiO_2$), kyanite, sillimanite, and quartz, suggesting that pressure-sensitive reactions of the type:

$$Pl = Grt + Al_2SiO_5 + Qtz \quad (4)$$

were responsible for garnet consumption. Muscovite is normally retrograde, but locally forms part of the equilibrium assemblage. Kyanite ranges from idioblastic prisms to strongly embayed relics. Sillimanite ranges from coarse-grained prisms to fibrolite, but mainly forms bundles of acicular grains aligned within the foliation. These textural relationships suggest that sillimanite crystallized after kyanite.

Metamorphic assemblages in coronitic metagabbro in the Ojibway assemblage and Shawanaga pluton record higher-grade conditions than those indicated by their host rocks (Table 2). Metastable preservation of early, high-grade assemblages in metabasite is common as reaction kinetics are relatively sluggish in these dry competent rocks (*e.g.*, Brodie & Rutter 1985, Indares 1993). Where undeformed or only mildly deformed, metagabbro (125) retains a subophitic texture and exhibits metamorphic coronas formed by reaction of primary olivine and Fe–Ti oxide with igneous plagioclase (Davidson & van Breemen 1988). Recrystallized domains contain the assemblage Grt ($Alm_{60}Prp_{15}Grs_{22}Sps_3$) + Hbl (magnesiopargasite) + Pl ($An_{30}$) + Cpx ($Wo_{42}En_{37}Fs_{18}$; 0.78% $Na_2O$) + Ilm + Bt ($X_{Fe} = 0.48$; 4% $TiO_2$) ± Opx (Fig. 8d). Where intensely recrystallized, coronitic metagabbro is reduced to fine-grained garnet amphibolite with vestiges of a subophitic texture.

A tectonic enclave of fine-grained, garnet–clinopyroxene-rich metabasite, hosted by straight gneiss of the Ojibway assemblage in the Shawanaga shear zone, contains a similar assemblage of minerals as found in the recrystallized coronitic metagabbro. The unfoliated core of this body, characterized by abundant clinopyroxene–plagioclase symplectite, is reduced to foliated amphibolite near the margins. Orthopyroxene is a relict matrix phase in symplectite. Reaction textures and mineral composition suggest that mafic bodies identical to this enclave throughout the Central Gneiss Belt are re-equilibrated relics of eclogite (Davidson 1990). Clinopyroxene–plagioclase symplectite is interpreted as the product of breakdown of omphacite during decompression from eclogite facies. Mineral assemblages in coronitic metagabbro and relict eclogite indicate eclogite-facies metamorphism in the Ojibway assemblage prior to initial re-equilibration in the granulite facies and final equilibration in the amphibolite facies (see also Needham 1992).

*Summary and interpretation*

The mineral assemblages presented above, together with evidence for partial melting (*i.e.*, quartzofeldspathic pods), place first-order constraints on the P–T conditions during thermal peak metamorphism and subsequent overprinting events in the Parry Sound and Shawanaga domains. In the interior Parry Sound assemblage, the presence of orthopyroxene in pelitic granulites (Table 1) suggests that temperature conditions were above the lower-T limit of the dehydration-melting reaction:

$$Bt + Qtz \pm Pl = Opx + Kfs + L \quad (5)$$

For typical pelitic rocks, this reaction is crossed at 800°C (*e.g.*, Spear 1993). The local occurrence of the peak assemblage Opx–Sil–Qtz in these granulites (Table 1; Davidson *et al.* 1990) constrains pressures to more than about 9 kbar at 800°C (*e.g.*, Carrington 1995, Aranovich & Berman 1996).

Rocks from the upper part of the basal Parry Sound assemblage are extensively retrograded to upper-amphibolite-facies assemblages (Fig. 5a). Textural features within Group-I pelitic gneisses (see above) are consistent with a P–T path that evolved from the stability field of sillimanite, then toward and probably across the Ky–Sil boundary, and back into the stability field of sillimanite. The coexistence of these aluminosilicates with K-feldspar indicates temperature conditions above the dehydration melting of muscovite according to the reaction:

$$Ms + Qtz \pm Pl = Ky \text{ or } Sil + Kfs + L \quad (6)$$

In addition, the presence of leucosomes with garnet in these gneisses indicates that the reaction:

$$Bt + Ky \text{ or } Sil + Qtz \pm Pl = Kfs + Grt + L \quad (7)$$

also occurred. For plagioclase-bearing pelitic rocks, reactions (6) and (7) occur at 680–740°C and *ca.* 750°C (for pressures between 6 and 10 kbar), respectively (LeBreton & Thompson 1988, Vielzeuf & Holloway 1988). The absence of orthopyroxene implies temperatures less than about 800°C.

In the lower part of the basal Parry Sound assemblage, there is evidence for an early granulite-facies metamorphic event that led to formation of the assemblage Opx + Hbl + Pl ± Grt ± Cpx (Table 1). The absence of leucosomes in the granulite-facies mafic dykes suggests peak metamorphic temperatures below 730–900°C (*e.g.*, Pattison 1991, Wolf & Wyllie 1994). The presence of (±coronitic) garnet in these granulites suggests relatively high-P conditions, probably in excess of 5 kbar (Beard & Lofgren 1991, Rushmer 1991).

Along the margins of, and adjacent to, the Parry Island anorthosite, the granulite-facies assemblages were

extensively overprinted by upper- to lower-amphibolite-facies assemblages (Fig. 5a). The coexistence of kyanite ± sillimanite and K-feldspar in the flanking upper-amphibolite-facies pelitic gneisses indicates that metamorphic temperatures exceeded those required for the dehydration-melting reaction (6) (*i.e.*, >680–740°C between 6 and 10 kbar). In the lower-amphibolite-facies pelitic schists (Group II) east of the Parry Island anorthosite, growth of sillimanite and biotite at the expense of garnet may be the result of back-reaction of the subsolidus equilibrium (3) (but with sillimanite as a product) or of the partial melting reaction (7).

In the Twelve Mile Bay assemblage, retrograde upper-amphibolite-facies assemblages dominate (Fig. 5b). The assemblage Grt + Bt + Sil + Qtz + Pl + Kfs + quartzofeldspathic pods in pelitic gneisses suggests the divariant dehydration-melting reaction (7), implying temperatures above *ca.* 750°C. The absence of kyanite provides an upper-P limit of *ca.* 8–10 kbar.

In the Shawanaga domain, migmatized pelitic rocks provide some constraints on the P–T conditions during upper-amphibolite-facies metamorphism. In pelitic gneisses of the Lighthouse assemblage (Fig. 2a), the occurrence of biotite and kyanite in melanosomes surrounding leucosomes suggests the partial melting reaction (7), implying temperatures of ≥750°C. The presence of kyanite places a lower-P limit of *ca.* 8–10 kbar. Textural features within the pelitic gneisses suggest that these P–T conditions were reached during thrust-related deformation. Furthermore, the presence of sillimanite in pelitic mylonites at the Parry Sound – Shawanaga contact indicates that P–T conditions in the Lighthouse assemblage entered the stability field of sillimanite during extensional shearing.

In the Ojibway assemblage, local persistence of texturally stable muscovite in kyanite–sillimanite-bearing pelitic gneisses suggests that the dehydration-melting reaction (6) did not go to completion. As noted above, this reaction implies temperatures of *ca.* 680–740°C between 6 and 10 kbar. Furthermore, textural features within these gneisses suggest that $Al_2SiO_5$ growth history was similar to that in pelitic rocks of the Lighthouse assemblage, implying a P–T path that progressed from the stability field of kyanite toward that of sillimanite.

## P–T Estimates

Twenty-seven samples of pelitic and mafic gneiss, garnet amphibolite, and coronitic metagabbro with granulite- or amphibolite-facies mineral assemblages appropriate for thermobarometric work were selected from the Parry Sound and Shawanaga domains for analysis. Sample sites (Figs. 2, 3) were chosen in order to determine the P–T conditions of the thermal peak of metamorphism and subsequent overprinting events and (2) constrain possible P–T paths for the Parry Sound and Shawanaga domains. The mineral compositions used for P–T estimates (Appendix I) are based on results of 8 to 93 electron-microprobe analyses per sample. In each polished thin section, compositional data were collected from two or more microdomains to check for consistency of mineral compositions. Where a given mineral composition was consistent within a sample, the data were averaged to yield a representative composition for use in thermobarometry. Where chemical heterogeneity was detected, averaged compositions from texturally well-equilibrated subdomains or results of individual analyses were used. Core-inclusion and rim compositions from strongly zoned minerals (*e.g.*, sample N71b) were treated separately. To minimize the potential effects of retrograde Fe–Mg exchange, all analyzed ferromagnesian minerals were separated by a neutral phase (*e.g.*, quartz, feldspar).

### *Approach*

All P–T estimates were calculated with the TWQ software program of Berman (1991) using an internally consistent thermodynamic dataset for end members and solution properties. Activities of end-member mineral components were calculated using the models of Berman (1990) for garnet, Aranovich (1991) for plagioclase, McMullin *et al.* (1991) for biotite, Newton (1983) for pyroxenes, and Mäder *et al.* (1994) for amphibole. The Aranovich (1991) solution model for plagioclase was favored over the widely used Fuhrman & Lindsley (1988) model for the following reasons: (1) for those samples that contain plagioclase with An content <20%, pressures estimated using the Fuhrman & Lindsley (1988) model were 3–4 kbar higher than those calculated using the Aranovich (1991) solution model, and P–T estimates fell in the kyanite stability field, which is not consistent with the observed assemblage of minerals, and (2) for those samples with An content >20%, good agreement (pressure differences ≤0.5 kbar) was obtained using either model. Unless stated otherwise, all other minerals were treated as pure phases.

TABLE 3. SELECTED EQUILIBRIA USED IN TWQ ANALYSIS OF PELITIC (1 to 5) AND MAFIC (4 to 11) SAMPLES

1. Alm + Phl = Prp + Ann
2. Alm + 3 Rt = Ky/Sil + 2 Qtz + 3 Ilm
3. 2 Ky/Sil + Qtz + Grs = 3 An
4. 3 Qtz + Grs + 2 Alm = 3 An + 6 Fsl
5. 3 En + 2 Alm = 3 Fsl + 2 Prp
6. Grs + 2 Prp + 3 Qtz = 6 En + 3 An
7. 3 Tr + 5 Alm = 5 Prp + 3 Ftr
8. 4 Grs + 2 Prp + 12 Qtz + 3 Ts = 3 Tr + 12 An
9. 2 Grs + Prp + 18 Qtz + 3 Prg = 3 Tr + 6 An + 3 Ab
10. Alm + 3 Di = Prp + 3 Hd
11. Alm + 2 Grs + 3 Qtz = 3 Hd + 3 An

All abbreviations are after Kretz (1983).

TABLE 4. P-T RESULTS AND ASSEMBLAGES USED IN TWQ ANALYSIS

| Sample No. | Assemblage | P (kbar) | SD (kbar)† | T (°C) | SD (°C)† |
|---|---|---|---|---|---|
| | **PARRY SOUND DOMAIN** | | | | |
| ***Northern interior Parry Sound assemblage*** | | | | | |
| N122b | Grt-Pl-Bt-Sil-Qtz-[Kfs] | 11.8* | 0.00 | 873* | 0 |
| N125b | Grt-Pl-Bt-Sil-Qtz-[Kfs] | 10.9* | 0.00 | 757* | 0 |
| N130a | Grt-Pl-Bt-Sil-Qtz-[Kfs] | 10.1* | 0.00 | 869* | 0 |
| N131a | Grt-Pl-Bt-Sil-Opx-Qtz-[Kfs-Rt-Ilm] | 7.6 | 0.40 | 729 | 27 |
| N144 | Grt-Pl-Hbl-Qtz | 13.3 | 0.73 | 976 | 5 |
| N171 | Grt-Pl-Hbl-Qtz-[Opx] | 12.7 | 0.49 | 883 | 3 |
| ***Southern interior Parry Sound assemblage*** | | | | | |
| N192a | Grt-Pl-Hbl-Qtz | 14.9 | 0.70 | 1008 | 5 |
| ***Upper part of basal Parry Sound assemblage*** | | | | | |
| *Group-I* | | | | | |
| N75c | Grt-Pl-Bt-Ky-Sil-Rt-Ilm-Qtz-[Kfs] | 7.9 | 0.92 | 868 | 5 |
| N76b | Grt-Pl-Bt-Ky-Sil-Rt-Ilm-Qtz-[Kfs] | 7.1 | 0.14 | 777 | 1 |
| N74c | Grt-Pl-Cpx-Hbl-Qtz | 8.5 | 0.66 | 725 | 36 |
| ***Lower part of basal Parry Sound assemblage*** | | | | | |
| N153c | Grt-Pl-Opx-Hbl-Qtz | 7.2 | 0.15 | 656 | 14 |
| *Group-II* | | | | | |
| N59 | Grt-Pl-Bt-Sil-Rt-Ilm-Qtz-[Kfs-St] | 5.5 | 0.67 | 615 | 3 |
| N73 | Grt-Pl-Bt-Sil-Rt-Ilm-Qtz-[Kfs-Ms] | 5.2 | 1.74 | 653 | 10 |
| N138 | Grt-Pl-Bt-Ky-Sil-Rt-Ilm-Qtz-[Kfs] | 6.5 | 0.51 | 691 | 3 |
| ***Twelve Mile Bay assemblage*** | | | | | |
| N205a | Grt-Pl-Bt-Sil-Rt-Ilm-Qtz-[Kfs] | 7.2 | 1.36 | 824 | 8 |
| N204b | Grt-Pl-Hbl-Qtz | 12.8 | 0.14 | 943 | 0.8 |
| | **SHAWANAGA DOMAIN** | | | | |
| ***Lighthouse assemblage*** | | | | | |
| N7f | Grt-Pl-Bt-Ky-Rt-Ilm-Qtz-[Kfs] | 7.1 | 0.53 | 702 | 3 |
| N31a | Grt-Pl-Bt-Ky-Rt-Ilm-Qtz-[Kfs] | 7.1 | 0.74 | 702 | 4 |
| N43b | Grt-Pl-Bt-Ky-Rt-Ilm-Qtz | 7.0 | 0.82 | 726 | 4 |
| N1d | Grt-Pl-Bt-Ky-Sil-Rt-Ilm-Qtz-[Kfs] | 5.7 | 0.68 | 687 | 4 |
| N58a | Grt-Pl-Bt-Ky-Sil-Rt-Ilm-Qtz-[Kfs] | 5.6 | 0.23 | 660 | 1 |
| N71b (core) | Grt-Pl-Bt-Ky-Sil-Qtz-[Kfs] | 10.9* | 0.00 | 831* | 0 |
| N71b (rim) | Grt-Pl-Bt-Ky-Sil-Rt-Ilm-Qtz-[Kfs] | 6.3 | 0.18 | 687 | 1 |
| N1c | Grt-Pl-Hbl-Qtz | 10.6 | 0.89 | 832 | 6 |
| ***Ojibway assemblage*** | | | | | |
| D47a | Grt-Pl-Bt-Ky-Sil-Rt-Ilm-Qtz-[Kfs] | 6.6 | 0.48 | 671 | 3 |
| 129b | Grt-Pl-Bt-Ky-Sil-Rt-Ilm-Qtz-[Kfs] | 5.0 | 0.48 | 581 | 3 |
| 125 | Grt-Pl-Cpx-Hbl-Qtz-[Bt] | 8.4 | 0.29 | 687 | 1 |
| 208b | Grt-Pl-Hbl-Qtz-[Bt] | 7.6 | 0.50 | 702 | 3 |

†The 1.0 sigma standard deviation (SD) calculated with the INTERSX program (Berman 1991). *P-T estimate based on only two independent reactions. [...] indicates minerals present but not used for P-T estimates. Abbreviations are as in Table 2.

For all samples, P–T estimates were computed from subsets of the most robust linearly independent equilibria for pelitic and mafic rocks (Table 3; *e.g.*, Mäder *et al.* 1994). The thermobarometric results and assemblages used in TWQ analysis are listed in Table 4. The P–T results are also presented graphically in Figures 9 and 10. We adopted a conservative uncertainty of ±1 kbar and ±50°C for our results, which probably closely reflects the maximum P–T uncertainty (*e.g.*, Essene 1989). We also report the standard deviations of the P–T intersections as calculated by Berman's (1991) INTERSX program (Table 4). These error bars allow an assessment of the overall consistency of the results, but do not represent statistically valid uncertainties in P–T, as they do not include errors in the electron-microprobe data, thermodynamic properties or solution models. The P–T estimates quoted below have been rounded to the nearest 5°C and 0.5 kbar.

*The Parry Sound domain*

The highest P–T estimates from the Parry Sound domain were obtained from interior Parry Sound assemblage rocks (Figs. 5, 9, Table 4). The mafic gneiss and granulite samples (N144 and N171) from the northern part of the assemblage (Fig. 2a) yielded P–T estimates of 12.5–13.0 kbar and 885–975°C, and plot within error of the stability field of the appropriate aluminosilicate (Fig. 9). We interpret these results as representing peak or near-peak granulite-facies conditions in the interior Parry Sound assemblage. These high pressures and temperatures are consistent with the presence of Opx + Sil + Qtz in nearby pelites and of Spr + Qtz in pelitic granulites to the northeast of the study area (Davidson *et al.* 1990). Sillimanite-bearing pelitic granulites (N122b, N125b, and N130a) from the northern part of the interior Parry Sound assemblage gave somewhat lower P–

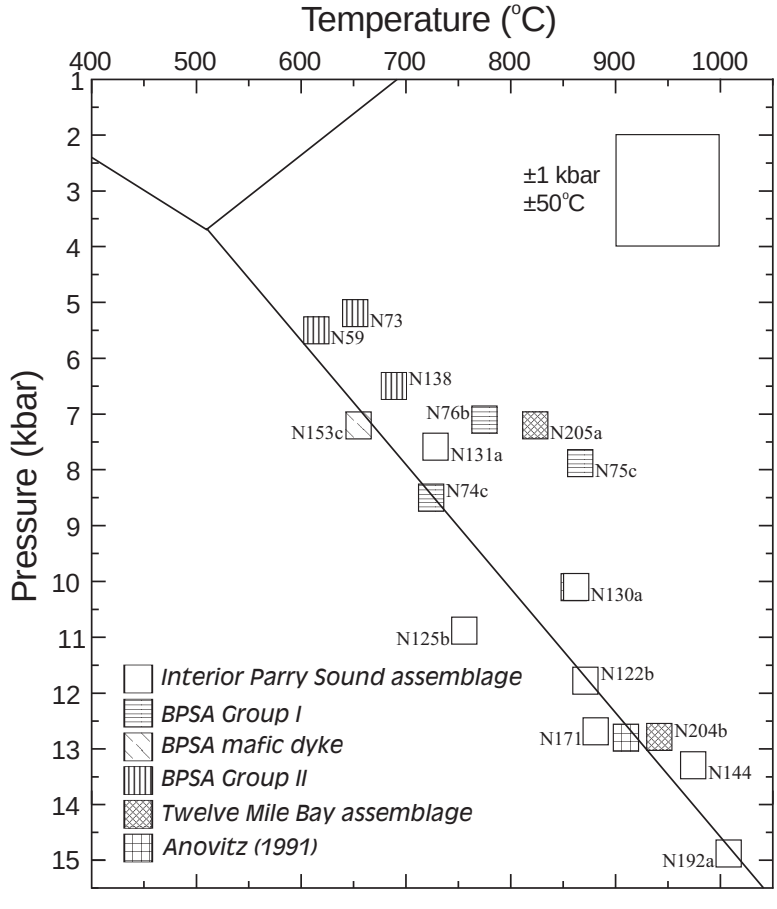


FIG. 9. P–T data for the Parry Sound domain. P–T estimates for individual samples are based on the reactions and mineral assemblages given in Tables 3 and 4, respectively. Error boxes are shown at ±0.25 kbar and ±12.5°C for clarity. BPSA: basal Parry Sound assemblage. See text for further details.

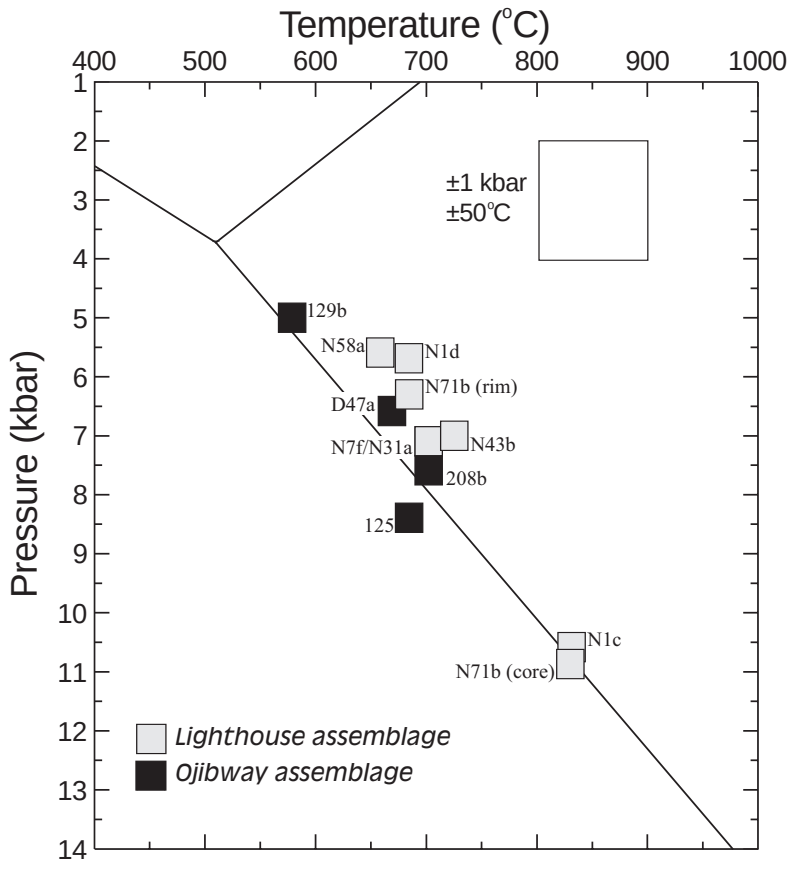


FIG. 10. P–T data for the Shawanaga domain. For details, see text and caption to Figure 9.

T estimates than the mafic rocks, in the range 10–12 kbar and 760–875°C. Since none of these samples contains rutile in equilibrium with ilmenite, these P–T determinations are based on only two independent equilibria involving garnet – plagioclase – biotite – sillimanite – quartz (Table 4). With the exception of N125b, the estimates plot within or close to the stability field of sillimanite and are similar to previously determined P–T estimates for this area (Anovitz 1991; Fig. 9). For these reasons, two of the three results (*i.e.*, 10–12 kbar, 870–875°C) are regarded as reliable and may reflect partial re-equilibration. The orthopyroxene-bearing pelitic granulite N131a yielded the lowest P–T estimate, 7.5 kbar and 730°C, and may reflect re-equilibration at a later stage. Sample N192a, a garnet amphibolite from the retrograded area in the southern interior Parry Sound assemblage (Figs. 2b, 5b), gave the highest P–T estimate of 15 kbar and 1010°C. This estimate appears high for upper-amphibolite-facies metamorphism, but there are insufficient data from this area to determine the significance of this result.

In the upper part of the basal Parry Sound assemblage, Group-I pelitic gneisses (N75c and N76b) yielded P–T estimates of 7–8 kbar and 780–870°C (Figs. 5a, 9, Table 4). The partially hydrated garnet amphibolite (N74c) yielded a slightly higher P of 8.5 kbar and a lower T of 725°C. All three estimates straddle the Ky–Sil boundary or plot within the stability field of sillimanite, consistent with sillimanite outlasting kyanite in the pelitic gneiss samples. However, sample N75c records a temperature well above the dehydration melting reaction (5), inconsistent with the absence of orthopyroxene in this pelitic rock. Given the petrogenetic constraints outlined above, we suggest that the results from samples N74c and N76b may closely reflect the P–T conditions during the upper-amphibolite-facies overprinting event in this part of the basal Parry Sound assemblage.

In the lower part of the basal Parry Sound assemblage, the granulite-facies mafic dyke N153c (Fig. 2a) that cuts the Parry Island anorthosite yielded a P–T estimate of 7.0 kbar and 660°C (Fig. 9, Table 4). We interpret this P–T

result as recording peak or near-peak granulite-facies conditions during orogen-parallel deformation within the basal Parry Sound assemblage, although minor re-equilibration during cooling cannot be ruled out.

Group-II pelitic schists (N59, N73, and N138), located in the low-strain area east of the Parry Island anorthosite (Fig. 2a), yielded the lowest P–T estimates (Figs. 5a, 9, Table 4), consistent with the observation of lower-amphibolite-facies retrogression in this area. P–T determinations for these samples are in the range 5.0–6.5 kbar and 615–690°C. Although sample N73 shows a large degree of scatter in P (±1.7 kbar), it yielded a P–T estimate that falls within error of the other two samples (Table 4).

The sillimanite-bearing pelitic gneiss N205a from the Twelve Mile Bay assemblage yielded a P–T estimate of 7.0 kbar and 825°C, whereas the garnet amphibolite N204b gave a much higher P of 13.0 kbar and T of 940°C (Figs. 5b, 9, Table 4). Both results fall within the stability field of the appropriate aluminosilicate. However, the garnet amphibolite records a pressure and temperature well above the dehydration–melting reaction (7), inconsistent with the mineral assemblage observed in the pelitic gneiss (see above). It is thus possible that the garnet amphibolite escaped re-equilibration to upper-amphibolite-facies conditions and records P–T conditions during granulite-facies metamorphism. Thermobarometric data from this area are currently insufficient to test this hypothesis. In contrast, although the pelitic gneiss shows a large scatter in P (±1.4 kbar), its P–T estimate is consistent with mineral equilibria and may thus reflect the P–T conditions during the upper-amphibolite-facies overprinting event.

*The Shawanaga domain*

TWQ results for the pelitic gneisses and mylonites from the Lighthouse assemblage show remarkable intersample consistency (Figs. 5a, 10, Table 4), suggesting that local equilibrium was achieved in the immediate footwall to and at the Parry Sound – Shawanaga contact. P–T determinations for the kyanite-bearing pelitic gneiss samples (N7f, N31a, and N43b) are in the range 7.0 kbar and 700–725°C. All three points fall within the stability field of sillimanite, suggesting that the calculated pressures and temperatures represent minimum estimates of upper-amphibolite-facies conditions. Data from the pelitic mylonites (N1d and N58a), including matrix and rim compositions from sample N71b, yielded lower P–T estimates of 5.5–6.5 kbar and 660–690°C that may reflect ambient P–T conditions during extensional shearing along the Parry Sound – Shawanaga contact. In contrast, the garnet core – inclusion assemblage in the pelitic mylonite N71b and the mylonitized garnet amphibolite N1c yielded much higher P–T estimates, 10.5–11.0 kbar and 830°C (Fig. 10, Table 4). These two samples may thus record an earlier point on the P–T path for the Lighthouse assemblage rocks.

In the structurally lower Ojibway assemblage, the highest pressure estimate (8.5 kbar, 685°C; Figs. 7, 10, Table 4) was obtained from recrystallized domains within coronitic metagabbro (sample 125; Fig. 8d) in the Shawanaga pluton. The amphibolite sample 208b yielded a lower P of 7.5 kbar and a slightly higher T of 700°C. These P–T estimates suggest that peak conditions of metamorphism in the Ojibway assemblage may have reached at least 8.5–7.5 kbar and 700–685°C. Similar results were reported from the northern Shawanaga domain by Anovitz & Essene (1990) for coronitic metagabbro (<10.2 kbar, 700–710°C) and by Tuccillo *et al.* (1992) for garnet metagabbro and pelite (~7–9 kbar at 700°C). Pelitic gneisses yielded lower P–T estimates than the coronitic metagabbro and amphibolite, consistent with the greater resistance of mafic rocks to fluid influx and retrograde reaction (*e.g.*, Brodie & Rutter 1985). The pelitic gneiss sample D47a, collected from the large exposure of supracrustal rock (Fig. 3), yielded an estimate of 6.5 kbar and 670°C, whereas the pelitic gneiss enclave 129b gave a lower P–T estimate, 5.0 kbar and 580°C (Figs. 7, 10, Table 4). Both results fall within error of the Ky–Sil univariant curve, consistent with the presence of both phases in these gneisses. We suggest that P–T estimates from the pelitic gneiss reflect partial re-equilibration during cooling.

## P–T–t Paths

Figure 11 shows possible P–T–t paths for Parry Sound and Shawanaga domain rocks. The paths were generated from P–T data from various samples that (1) shared a common metamorphic history and (2) were either sufficiently closely spaced or from the same structural level that significant differences in P–T–t history between outcrops are unlikely (*cf.* Jamieson *et al.* 1995). Furthermore, we assume that the P–T estimates used to construct the P–T–t paths reflect either conditions approaching the thermal peak or re-equilibration at a later stage. For these reasons, we believe it to be unlikely that the paths shown in Figure 11 represent metamorphic field-gradients. P–T–t paths could not be reconstructed for the basal Parry Sound or Twelve Mile Bay assemblages because of insufficient data.

*The Parry Sound domain*

P–T data from the interior Parry Sound assemblage lie on a P–T–t path suggesting initial near-isothermal decompression over the range 13–10 kbar and 950–870°C, followed by decompression (10→8 kbar) accompanied by more cooling (870 →730°C) (Fig. 11a). The higher-P segment of the P–T–t path resembles that proposed by Anovitz (1991), whereas the lower-P segment has a much steeper slope than the one obtained by

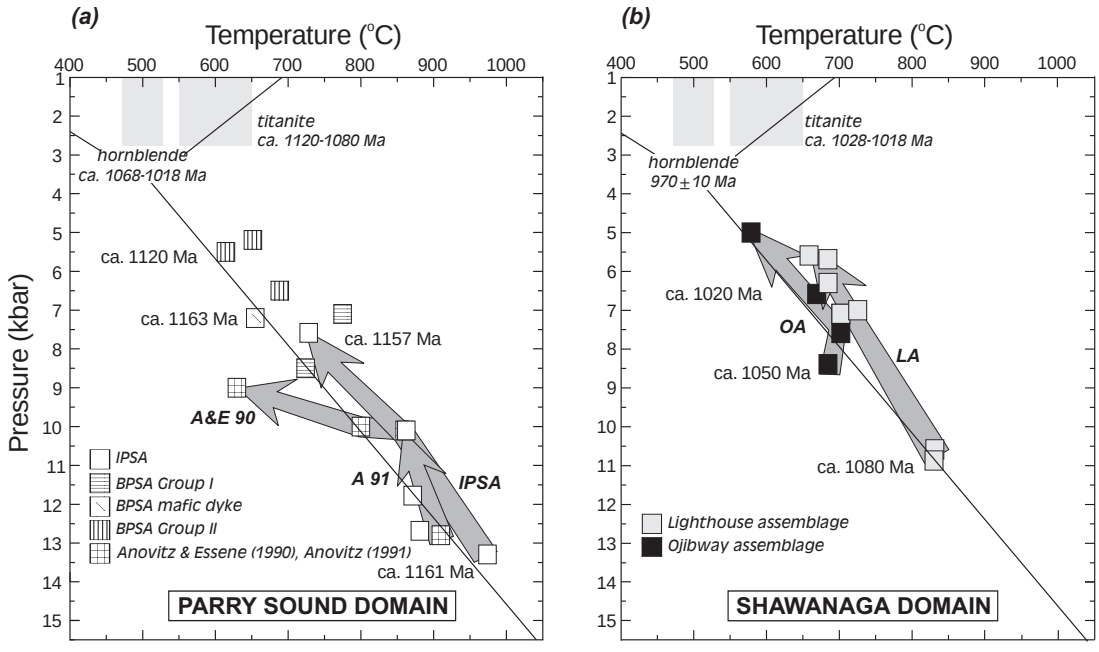


FIG. 11. Possible P–T–t paths for the (a) Parry Sound domain and (b) Shawanaga domain. Sample numbers and P–T estimates regarded as unreliable (see text) are omitted for clarity. Paths "IPSA" (interior Parry Sound assemblage), "LA" (Lighthouse assemblage), and "OA" (Ojibway assemblage) are based on our data, whereas paths "A&E 90" and "A 91" are after Anovitz & Essene (1990) and Anovitz (1991), respectively. Also shown are U–Pb and $^{40}Ar/^{39}Ar$ dates for high-grade metamorphism, extensional deformation, and cooling in the Parry Sound and Shawanaga domains (van Breemen *et al.* 1986, Davidson & van Breemen 1988, Culshaw *et al.* 1991, Tuccillo *et al.* 1992, Heaman & LeCheminant 1993, Wodicka 1994, Ketchum 1995, Krogh 1997, Ketchum *et al.* 1998) and the generally accepted ranges of closure temperatures for the U–Pb system in titanite (Heaman & Parrish 1991) and for the $^{40}Ar/^{39}Ar$ system in hornblende (*e.g.*, Baldwin *et al.* 1990). As noted in text, not all titanite data can be interpreted as cooling dates, and the temperature shown may not be applicable in all cases. BPSA: basal Parry Sound assemblage.

Anovitz & Essene (1990). These investigators interpreted their P–T–t path to reflect a composite history involving a significant period of pre-peak unloading followed by isobaric cooling (Anovitz 1991). The isobaric cooling path was modeled by postulating a post–thrusting period of extension at or near the peak of metamorphism (Anovitz & Chase 1990). In contrast, our data suggest that the post-peak P–T–t evolution of interior Parry Sound assemblage rocks involved decompression and cooling which, as discussed below, can be attributed to thrusting.

The final part of the P–T–t path followed by interior Parry Sound assemblage granulites overlaps with P–T data from the upper part of the basal Parry Sound assemblage, when realistic uncertainties in P–T estimates are taken into account (Fig. 11a). Retrograde amphibolite-facies minerals in rocks from the upper part of the basal Parry Sound assemblage define the tectonic fabric associated with thrust-related deformation below the interior Parry Sound – basal Parry Sound contact (Fig. 4b). On the basis of these observations, we suggest that granulite-facies assemblages in this part of the basal Parry Sound assemblage were re-equilibrated to upper-amphibolite-facies conditions in response to overthrusting by interior Parry Sound assemblage rocks.

P–T data from Group-II pelitic schists from the lower part of the basal Parry Sound assemblage record the lowest pressures and temperatures from the Parry Sound domain (5.0–6.5 kbar, 615–690°C; Fig. 11a), and likely reflect conditions during the lower-amphibolite-facies metamorphic overprint. Textural evidence for an earlier, high-grade Ky–Kfs assemblage in these schists does not justify construction of a path that directly links these data with those from the granulite-facies mafic dyke N153c. Unfortunately, there are currently no thermobarometric data for the Ky–Kfs assemblage, but petrogenetic constraints suggest that Group-II pelitic schists likely reached $T \geq 680–740°C$ and $P \geq 8–10$ kbar (see above) following granulite-facies metamorphism at intermediate P and T (7.0 kbar and 660°C) and prior to re-equilibration to lower-amphibolite-facies conditions (5.0–6.5 kbar and 615–690°C).

*The Shawanaga domain*

Core and rim thermobarometric data from the pelitic mylonite N71b of the Lighthouse assemblage lie on a P–T–t path showing decompression (11→6.5 kbar) accompanied by cooling (830→685°C) (Fig. 11b). Several features suggest that the relative shape of this path in P–T space is correct: (1) P–T points from the other Lighthouse assemblage rocks within and adjacent to the Parry Sound – Shawanaga contact all fall along the same path defined by the core and rim P–T estimates, and (2) the path progresses from the kyanite field toward the stability field of sillimanite, consistent with the observed sequence of aluminosilicate polymorphs. However, given the magnitude of P–T uncertainties, the possibility that the Ky–Sil transition occurred at a lower P than that shown in Figure 11 cannot be ruled out.

Three of the four P–T points from the Ojibway assemblage lie on a P–T–t path suggesting decompression over the range 7.5–5.0 kbar and 700–580°C (Fig. 11b). A steeper P–T–t path segment is defined by linking these data with the fourth P–T point, coronitic metagabbro 125, which lies at a higher pressure (8.5 kbar). The initial part of the P–T–t path crosses from the kyanite field to the sillimanite field, consistent with mineral textures in Ojibway pelitic gneisses, which indicate sillimanite growth after kyanite. The middle part of the path overlaps with the final P–T–t path segment followed by Lighthouse assemblage rocks, suggesting that these rocks had, at least in part, a similar exhumation history as the Ojibway assemblage rocks. However, final equilibration in the Ojibway assemblage occurred at a lower P and T than in the Lighthouse assemblage (Fig. 11b).

In general, the P–T–t paths shown in Figure 11 for the interior Parry Sound, Lighthouse, and Ojibway assemblages closely resemble those previously determined by Wodicka (1994) and Ketchum (1995) for the same areas (see Culshaw *et al.* 1997). Minor differences, particularly in the location of the paths in P–T space, probably result from the use of (1) a different thermobarometric approach and (2) different solution-models for plagioclase. Wodicka (1994) and Ketchum (1995) generally used all possible equilibria (*i.e.*, the multi-equilibrium approach of Berman 1991) and the Fuhrman & Lindsley (1988) solution model to calculate P and T in the Parry Sound and Shawanaga domains, whereas in this paper we used only the most robust linearly independent equilibria and the Aranovich (1991) model. Our results tend to be up to 1.5 kbar lower for pelitic rocks and about 3 kbar higher for mafic rocks than those estimated by Wodicka (1994) and Ketchum (1995).

## Timing of Metamorphism, Deformation and Cooling

*The Parry Sound domain*

Geochronological data show that the granulite- and amphibolite-facies assemblages in the northern Parry Sound domain formed as a result of more than one metamorphic event (Fig. 4b). High-P – high-T granulite-facies metamorphism in the interior Parry Sound assemblage has been dated at 1161 ± 3 Ma (Fig. 11a; van Breemen *et al.* 1986). This metamorphism was approximately coeval with the upper-amphibolite-facies overprinting event in the upper part of the basal Parry Sound assemblage, which is constrained by a 1157 ± 3 Ma kyanite-bearing pegmatitic leucosome from a Group-I kyanite–sillimanite pelitic gneiss and by metamorphic zircon from a nearby garnet amphibolite, which yielded a slightly younger, minimum age of 1148 ± 6 Ma (Fig. 11a; Wodicka 1994). Tuccillo *et al.* (1992) obtained an identical $^{207}Pb/^{206}Pb$ age of 1157 ± 1 Ma on monazite from a metasedimentary rock lying at the same structural level as Group-I rocks. Thrust deformation along the interior Parry Sound – basal Parry Sound contact has been dated at *ca.* 1159 Ma (Fig. 4b; van Breemen *et al.* 1986), consistent with the suggestion that conversion of granulite-facies rocks to amphibolite within this part of the basal Parry Sound assemblage was a consequence of overthrusting by interior Parry Sound assemblage rocks (see above).

In the lower part of the basal Parry Sound assemblage, field relationships indicate that intermediate-P granulite-facies metamorphism was coeval with emplacement of the 1163 ± 3 Ma Parry Island anorthosite (Figs. 4b, 11a; Wodicka 1994). The lower-amphibolite-facies metamorphic overprint in this part of the basal Parry Sound assemblage appears to postdate both kyanite-grade metamorphism at higher structural levels and granulite-facies metamorphism in the basal Parry Sound assemblage by *ca.* 40 m.y. Monazite from a Group-II pelitic schist from the low-strain area east of the Parry Island anorthosite yielded an age of $1116^{+16}_{-10}$ Ma (Wodicka 1994), and a comparable $^{207}Pb/^{206}Pb$ garnet age of *ca.* 1123 Ma was reported from another pelitic unit from the lower part of the basal Parry Sound assemblage (Tuccillo *et al.* 1992). These data are interpreted to date the time of thrust-related, upper- to lower-amphibolite-facies metamorphic overprint at *ca.* 1120 Ma in the lower part of the basal Parry Sound assemblage (Fig. 11a; Wodicka 1994). This interpretation is consistent with recently reported U–Pb zircon ages of *ca.* 1129–1104 Ma for boudin infills in amphibolitized rocks from the lower part of the basal Parry Sound assemblage (Krogh 1997). At higher structural levels within the interior Parry Sound assemblage, evidence for minor deformation and associated amphibolite-facies metamorphism at about the same time comes from an 1121 ± 5 Ma late tectonic pegmatite (van Breemen *et al.* 1986) and 1114 ± 2 Ma metamorphic zircon from a deformed and amphibolitized mafic dyke (Bussy *et al.* 1995). Thus, these data combine to suggest a significant time-gap between granulite-facies metamorphism (*ca.* 1163 Ma) and deformation and associated hydration (*ca.* 1120 Ma) in the lower part of the basal Parry Sound assemblage, *i.e.*, retrogression did not occur

during cooling of the granulite-facies rocks soon after *ca.* 1163 Ma.

U–Pb titanite data from the basal and northern interior Parry Sound assemblages record ages between *ca.* 1120 and 1080 Ma (Fig. 11a; Tuccillo *et al.* 1992, Wodicka 1994). These data likely reflect cooling through ≥600°C following high-grade metamorphism (Culshaw *et al.* 1997), although the possibility that the ages represent the times of late shearing or recrystallization (or both) (*e.g.*, Tuccillo *et al.* 1992, Wodicka 1994) cannot be excluded. Decompression in the interior Parry Sound assemblage must have occurred before 1120–1080 Ma, as all the metamorphic temperatures exceed the closure temperature of titanite (Fig. 11a). Textural observations, together with U–Pb data on timing of thrusting along the interior Parry Sound – basal Parry Sound contact, suggest that decompression of rocks of the interior Parry Sound assemblage can be linked to thrusting soon after peak granulite-facies metamorphism.

Cooling through closure temperatures of hornblende (*ca.* 500°C) took place between *ca.* 1068 Ma and 1018 Ma (Fig. 11a; Wodicka 1994). $^{40}Ar/^{39}Ar$ muscovite ages are considerably younger and indicate cooling of the basal Parry Sound domain through *ca.* 300°C by *ca.* 890 Ma (Reynolds *et al.* 1995).

Overall, the geochronological data from the northern Parry Sound domain indicate that the rocks experienced polyphase metamorphism and deformation. With increasing structural depth, *i.e.*, from the northern interior Parry Sound assemblage to the lowest structural level of the basal Parry Sound assemblage, there appears to be a systematic younging of amphibolite-facies metamorphism, associated deformation, and subsequent cooling through ≥600–500°C (Wodicka 1994, Krogh 1997). This pattern is consistent with northwestward propagation of the Grenville orogen into its foreland (*e.g.*, Jamieson *et al.* 1992, 1995, Haggart *et al.* 1993, Culshaw *et al.* 1994, 1997). In the Twelve Mile Bay assemblage, the absolute time of metamorphism is currently unknown. However, metamorphism must have postdated the deposition of quartzites at *ca.* 1140–1120 Ma (Wodicka *et al.* 1996), and either predated or was synchronous with widespread upper-amphibolite-facies metamorphism in the CGB at *ca.* 1080–1035 Ma (*e.g.*, Culshaw *et al.* 1997).

*The Shawanaga domain*

U–Pb zircon dates derived from garnet–clinopyroxene-rich rocks within the Shawanaga domain and its bounding shear zones indicate a major phase of eclogite-facies metamorphism at *ca.* 1090–1085 Ma (Fig. 4b; Ketchum & Krogh 1997). An older age of *ca.* 1120 Ma has also been obtained from these rocks, but the significance of this age is currently not very well constrained. Though not yet dated, granulite-facies metamorphism must be younger than *ca.* 1170–1150 Ma, the age of coronitic metagabbro bodies that preserve granulite-facies assemblages. On the basis of petrographic considerations, this metamorphism is likely also younger than the age of the eclogite-facies event. Upper-amphibolite-facies metamorphism in the Shawanaga domain is distinctly younger than that recorded in the Parry Sound domain (Fig. 4b). Migmatite in the immediate footwall of the Parry Sound domain has recently been dated at *ca.* 1082 Ma (Krogh 1997), and a somewhat younger metamorphic zircon age of *ca*. 1050 Ma (Heaman & LeCheminant 1993) and a discordant titanite age of *ca.* 1058 Ma (Tuccillo *et al.* 1992) have been obtained from rocks at lower structural levels within the Shawanaga domain (Fig. 11b). It is not yet clear whether upper-amphibolite-facies metamorphism between about 1080 and 1050 Ma was continuous or episodic. Sillimanite-grade conditions were maintained until at least *ca.* 1020 Ma, the age of a late-syntectonic granitic pegmatite within the extensional Shawanaga shear zone (Ketchum *et al.* 1998). $^{40}Ar/^{39}Ar$ data on hornblende suggest that extensional displacement along the Parry Sound – Shawanaga contact occurred some time between *ca.* 1020 and 970 Ma (Wodicka 1994), *i.e.*, possibly at about the same time as along the Shawanaga shear zone. A *ca.* 990 Ma post-tectonic pegmatite indicates that ductile deformation in the northern Shawanaga domain ceased prior to this time (Ketchum *et al.* 1998).

U–Pb titanite data from the Shawanaga domain define two distinct age-populations. The older group of ages (1028–1018 Ma; Fig. 11b) is interpreted to mark regional cooling through the closure temperature of titanite during or immediately following extensional unroofing, whereas the younger group of ages (967–956 Ma) is considered to date postkinematic recrystallization (Ketchum *et al.* 1998). $^{40}Ar/^{39}Ar$ data indicate that the Shawanaga domain cooled through the closure temperature of hornblende at 970 ± 10 Ma (Fig. 11b; Culshaw *et al.* 1991, Wodicka 1994), some 50–80 m.y. later than the Parry Sound domain. Together with $^{40}Ar/^{39}Ar$ muscovite ages of $900^{+10}_{-20}$ Ma, the hornblende data indicate slow, uniform cooling of the domain at 2–4°C/m.y. (Culshaw *et al.* 1991, Reynolds *et al.* 1995) following extensional deformation at sillimanite-grade conditions.

Since most metamorphic temperatures in both the Lighthouse and Ojibway assemblages exceed the closure temperature of titanite, the initial stages of decompression must have occurred before 1028–1018 Ma (Fig. 11b), *i.e.*, prior to extensional displacement along the Shawanaga shear zone and the Parry Sound – Shawanaga contact. In the case of the Lighthouse assemblage, structural and petrological data suggest that initial decompression can be attributed to northwest-directed thrusting. In contrast, textural observations and U–Pb data suggest that final decompression in the Light-

house and Ojibway assemblages can be linked to extension on the Parry Sound – Shawanaga contact (Wodicka 1994, Ketchum 1995).

## Implications Concerning the Controls of Metamorphism

As geochronological data provide evidence for multiple phases of Grenvillian high-grade metamorphism in the Parry Sound and Shawanaga domains, construction and interpretation of P–T–t paths from these rocks require careful assessment of timing and overprinting relationships, and the degree to which estimates of maximum P–T really reflect peak P–T conditions (*e.g.*, Frost & Chacko 1989, Frost *et al.* 1998, Pattison 1998). Only then can the metamorphic data provide quantitative constraints on the tectonic processes operating during Grenvillian orogenesis. We argue here that the extent of overprinting of mineral assemblages, thermobarometers, and fabrics in the polymetamorphosed rocks of the Parry Sound and Shawanaga domains can be linked to three important factors: strain, fluid access, and high-temperature residence time.

The importance of deformation and associated infiltration of fluid in metamorphism is well known (*e.g.*, Brodie & Rutter 1985, Rubie 1990, Erambert & Austrheim 1993, Moecher & Wintsch 1994, St-Onge & Lucas 1995). In the Parry Sound domain, the preservation of granulite-facies assemblages and associated fabrics appears to have been largely dependent upon fluid availability and strain intensity. Both the northern interior Parry Sound assemblage and the Parry Island anorthosite of the basal Parry Sound assemblage remained relatively strong during Grenvillian deformation, preserving granulite-facies assemblages and structures that formed during an early phase of Grenvillian tectonism. Although these rocks are deformed, deformation was not pervasive and occurred under relatively anhydrous conditions (see above). Mafic rocks from these lithotectonic assemblages were the most resistant to resetting of thermobarometers, and thus appear to preserve a record of peak or near-peak P–T conditions.

In contrast, penetration of fluid, particularly along high-strain zones, facilitated weakening of the granulite-facies rocks by retrograde hydration. For example, rocks along the flanks of the Parry Island anorthosite and within the upper part of the basal Parry Sound assemblage underwent partial to complete compositional change as a result of interaction with a fluid during high-strain, thrust-related deformation. Any pre-existing structures were completely transposed into the dominant SE-dipping foliation in these highly strained, upper-amphibolite-facies rocks. In the southern interior Parry Sound assemblage, conversion of granulite-facies rocks to amphibolite likely occurred in response to thrust emplacement of the overlying Moon River domain, with fluid flow focused along the Parry Sound – Moon River boundary (Culshaw *et al.* 1997). Re-equilibration of Group-II rocks to lower-amphibolite-facies conditions was accompanied by extensive growth of muscovite, suggesting infiltration of aqueous fluids in the strain shadow of the Parry Island anorthosite. We believe that retrogression in this low-strain area took place at the same time as re-equilibration at upper-amphibolite-facies conditions in the adjacent high-strain zones flanking the anorthosite. Extensive growth of muscovite in the strain shadow of the Parry Island anorthosite presumably reflects both greater influx of fluid and further localization of intense retrogression in this area, and the influence of $X(H_2O)$ on reaction positions in P–T space.

In the Shawanaga domain, relict eclogite- and granulite-facies assemblages are only preserved in rocks of suitable composition in low-strain areas. Between *ca.* 1080 and 1050 Ma, penetrative ductile deformation at upper-amphibolite-facies conditions largely overprinted these mineral assemblages. Variable re-equilibration also occurred during high-temperature extensional deformation at *ca.* 1020 Ma. Ductile extensional flow along both the Shawanaga shear zone and the Parry Sound – Shawanaga contact overprinted earlier thrust fabrics. The widespread occurrence of retrograde muscovite and chlorite in rocks of the Sand Bay assemblage provides direct evidence for fluid infiltration.

Extended residence time in the deep crust may have also led to significant resetting of thermobarometers in both Parry Sound and Shawanaga domain rocks. Although rocks of the Parry Sound domain may have cooled slightly following *ca.* 1160 Ma granulite-facies metamorphism, final cooling through the closure temperature of titanite did not take place until *ca.* 1120–1080 Ma (Fig. 11a). Similarly, U–Pb and Ar–Ar data indicate that high-grade metamorphism in the Shawanaga domain probably took place over an interval of *ca.* 40 m.y., and that the crust remained above *ca.* 500°C for another 40–50 m.y. following high-temperature extensional deformation at *ca.* 1020 Ma (Fig. 11b).

## Interpretation of Tectonic History

A tectonic interpretation for high-grade metamorphism and assembly of the Parry Sound and Shawanaga domains during the Grenvillian orogeny is shown in Figure 12. The reconstruction is largely based on geological, geometrical, and chronological constraints from the CGB along Georgian Bay (Culshaw *et al.* 1997, and references therein).

At *ca.* 1163–1161 Ma, granulite-facies metamorphism affected both the interior and basal Parry Sound assemblages. This metamorphism was coeval with the late stages of upper-amphibolite-facies metamorphism and thrust deformation in the Central Metasedimentary Belt boundary thrust zone (McEachern & van Breemen 1993), with the waning stages of the "Elzevirian" orogeny in the CMB and Adirondack Highlands (*e.g.*, Moore & Thompson 1980, McLelland *et al.* 1996), and with widespread anorthosite – mangerite – charnockite –

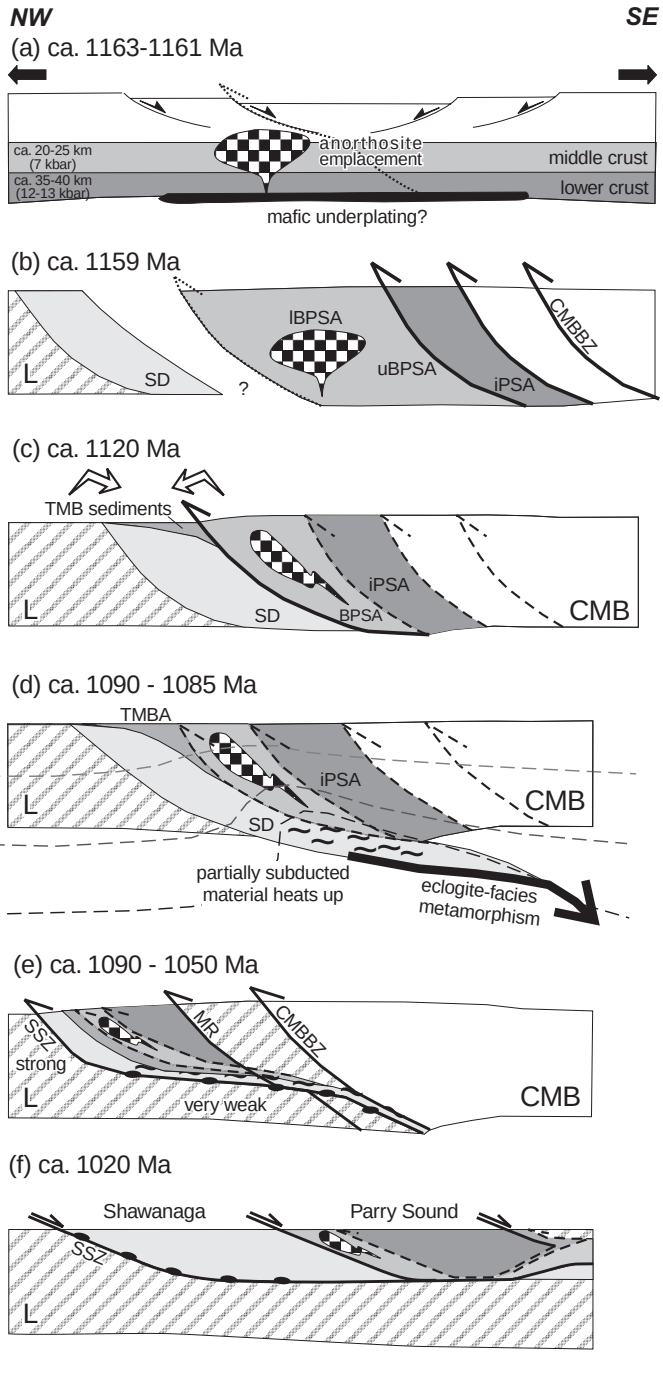


FIG. 12. Cartoons illustrating proposed tectonic evolution of the Parry Sound and Shawanaga domains between *ca.* 1163 and 1020 Ma. Dotted lines show future thrust faults, heavy lines show active thrust and extensional faults, and dashed lines show inactive thrust faults. (a) The *ca.* 1163–1161 Ma panel shows the possible setting for granulite-facies metamorphism in the lower part of the basal Parry Sound assemblage (*i.e.*, middle crust) and in the interior Parry Sound assemblage (*i.e.*, lower crust) and for emplacement of the Parry Island anorthosite in an overall convergent orogen (not shown for simplicity). (b) The *ca.* 1159 Ma panel shows thrust emplacement of the interior Parry Sound granulites (iPSA) onto the upper part of the basal Parry Sound assemblage (uBPSA). The amount of separation, if any, between the Parry Sound domain, CMB, and Laurentia (L) at this time is not known. lBPSA: lower part of the basal Parry Sound assemblage. (c) The *ca.* 1120 Ma panel shows the initial encounter of the Parry Sound domain with Laurentia and deposition of the Twelve Mile Bay (TMB) supracrustal unit. (d) The *ca.* 1090–1085 Ma panel shows the formation of eclogite-facies metamorphism in the Shawanaga domain (SD). The partially subducted or deeply buried material beneath the CMB was heated up to form the leucosome-rich migmatites in the SD. The Twelve Mile Bay assemblage (TMBA) was overridden by, and incorporated into, the Parry Sound domain some time between *ca.* 1120 and 1080 Ma. (e) The *ca.* 1090–1050 Ma panel shows thrusting along the Shawanaga shear zone (SSZ) and Central Metasedimentary Belt boundary thrust zone (CMBBZ) and out-of-sequence thrusting in the Moon River domain (MR). The SSZ facilitated both the emplacement of the Parry Sound and Shawanaga allochthons onto the Laurentian craton and the transport of garnet–clinopyroxene-rich rocks (filled ellipses) to middle crust levels. NW-directed thrusting resulted in telescoping of the Laurentian margin and craton. The SD was affected by upper-amphibolite-facies metamorphism at *ca.* 1080–1050 Ma. (f) Extension along the SSZ, and possibly also along the Parry Sound – Shawanaga contact, took place at *ca.* 1020 Ma, and resulted in SE-directed transport of allochthonous rocks. This panel shows the present-day architecture of the crust in the Parry Sound and Shawanaga domains (see Fig. 4a). See text for further details.

granite (AMCG) magmatism between *ca.* 1180 and 1125 Ma in the southeastern, central, and eastern parts of the Grenville orogen (*e.g.*, Emslie & Hunt 1990, McLelland & Chiarenzelli 1991, Higgins & van Breemen 1996). In contrast, with the exception of the emplacement of gabbro at *ca.* 1170–1150 Ma, there is no tectonic activity of this age known from the Laurentian craton and margin. Thus, at the time of high-grade metamorphism, the Parry Sound domain cannot have been contiguous with the Laurentian rocks that now underlie it (Wodicka *et al.* 1996, Timmermann *et al.* 1997). Our data do not show whether the convergence responsible for *ca.* 1163–1161 Ma high-grade metamorphism and thrusting in the Parry Sound domain occurred at a distal margin of Laurentia which is not preserved, or within some part of the composite arc system now represented by the Central Metasedimentary Belt.

Peak metamorphic conditions of *ca.* 12–13 kbar and 885–975°C have been estimated for the interior Parry Sound assemblage rocks. The high pressures require either substantial thickening of the crust or exhumation of these rocks from synorogenic lower crust corresponding to depths of 35–40 km. Although there is no compelling evidence one way or the other, the latter hypothesis may be favored by the lack of clear evidence for continental collision in this part of the orogen, and by the P–T–t path segment suggesting near-isothermal decompression (Fig. 11a). In addition, if granulites of the interior Parry Sound assemblage reached peak conditions in the middle part of a thick orogenic crust, Moho temperatures must have been substantially above 1000°C; this seems unlikely by comparison with modern orogenic settings, and should have led to widespread melting in the lower crust at this time, for which there is no evidence.

Possible explanations for high temperatures of metamorphism in the interior Parry Sound assemblage include tectonic accretion of heat-producing material, heat transfer from coeval anorthosite, or underplating by voluminous mafic magma. Lateral accretion or tectonic underplating of heat-producing crustal material can produce the necessary temperatures (Huerta *et al.* 1998, Jamieson *et al.* 1998), but this part of the Parry Sound domain is dominated by mafic to intermediate metaigneous rocks, with relatively little granitic or metasedimentary material. If accretion of heat-producing material was responsible, this material is now gone.

The interval 1180–1125 Ma coincides with a major episode of AMCG magmatism in much of the Grenville orogen. Heat advected from anorthosite could account for intermediate-P (≥7.0 kbar and ≥660°C) granulite-facies metamorphism in the lower part of the basal Parry Sound assemblage (Fig. 12a), but the absence of syn-metamorphic anorthosite or any other intrusive rocks in the interior Parry Sound assemblage suggests that another mechanism is required. It has recently been suggested that this AMCG magmatism was associated with widespread mafic underplating and lithosphere delamination in the CMB and Adirondack Highlands (Corrigan 1995, McLelland *et al.* 1996, Corrigan & Hanmer 1997). Although the proposed mechanism, convective removal of over-thickened suborogenic lithospheric mantle, seems incompatible with the lack of evidence for collision in the study area, underplating by voluminous mafic magma, whatever its origin, is likely to have accompanied AMCG magmatism and is also likely to have transferred a significant amount of heat to the immediately overlying crust. The postulated underplated material, which on cooling would have been both denser and stronger than the overlying crust, is unlikely to have been incorporated into the orogenic crust during subsequent tectonic shortening. We conclude that the most likely setting for 1161 ± 3 Ma high-P – high-T granulite-facies metamorphism in the interior Parry Sound assemblage was at or near the base of crust underplated by voluminous mafic magma at or shortly before 1161 Ma (Fig. 12a). In contrast, barometric data suggest that rocks of the basal Parry Sound assemblage lay at much higher levels in the crust (*ca.* 20–25 km, 7 kbar) at the time of emplacement of the 1163 ± 3 Ma Parry Island anorthosite (Fig. 12a). At *ca.* 1159 Ma, tectonic emplacement of the interior Parry Sound assemblage onto the upper part of the basal Parry Sound assemblage probably resulted in conversion of these rocks to amphibolite (≥7.0–8.5 kbar, 725–775°C; Fig. 12b). The position of rocks of the Parry Sound domain relative to Laurentia at the time is unknown.

At *ca.* 1120 Ma, amphibolite-facies metamorphism and thrust deformation affected the lower part of the basal Parry Sound assemblage (Fig. 12c). We suggest that at this time, the pre-assembled interior Parry Sound assemblage and upper part of the basal Parry Sound assemblage were transported northwestward onto rocks of the lower part of the basal Parry Sound assemblage. Petrological and structural data from the lower part of the basal Parry Sound assemblage suggest that thrusting and concomitant erosion brought the Parry Sound domain into the middle to upper crust (5–6.5 kbar, 15–20 km) at *ca.* 1120 Ma. At about the same time, the Twelve Mile Bay quartzite was deposited from a varied source that included AMCG and Laurentian rocks (Wodicka *et al.* 1996; Fig. 12c). As suggested by Culshaw *et al.* (1997), this period may mark the initial encounter of the Parry Sound domain and correlative rocks (*i.e.*, Central Metasedimentary Belt boundary thrust zone allochthons) with the outer margin of Laurentia.

Apart from *ca.* 1100 Ma syntectonic granitic pegmatites near the boundaries of the Moon River and Seguin domains (van Breemen & Davidson 1990, Nadeau 1990), few data indicate that the interval 1120–1090 Ma represents a major phase of thrust deformation in the southwestern CGB or CMB, which suggests that convergence slowed down or stopped. Whether this was due to aborted subduction of the buoyant Laurentian

margin or to a far-field change in plate motions, perhaps associated with the formation of the 1109–1087 Ma Midcontinent rift (Van Schmus 1992, Cannon 1994), remains unknown.

The recent recognition of eclogite-facies metamorphism at *ca.* 1090–1085 Ma in the Shawanaga domain and other allochthonous domains of the CGB (Ketchum & Krogh 1997) suggests deep burial or partial subduction of the Laurentian margin beneath the CMB at this time (Fig. 12d). Seismic and geological evidence indicating that the CGB extends beneath the CMB (*e.g.*, Culshaw *et al.* 1983, Hanmer & McEachern 1992, Milkereit *et al.* 1992, White *et al.* 1994) supports this interpretation. Heating of this deeply buried or partially subducted material formed leucosome-rich migmatites in the Shawanaga domain approximately 10 m.y. after eclogite-facies metamorphism (Culshaw *et al.* 1997). At some time between *ca.* 1120 and 1080 Ma, the Twelve Mile Bay assemblage was affected by upper-amphibolite-facies metamorphism and was overridden by the Parry Sound domain.

Eclogite-facies metamorphism in the Shawanaga domain broadly coincided with *ca.* 1090–1080 Ma thrusting and high-grade metamorphism in the Central Metasedimentary Belt boundary thrust zone, suggesting renewed convergence near the Laurentian margin at this time (McEachern & van Breemen 1993, Timmermann *et al.* 1997; Fig. 12e). Between *ca.* 1080 and 1050 Ma, the Shawanaga domain was affected by upper-amphibolite-facies metamorphism and deformation, which coincided with widespread metamorphism in the CGB, with the exception of the Parry Sound domain and the Grenville Front Tectonic Zone. Metamorphic conditions recorded by our data suggest that rocks of the Lighthouse assemblage lay at crustal depths of *ca.* 30–35 km (10.5–11.0 kbar) and temperatures of *ca.* 830°C, whereas rocks of the Ojibway assemblage lay at depths of at least *ca.* 22 km (7.5–8.5 kbar and 700–685°C) at this time. Upper-amphibolite-facies metamorphism is interpreted as a response to the *ca.* 1090–1080 Ma thrusting (Culshaw *et al.* 1997). Transport of the Shawanaga and Parry Sound allochthons over the Laurentian craton may have been facilitated by the Shawanaga domain migmatite, acting as a thin, extremely weak, intra-crustal *décollement* (*i.e.*, the thrust stage of the Shawanaga shear zone; Jamieson *et al.* 1992, White *et al.* 1994, Ketchum 1995, Culshaw *et al.* 1997). Transport of eclogite to higher levels in the crust, accompanied by recrystallization to upper-amphibolite-facies assemblages, was probably associated with thrusting along the Shawanaga shear zone or similar structures. Subsequent out-of-sequence thrusting in the Moon River domain caused reworking and retrogression of the southern interior Parry Sound assemblage (Culshaw *et al.* 1997).

At *ca.* 1020 Ma, extension on the Shawanaga shear zone (Ketchum 1995, Ketchum *et al.* 1998) generally postdated thrusting in the CGB, and resulted in SE-directed transport of allochthonous rocks (Fig. 12f). Ductile extensional fabrics at the Parry Sound – Shawanaga contact may have developed at about the same time (Wodicka 1994). Extensional displacement along these shear zones postdated peak metamorphism, although growth of sillimanite parallel to the extension lineation indicates that these rocks were hot during extensional shear (Wodicka 1994, Ketchum 1995). Our data suggest that extensional unroofing brought rocks of the Lighthouse and Ojibway assemblages into the middle to upper crust (5–6.5 kbar; 15–20 km) at *ca.* 1020 Ma. Extension could have been driven by reduced rates of convergence, excess gravitational potential related to the development of thick orogenic crust and high topography, or reduced strength of the lower crust associated with high temperatures and partial melting (Culshaw *et al.* 1994, 1997); it is not clear which of these mechanisms was most important in the study area.

In summary, the metamorphic and age data are consistent with progressive NW-directed juxtaposition of lithotectonic assemblages metamorphosed at progressively later times, and appear to record progressive or multi-stage convergence at the southeastern margin of Laurentia. The earliest phase of convergence took place southeast of the Laurentian craton between *ca.* 1163 and 1120 Ma, and resulted in assembly and granulite- to amphibolite-facies metamorphism of lithotectonic assemblages within the Parry Sound domain. The second phase of convergence, which began at or shortly before 1090–1080 Ma, involved deep burial or partial subduction of the Laurentian margin beneath the CMB. Continued convergence resulted in thrust imbrication and upper-amphibolite-facies metamorphism of the weakened Laurentian craton (including the Shawanaga domain) beneath the Parry Sound domain, transport of garnet–clinopyroxene-rich rocks to mid-crust levels, and assembly and transport of CGB lithotectonic units over the craton. A major episode of extension at *ca.* 1020 Ma followed convergence and resulted in SE-directed transport of allochthonous rocks.

## Conclusions

1. The Parry Sound and Shawanaga domains contain monocyclic rocks that originated at or near the southeastern margin of Laurentia between *ca.* 1450 and 1120 Ma. Their metamorphism and deformation are entirely attributable to Grenvillian orogenesis.

2. In the Parry Sound domain, both the interior and basal Parry Sound assemblages preserve granulite-facies assemblages and structures that formed during an early phase of Grenvillian tectonism. The most likely setting for *ca.* 1161 Ma high-P – high-T (*ca.* 12–13 kbar and 885–975°C) granulite-facies metamorphism in the interior Parry Sound assemblage was at or near the base of crust that was underplated by voluminous mafic magma. In contrast, heat advected from anorthosite could account for *ca.* 1163 Ma intermediate-P (≥7 kbar

and 660°C) granulite-facies metamorphism in the basal Parry Sound assemblage. In the upper part of the basal Parry Sound assemblage, retrogression of granulite-facies assemblages to upper-amphibolite-facies conditions (≥7–8.5 kbar and 725–775°C) likely occurred in response to thrust emplacement of the interior Parry Sound granulites onto this portion of the basal Parry Sound assemblage at *ca.* 1159 Ma. In the lower part of the basal Parry Sound assemblage, thrust deformation and re-equilibration at lower-amphibolite-facies conditions (5–6.5 kbar and 615–690°C) took place at *ca.* 1120 Ma. In the Twelve Mile Bay assemblage, a highly attenuated sequence of quartzites and mafic rocks deposited some time after 1140–1120 Ma was affected by upper-amphibolite-facies metamorphism before or at 1080 Ma.

3. Northwest of and structurally below the Parry Sound domain, rocks in the Shawanaga domain were affected by eclogite-facies metamorphism at *ca.* 1090–1085 Ma, suggesting deep burial or partial subduction of the Laurentian margin beneath the Central Metasedimentary Belt at this time. Widespread upper-amphibolite-facies metamorphism after *ca.* 1080 Ma was associated with a major phase of northwest-directed thrusting and crustal thickening. Our data suggest that rocks from the uppermost Lighthouse assemblage lay at depths of *ca.* 30–35 km in the crust (10.5–11.0 kbar) and temperatures of *ca.* 830°C, whereas those from the structurally lower Ojibway assemblage lay at depths of at least *ca.* 22 km (7.5–8.5 kbar and 700–685°C) at this time. Sillimanite-grade conditions in the Shawanaga domain were maintained until at least *ca.* 1020 Ma, the time of major extensional deformation.

4. P–T–t paths for the Parry Sound and Shawanaga domains generally show decompression accompanied by some cooling. Petrological and structural data suggest that decompression of the interior Parry Sound granulites can be linked to thrusting soon after peak metamorphism, whereas exhumation of Shawanaga domain rocks was likely associated with both thrusting and extension.

5. Evidence for multiple phases of Grenvillian high-grade metamorphism in the Parry Sound and Shawanaga domains suggests that construction and interpretation of P–T–t paths from these rocks require careful assessment of timing and overprinting relationships. Only then can the metamorphic data provide quantitative constraints on the tectonic processes operating during Grenvillian orogenesis. In the study area, the extent of overprinting of mineral assemblages, thermobarometers, and fabrics can be linked to strain, fluid access, and high-temperature residence time.

6. The metamorphic and age data are consistent with progressive NW-directed juxtaposition of lithotectonic assemblages metamorphosed at progressively later times, and appear to record progressive or multistage convergence at the southeastern margin of Laurentia.

## Acknowledgements

This research was funded by NSERC Postgraduate Scholarships and Dalhousie Graduate Fellowships to NW and JWFK, and NSERC Research and Lithoprobe Supporting Geoscience grants to RAJ and N.G. Culshaw. The work would not have been possible without the field assistance of Robbie Hicks and Steve Grant. We thank G. Brown for thin-section preparation, and R. MacKay for assistance with the electron microprobe. We are particularly grateful to R. Berman for assistance with the application and interpretation of TWQ analysis. Discussions with numerous colleagues, including D. Corrigan and N. Culshaw, are gratefully acknowledged. The manuscript greatly benefitted from constructive reviews by M.R. St-Onge, A. Indares, M. Williams, and R.M. Easton.

## References

Anovitz, L.M. (1991): Al zoning in pyroxene and plagioclase: window on late prograde to early retrograde *P–T* paths in granulite terranes. *Am. Mineral.* **76**, 1328-1343.

_____ & Chase, C.G. (1990): Implications of post-thrusting extension and underplating for P–T–t paths in granulite terranes: a Grenville example. *Geology* **18**, 466-469.

_____ & Essene, E.J. (1990): Thermobarometry and pressure–temperature paths in the Grenville Province of Ontario. *J. Petrol.* **31**, 197-241.

Aranovich, L.Ya. (1991): *Mineral Equilibria of Multicomponent Solid Solutions*. Nauka Press, Moscow, Russia (in Russ.).

_____ & Berman, R.G. (1996): Optimized standard state and mixing properties of minerals. II. Comparisons, predictions, and applications. *Contrib. Mineral. Petrol.* **126**, 25-37.

Baldwin, S.L., Harrison, T.M. & FitzGerald, J.D. (1990): Diffusion of $^{40}$Ar in metamorphic hornblende. *Contrib. Mineral. Petrol.* **105**, 691-703.

Beard, J.S. & Lofgren, G.E. (1991): Dehydration melting and water saturated melting of basaltic and andesitic greenstones and amphibolites at 1, 3 and 6.9 kb. *J. Petrol.* **32**, 365-401.

Berman, R.G. (1990): Mixing properties of Ca–Mg–Fe–Mn garnets. *Am. Mineral.* **75**, 328-344.

_____ (1991): Thermobarometry using multi-equilibrium calculations: a new technique, with petrological applications. *Can. Mineral.* **29**, 833-855.

Brodie, K.H. & Rutter, E.H. (1985): On the relationship between deformation and metamorphism, with special reference to the behaviour of basic rocks. *In* Advances in Physical Geochemistry **4** (A.B. Thompson & D.C. Rubie, eds.). Springer-Verlag, New York, N.Y. (138-179).

BUSCH, J.P. & VAN DER PLUIJM, B.A. (1996): Late orogenic, plastic to brittle extension along the Robertson Lake shear zone: implications for the style of deep-crustal extension in the Grenville orogen, Canada. *Precamb. Res.* **77**, 41-57.

_____, _____, HALL, C.M. & ESSENE, E.J. (1996): Listric normal faulting during postorogenic extension revealed by $^{40}Ar/^{39}Ar$ thermochronology near the Robertson Lake shear zone, Grenville orogen, Canada. *Tectonics* **15**, 387-402.

BUSSY, F., KROGH, T.E., KLEMENS, W.P. & SCHWERDTNER, W.M. (1995): Tectonic and metamorphic events in the westernmost Grenville Province, central Ontario: new results from high-precision U–Pb zircon geochronology. *Can. J. Earth Sci.* **32**, 660-671.

CANNON, W.F. (1994): Closing of the Midcontinent rift – a far-field effect of Grenvillian compression. *Geology* **22**, 155-158.

CARLSON, K.A., VAN DER PLUIJM, B.A. & HANMER, S. (1990): Marble mylonites of the Bancroft shear zone: evidence for extension in the Canadian Grenville. *Geol. Soc. Am., Bull.* **102**, 174-181.

CARRINGTON, D.P. (1995): The relative stability of garnet – cordierite and orthopyroxene – sillimanite – quartz assemblages in metapelitic granulites: experimental data. *Eur. J. Mineral.* **7**, 949- 960.

CORRIGAN, D. (1995): *Mesoproterozoic Evolution of the South-Central Grenville Orogen: Structural, Metamorphic, and Geochronologic Constraints from the Mauricie Transect.* Ph.D. thesis, Carleton Univ., Ottawa, Ontario.

_____ & HANMER, S. (1997): Anorthosites and related granitoids in the Grenville orogen: a product of convective thinning of the lithosphere? *Geology* **25**, 61-64.

CULSHAW, N.G., CHECK, G., CORRIGAN, D., DRAGE, J., GOWER, R., HAGGART, M.J., WALLACE, P. & WODICKA, N. (1989): Georgian Bay geological synthesis: Dillon to Twelve Mile Bay, Grenville Province of Ontario. *Geol. Surv. Can., Pap.* **89-1C**, 157-163.

_____, CORRIGAN, D., DRAGE, J. & WALLACE, P. (1988): Georgian Bay geological synthesis: Key Harbour to Dillon, Grenville Province of Ontario. *Geol. Surv. Can., Pap.* **88-1C**, 129-133.

_____, _____, KETCHUM, J. & WALLACE, P. (1990): Georgian Bay geological synthesis. III. Twelve Mile Bay to Port Severn, Grenville Province of Ontario. *Geol. Surv. Can., Pap.* **90-1C**, 107- 112.

_____, DAVIDSON, A. & NADEAU, L. (1983): Structural subdivisions of the Grenville Province in the Parry Sound – Algonquin Region, Ontario. *Geol. Surv. Can., Pap.* **83-1B**, 243-252.

_____ & DOSTAL, J. (1997): Sand Bay gneiss association, Grenville Province, Ontario: a Grenvillian rift- (and -drift) assemblage stranded in the Central Gneiss Belt. *Precamb. Res.* **85**, 97- 113.

_____, JAMIESON, R.A., KETCHUM, J.W.F., WODICKA, N., CORRIGAN, D. & REYNOLDS, P.H. (1997): Transect across the northwestern Grenville orogen, Georgian Bay, Ontario: polystage convergence and extension in the lower orogenic crust. *Tectonics* **16**, 966-982.

_____, KETCHUM, J.W.F., WODICKA, N. & WALLACE, P. (1994): Deep crustal ductile extension following thrusting in the southwestern Grenville Province, Ontario. *Can. J. Earth Sci.* **31**, 160-175.

_____, REYNOLDS, P.H. & CHECK, G. (1991): A $^{40}Ar/^{39}Ar$ study of post-tectonic cooling in the Britt domain of the Grenville Province, Ontario. *Earth Planet. Sci. Lett.* **105**, 405-415.

DAVIDSON, A. (1984): Identification of ductile shear zones in the southwestern Grenville Province of the Canadian Shield. *In* Precambrian Tectonics Illustrated (A. Kröner & R. Greiling, eds.). E. Schweizerbart'sche Verlagsbuchhandlung, Stuttgart, Germany (263-279).

_____ (1986): New interpretations in the southwestern Grenville Province. *In* The Grenville Province (J.M. Moore, A. Davidson & A. J. Baer, eds.). *Geol. Assoc. Can., Spec. Pap.* **31**, 61-74.

_____ (1990): Evidence for eclogite metamorphism in the southwest Grenville Province, Ontario. *Geol. Surv. Can., Pap.* **90-1C**, 113-118.

_____ (1991): Metamorphism and tectonic setting of gabbroic and related rocks in the Central Gneiss Belt, Grenville Province, Ontario. *Geol. Assoc. Can. – Mineral. Assoc. Can., Field Trip Guidebook* **A2**.

_____ (1995): A review of the Grenville orogen in its North American type area. *Aust. Geol. Surv. Org., J. Aust. Geol. Geophys.* **16**, 3-24.

_____, CARMICHAEL, D.M. & PATTISON, D.M.R. (1990): Metamorphism and geodynamics of the southwestern Grenville Province, Ontario. *Int. Geol. Correlation Program, Project* **235/304,** *Field Trip Guide* **1**.

_____, CULSHAW, N.G. & NADEAU, L. (1982): A tectono-metamorphic framework for part of the Grenville Province, Parry Sound region, Ontario. *Geol. Surv. Can., Pap.* **82-1A**, 175-190.

_____ & MORGAN, W.C. (1981): Preliminary notes on the geology east of Georgian Bay, Grenville Structural Province, Ontario. *Geol. Surv. Can., Pap.* **81-1A**, 291-298.

_____ & VAN BREEMEN, O. (1988): Baddeleyite–zircon relationships in coronitic metagabbro, Grenville Province, Ontario: implications for geochronology. *Contrib. Mineral. Petrol.* **100**, 291-299.

DEWEY, J.F. & BURKE, K.C.A. (1973): Tibetan, Variscan, and Precambrian basement reactivation: products of continental collision. *J. Geol.* **81**, 683-692.

EASTON, R.M. (1992): The Grenville Province and the Proterozoic history of central and southern Ontario. *In* Geology of Ontario (P.C. Thurston, ed.). *Ontario Geol. Surv., Spec. Vol.* **4**, 714-904.

EMSLIE, R.F. & HUNT, P.A. (1990): Ages and petrogenetic significance of igneous mangerite–charnockite suites associated with massif anorthosites, Grenville Province. *J. Geol.* **98**, 213-231.

ENGLAND, P.C. & RICHARDSON, S.W. (1977): The influence of erosion upon mineral facies of rocks from different metamorphic environments. *J. Geol. Soc. London* **134**, 201-213.

_____ & THOMPSON, A.B. (1984): Pressure – temperature – time paths of regional metamorphism. I. Heat transfer during the evolution of regions of thickened continental crust. *J. Petrol.* **25**, 894-928.

ERAMBERT, M. & AUSTRHEIM, H. (1993): The effect of fluid and deformation on zoning and inclusion patterns in polymetamorphic garnets. *Contrib. Mineral. Petrol.* **115**, 204-214.

ESSENE, E.J. (1989): The current status of thermobarometry in metamorphic rocks. *In* Evolution of Metamorphic Belts (J.S. Daly, R.A. Cliff & B.W.D. Yardley, eds.). *Geol. Soc., Spec. Publ.* **43**, 1-44.

FROST, B.R. & CHACKO, T. (1989): The granulite uncertainty principle: limitations on thermobarometry in granulites. *J. Geol.* **97**, 435-450.

_____, CHAMBERLAIN, K.R., SWAPP, S.M. & FROST, C.D. (1998): The age of granulite metamorphism in the Wind River range, Wyoming: the granulite uncertainty principle compounded. *Geol. Soc. Am., Abstr. Programs* **30**, A-154.

FUHRMAN, M.L. & LINDSLEY, D.H. (1988): Ternary-feldspar modeling and thermometry. *Am. Mineral.* **73**, 201-215.

GOWER, R.J.W. (1992): Nappe emplacement direction in the Central Gneiss Belt, Grenville Province, Ontario, Canada: evidence for oblique collision. *Precamb. Res.* **59**, 73-94.

GRANT, S.M. (1987): *The Petrology and Structural Relations of Metagabbros from the Western Grenville Province, Canada.* Ph.D. thesis, Leicester Univ., Leicester, U.K.

GREEN, A.G., MILKEREIT, B., DAVIDSON, A., SPENCER, C., HUTCHINSON, D.R., CANNON, W., LEE, M.W., AGENA, W.F., BEHRENDT, J.C. & HINZE, W.J. (1988): Crustal structure of the Grenville Front and adjacent terranes. *Geology* **16**, 788-792.

HAGGART, M.J., JAMIESON, R.A., REYNOLDS, P.H., KROGH, T.E., BEAUMONT, C. & CULSHAW, N.G. (1993): Last gasp of the Grenville Orogeny: thermochronology of the Grenville Front Tectonic Zone near Killarney, Ontario. *J. Geol.* **101**, 575-589.

HANMER, S. (1984): Structure of the junction of three tectonic slices; Ontario gneiss segment, Grenville Province. *Geol. Surv. Can., Pap.* **84-1B**, 109-120.

_____ & MCEACHERN, S.J. (1992): Kinematical and theological evolution of a crustal-scale ductile thrust zone, Central Metasedimentary Belt, Grenville orogen, Ontario. *Can. J. Earth Sci.* **29**, 1779-1790.

HEAMAN, L.M. & LECHEMINANT, A.N. (1993): Paragenesis and U–Pb systematics of baddeleyite ($ZrO_2$). *Chem. Geol.* **110**, 95-126.

_____ & PARRISH, R.R. (1991): U–Pb geochronology of accessory minerals. *In* Applications of Radiogenic Isotope Systems to Problems in Geology (L. Heaman & J.N. Ludden, eds.). *Mineral. Assoc. Can., Short Course Handbook* **19**, 59-102.

HICKS, R.J. (1992): *Metamorphism of Metabasites from Parry Island, Georgian Bay, Ontario*. B.Sc. Honours thesis, Dalhousie Univ., Halifax, Nova Scotia.

HIGGINS, M.D. & VAN BREEMEN, O. (1996): Three generations of anorthosite – mangerite – charnockite – granite (AMCG) magmatism, contact metamorphism and tectonism in the Saguenay – Lac-Saint-Jean region of the Grenville Province, Canada. *Precamb. Res.* **79**, 327-349.

HUERTA, A.D., ROYDEN, L.H. & HODGES, K.V. (1998): The thermal structure of collisional orogens as a response to accretion, erosion, and radiogenic heating. *J. Geophys. Res.* **103**, 15287-15302.

INDARES, A. (1993): Eclogitized gabbros from the eastern Grenville Province: textures, metamorphic context, and implications. *Can. J. Earth Sci.* **30**, 159-173.

JAMIESON, R.A. (1988): Textures, sequences of events, and assemblages in metamorphic rocks. *In* Heat, Metamorphism, and Tectonics (E.G. Nisbet, C.M.R. Fowler & E.D. Ghent, eds.). *Mineral. Assoc. Can., Short Course Handbook* **14**, 189-212.

_____, BEAUMONT, C. FULLSACK, P. & LEE, B. (1998): Barrovian regional metamorphism: where's the heat? *In* What Drives Metamorphism and Metamorphic Reactions? (P.J. Treloar & P. O'Brien, eds.). *Geol. Soc., Spec. Publ.* **138**, 23-51.

_____, CULSHAW, N.G. & CORRIGAN, D. (1995): Northwest propagation of the Grenville orogen: Grenvillian structure and metamorphism near Key Harbour, Georgian Bay, Ontario, Canada. *J. Metamorph. Geol.* **13**, 185-207.

_____, _____, WODICKA, N., CORRIGAN, D. & KETCHUM, J.W.F. (1992): Timing and tectonic setting of Grenvillian metamorphism – constraints from a transect along Georgian Bay, southwestern Ontario. *J. Metamorph. Geol.* **10**, 321-332.

KETCHUM, J.W.F. (1995): *Extensional Shear Zones and Lithotectonic Domains in the Southwest Grenville Orogen: Structure, Metamorphism, and U–Pb Geochronology of the Central Gneiss Belt near Pointe-au-Baril, Ontario.* Ph.D. thesis, Dalhousie Univ., Halifax, Nova Scotia.

_____ & DAVIDSON, A. (2000): Crustal architecture and tectonic assembly of the Central Gneiss Belt, southwestern Grenville Province, Canada – a new interpretation. *Can. J. Earth Sci.* **37**, 217-234.

_____, HEAMAN, L.M., KROGH, T.E., CULSHAW, N.G. & JAMIESON, R.A. (1998): Timing and thermal influence of late orogenic extension in the lower crust: a U–Pb geochronological study from the southwest Grenville orogen, Canada. *Precamb. Res.* **89**, 25-45.

_____, JAMIESON, R.A., HEAMAN, L.M., CULSHAW, N.G. & KROGH, T.E. (1994): 1.45 Ga granulites in the southwestern Grenville Province: geologic setting, *P–T* conditions, and U–Pb geochronology. *Geology* **22**, 215-218.

_____ & KROGH, T.E. (1997): U–Pb constraints on high-pressure metamorphism in the Central Gneiss Belt, southwestern Grenville orogen. *Geol. Assoc. Can. - Mineral. Assoc. Can., Program Abstr.* **22**, A78.

KRETZ, R. (1983): Symbols for rock-forming minerals. *Am. Mineral.* **68**, 277-279.

KROGH, T.E. (1994): Precise U–Pb ages for Grenvillian and pre-Grenvillian thrusting of Proterozoic and Archean metamorphic assemblages in the Grenville Front tectonic zone, Canada. *Tectonics* **13**, 963-982.

_____ (1997): Seventy-five million years of convergence recorded in the Parry Sound shear zone in the Central Gneiss Belt of the Grenville Province. *In* Proterozoic Orogenies and Plate Interactions: The North Atlantic Region in Space and Time. *COPENA Conf., Norsk Geol. Unders., Abstr. Proc.*

LEBRETON, N. & THOMPSON, A.B. (1988): Fluid absent (dehydration) melting of biotite in metapelites in the early stages of crustal anatexis. *Contrib. Mineral. Petrol.* **99**, 226-237.

MÄDER, U.K., PERCIVAL, J.A. & BERMAN, R.G. (1994): Thermobarometry of garnet – clinopyroxene – hornblende granulites from the Kapuskasing structural zone. *Can. J. Earth Sci.* **31**, 1134-1145.

MCEACHERN, S.J. & VAN BREEMEN, O. (1993): Age of deformation within the Central Metasedimentary Belt boundary thrust zone, southwest Grenville Orogen: constraints on the collision of the Mid-Proterozoic Elzevir terrane. *Can. J. Earth Sci.* **30**, 1155-1165.

MCLELLAND, J. & CHIARENZELLI, J. (1991): Geochronological studies in the Adirondack Mountains and the implications of a Middle Proterozoic tonalitic suite. *In* Mid-Proterozoic Laurentia and Baltica (C.F. Gower, T. Rivers & B. Ryan). *Geol. Assoc. Can., Spec. Pap.* **38**, 175-194.

_____, DALY, J.S. & MCLELLAND, J.M. (1996): The Grenville orogenic cycle (*ca.* 1350–1000 Ma): an Adirondack perspective. *Tectonophys.* **265**, 1-28.

MCMULLIN, D., BERMAN, R.G. & GREENWOOD, H.J. (1991): Calibration of the SGAM thermobarometer for pelitic rocks using data from equilibrium experiments and natural assemblages. *Can. Mineral.* **29**, 889-908.

MILKEREIT, B., FORSYTH, D.A., GREEN, A.G., DAVIDSON, A., HANMER, S., HUTCHINSON, D.R., HINZE, W.J. & MEREU, R.F. (1992): Seismic images of a Grenvillian terrane boundary. *Geology* **20**, 1027-1030.

MOECHER, D.P. & WINTSCH, R.P. (1994): Deformation-induced reconstitution and local resetting of mineral equilibria in polymetamorphic gneisses: tectonic and metamorphic implications. *J. Metamorph. Geol.* **12**, 523-538.

MOORE, J.M. & THOMPSON, P.H. (1980): The Flinton Group: a late Precambrian metasedimentary succession in the Grenville Province of eastern Ontario. *Can. J. Earth Sci.* **17**, 1685-1707.

NADEAU, L. (1990): *Tectonic, Thermal and Magmatic Evolution of the Central Gneiss Belt, Huntsville Region, Southwestern Grenville Orogen.* Ph.D. thesis, Carleton Univ., Ottawa, Ontario.

NEEDHAM, T.W. (1992): *The Metamorphic Evolution of the Frederic Inlet Metagabbros, Southwestern Grenville Province, Ontario, Canada.* M.Sc. thesis, Queen's Univ., Kingston, Ontario.

NEWTON, R.C. (1983): Geobarometry of high-grade metamorphic rocks. *Am. J. Sci.* **283-A**,1-28.

OXBURGH, E.R. & TURCOTTE, D.L. (1974): Thermal gradients and regional metamorphism in overthrust terrains with specific reference to the Eastern Alps. *Schweiz. Mineral. Petrogr. Mitt.* **54**, 641-662.

PATTISON, D.R.M. (1991): Infiltration-driven dehydration and anatexis in granulite facies metagabbro, Grenville Province, Ontario, Canada. *J. Metamorph. Geol.* **9**, 315-332.

_____ (1998): Re-assessment of temperatures of granulite facies rocks using refractory cationic systems corrected for late resetting. *Geol. Soc. Am., Abstr. Programs* **30**, A-154.

REYNOLDS, P.H., CULSHAW, N.G., JAMIESON, R.A., GRANT, S.L. & MCKENZIE, K.J. (1995): $^{40}Ar/^{39}Ar$ traverse – Grenville Front Tectonic Zone to Britt Domain, Grenville Province, Ontario, Canada. *J. Metamorph. Geol.* **13**, 209-221.

RIVERS, T. (1997): Lithotectonic elements of the Grenville Province: review and tectonic implications. *Precamb. Res.* **86**, 117-154.

_____, MARTIGNOLE, J., GOWER, C.F. & DAVIDSON, A. (1989): New tectonic divisions of the Grenville Province, southeast Canadian Shield. *Tectonics* **8**, 63-84.

RUBIE, D.C. (1990): Mechanisms of reaction enhanced deformability in minerals and rocks. *In* Deformation Processes in Minerals, Ceramics and Rocks (D.J. Barber & P.G. Meredith, eds.). Unwin-Hyman, London, U.K. (262-295).

RUPPEL, C. & HODGES, K.V. (1994): Pressure – temperature – time paths from two-dimensional thermal models:

prograde, retrograde, and inverted metamorphism. *Tectonics* **13**, 17-44.

RUSHMER, T. (1991): Partial melting of two amphibolites: contrasting experimental results under fluid-absent conditions. *Contrib. Mineral. Petrol.* **107**, 41-59.

SELVERSTONE, J., SPEAR, F.S., FRANZ, G. & MORTEANI, G. (1984): High-pressure metamorphism in the SW Tauern Window, Austria: P–T paths from hornblende – kyanite – staurolite-schists. *J. Petrol.* **25**, 501-532.

SPEAR, F.S. (1993): *Metamorphic Phase Equilibria and Pressure – Temperature – Time Paths.* Mineralogical Society of America, Washington, D.C.

_____, SELVERSTONE, J., HICKMOTT, D., CROWLEY, P. & HODGES, K.V. (1984): P–T paths from garnet zoning: a new technique for deciphering tectonic processes in crystalline terranes. *Geology* **12**, 87-90.

ST-ONGE, M.R. & LUCAS, S.B. (1995): Large-scale fluid infiltration, metasomatism and re-equilibration of Archaean basement granulites during Palaeoproterozoic thrust belt construction, Ungava Orogen, Canada. *J. Metamorph. Geol.* **13**, 509-535.

TIMMERMANN, H., PARRISH, R.R., JAMIESON, R.A. & CULSHAW, N.G. (1997): Time of metamorphism beneath the Central Metasedimentary Belt boundary thrust zone, Grenville Orogen, Ontario: accretion at 1080 Ma? *Can. J. Earth Sci.* **34**, 1023-1029.

TUCCILLO, M.E., ESSENE, E.J. & VAN DER PLUIJM, B.A. (1990): Growth and retrograde zoning in garnets from high-grade metapelites: implications for pressure–temperature paths. *Geology* **18**, 839- 842.

_____, MEZGER, K., ESSENE, E.J. & VAN DER PLUIJM, B.A. (1992): Thermobarometry, geochronology and the interpretation of P–T–t data in the Britt domain, Ontario Grenville orogen, Canada. *J. Petrol.* **33**, 1225-1259.

VAN BREEMEN, O. & DAVIDSON, A. (1990): U–Pb zircon and baddeleyite ages from the Central Gneiss Belt, Ontario. *In* Radiogenic Age and Isotopic Studies: Report 3. *Geol. Surv. Can., Pap.* **89-2**, 85-92.

_____, _____, LOVERIDGE, W.D. & SULLIVAN, R.W. (1986): U–Pb zircon geochronology of Grenville tectonites, granulites and igneous precursors, Parry Sound, Ontario. *In* The Grenville Province (J.M. Moore, A. Davidson & A.J. Baer. eds.). *Geol. Assoc. Can., Spec. Pap.* **31**, 191-207.

VAN SCHMUS, W.R. (1992): Tectonic setting of the Midcontinent Rift system. *Tectonophys.* **213**, 1- 15.

VERNON, R.H. (1996): Problems with inferring P–T–t paths in low-P granulite facies rocks. *J. Metamorph. Geol.* **14**, 143-153.

VIELZEUF, D. & HOLLOWAY, J.R. (1988): Experimental determination of the fluid-absent melting relations in the pelitic system. *Contrib. Mineral. Petrol.* **98**, 257-276.

WHITE, D.J., EASTON, R.M., CULSHAW, N.G., MILKEREIT, B., FORSYTH, D.A., CARR, S., GREEN, A.G. & DAVIDSON, A. (1994): Seismic images of the Grenville Orogen in Ontario. *Can. J. Earth Sci.* **31**, 293-307.

WINDLEY, B.F. (1986): Comparative tectonics of the western Grenville and western Himalaya. *In* The Grenville Province (J.M. Moore, A. Davidson & A.J. Baer, eds.). *Geol. Assoc. Can., Spec. Pap.* **31**, 341-348.

_____ (1989): Anorogenic magmatism and the Grenville Orogeny. *Can. J. Earth Sci.* **26**, 479- 489.

WODICKA, N. (1994): *Middle Proterozoic Evolution of the Parry Sound Domain, Southwestern Grenville Orogen, Ontario: Structural, Metamorphic, U/Pb, and $^{40}Ar/^{39}Ar$ Constraints.* Ph.D. thesis, Dalhousie Univ., Halifax, Nova Scotia.

_____, PARRISH, R.R. & JAMIESON, R.A. (1996): The Parry Sound domain: a far-travelled allochthon? New evidence from U–Pb zircon geochronology. *Can. J. Earth Sci.* **33**, 1087-1104.

WOLF, M.B. & WYLLIE, P.J. (1994): Dehydration-melting of amphibolite at 10 kbar: the effects of temperature and time. *Contrib. Mineral. Petrol.* **115**, 369-383.

WYNNE-EDWARDS, H.R. (1972): The Grenville Province. *In* Variations in Tectonic Styles in Canada (R.A. Price & R.J.W. Douglas, eds.). *Geol. Assoc. Can., Spec. Pap.* **11**, 263-334.

*Received February 4, 1998, revised manuscript accepted November 2, 1999.*

# TABLE A1. GARNET COMPOSITIONS* USED IN TWQ ANALYSIS

| Area | PARRY SOUND DOMAIN | | | | | | | | | | | | | | | |
|---|---|---|---|---|---|---|---|---|---|---|---|---|---|---|---|---|
| | IPSA | | | | | | | BPSA | | | | | | | TMBA | |
| | | | | | | | | GROUP I | | | | GROUP II | | | | |
| Sample | N122B | N125B | N130A | N131A | N144 | N171 | N192A | N75C | N76B | N74C | N153C | N59 | N73 | N138 | N205A | N204B |
| Lithology | PGR | PGR | PGR | PGR | MGN | MGR | MGN | PGN | PGN | AM | MD | PS | PS | PS | PGN | AM |
| Location | R | R | R | R | R | R | R | R | R | R | R | R | R | R | R | R |
| *n* | 7 | 6 | 16 | 12 | 15 | 10 | 10 | 18 | 13 | 11 | 14 | 30 | 16 | 9 | 28 | 14 |
| $SiO_2$ | 39.52 | 39.50 | 39.15 | 39.87 | 37.55 | 37.41 | 37.45 | 38.62 | 37.40 | 38.10 | 38.40 | 37.11 | 36.95 | 37.33 | 37.81 | 37.84 |
| $Al_2O_3$ | 22.72 | 22.30 | 22.68 | 22.93 | 20.83 | 20.42 | 20.81 | 21.46 | 21.24 | 20.84 | 21.89 | 21.22 | 21.51 | 19.78 | 21.67 | 20.94 |
| FeO | 25.52 | 23.54 | 24.34 | 22.00 | 29.58 | 27.29 | 30.51 | 32.27 | 33.41 | 25.65 | 25.34 | 34.34 | 35.50 | 35.34 | 30.70 | 26.01 |
| MnO | 0.67 | 1.50 | 1.86 | 0.92 | 2.53 | 3.93 | 2.10 | 0.94 | 1.43 | 2.24 | 1.43 | 1.43 | 1.95 | 0.76 | 1.48 | 1.81 |
| MgO | 11.79 | 11.80 | 11.89 | 13.92 | 2.93 | 2.64 | 2.18 | 6.17 | 4.82 | 4.18 | 6.62 | 3.59 | 3.50 | 3.76 | 6.79 | 3.80 |
| CaO | 0.84 | 1.63 | 0.51 | 0.99 | 7.12 | 8.02 | 8.42 | 1.49 | 1.60 | 9.67 | 7.22 | 2.20 | 1.04 | 2.05 | 1.72 | 10.19 |
| Total | 101.06 | 100.27 | 100.43 | 100.63 | 100.54 | 99.71 | 101.47 | 100.95 | 99.90 | 100.68 | 101.11 | 99.89 | 100.45 | 99.02 | 100.17 | 100.59 |
| Si | 2.967 | 2.982 | 2.958 | 2.963 | 2.985 | 2.996 | 2.970 | 3.009 | 2.983 | 2.986 | 2.946 | 2.980 | 2.959 | 3.032 | 2.963 | 2.974 |
| Al | 2.008 | 1.982 | 2.019 | 2.006 | 1.951 | 1.928 | 1.943 | 1.969 | 1.995 | 1.924 | 1.980 | 2.007 | 2.030 | 1.891 | 2.000 | 1.938 |
| Fe | 1.602 | 1.486 | 1.538 | 1.367 | 1.967 | 1.828 | 2.023 | 2.103 | 2.229 | 1.681 | 1.626 | 2.306 | 2.378 | 2.400 | 2.012 | 1.710 |
| Mn | 0.043 | 0.096 | 0.119 | 0.058 | 0.171 | 0.267 | 0.141 | 0.062 | 0.096 | 0.149 | 0.093 | 0.098 | 0.132 | 0.052 | 0.098 | 0.121 |
| Mg | 1.319 | 1.327 | 1.339 | 1.541 | 0.347 | 0.315 | 0.258 | 0.716 | 0.572 | 0.489 | 0.757 | 0.430 | 0.418 | 0.455 | 0.793 | 0.445 |
| Ca | 0.067 | 0.132 | 0.042 | 0.079 | 0.607 | 0.689 | 0.716 | 0.124 | 0.137 | 0.812 | 0.594 | 0.189 | 0.090 | 0.178 | 0.144 | 0.858 |
| Sum | 8.006 | 8.005 | 8.015 | 8.014 | 8.028 | 8.023 | 8.051 | 7.983 | 8.012 | 8.041 | 8.000 | 8.010 | 8.007 | 8.008 | 8.010 | 8.046 |
| Mg# | 0.453 | 0.472 | 0.466 | 0.530 | 0.150 | 0.146 | 0.113 | 0.250 | 0.204 | 0.225 | 0.318 | 0.157 | 0.148 | 0.160 | 0.280 | 0.205 |
| Alm | 0.528 | 0.489 | 0.506 | 0.449 | 0.626 | 0.575 | 0.635 | 0.700 | 0.734 | 0.523 | 0.511 | 0.763 | 0.788 | 0.777 | 0.660 | 0.532 |
| Grs | 0.022 | 0.043 | 0.014 | 0.026 | 0.202 | 0.230 | 0.234 | 0.041 | 0.045 | 0.267 | 0.201 | 0.063 | 0.030 | 0.058 | 0.047 | 0.282 |
| Prp | 0.435 | 0.437 | 0.441 | 0.506 | 0.115 | 0.106 | 0.084 | 0.238 | 0.189 | 0.161 | 0.257 | 0.142 | 0.138 | 0.147 | 0.260 | 0.146 |
| Sps | 0.015 | 0.032 | 0.039 | 0.019 | 0.057 | 0.089 | 0.047 | 0.021 | 0.032 | 0.049 | 0.032 | 0.032 | 0.044 | 0.017 | 0.032 | 0.040 |
| Fe3+ | 0.062 | 0.057 | 0.078 | 0.081 | 0.105 | 0.100 | 0.164 | 0.000 | 0.054 | 0.139 | 0.120 | 0.044 | 0.057 | 0.051 | 0.082 | 0.157 |
| Fe2+ | 1.539 | 1.428 | 1.458 | 1.284 | 1.855 | 1.723 | 1.846 | 2.106 | 2.171 | 1.533 | 1.507 | 2.259 | 2.319 | 2.345 | 1.926 | 1.543 |

*All analyses performed at Dalhousie University on a JEOL 733 Superprobe with Link automation. Operating conditions: 15 kV and 5-13 nA. Mg# = $Mg/(Mg+Fe_{tot})$. Minor components (<0.1 wt%) for some minerals have been omitted. Abbreviations in all tables are: PSD = Parry Sound domain; SD = Shawanaga domain; BPSA = Basal Parry Sound assemblage; IPSA = Interior Parry Sound assemblage; LA = Lighthouse assemblage; OA = Ojibway assemblage; SBA = Sand Bay assemblage; TMBA = Twelve Mile Bay assemblage; AM = amphibolite; CM = coronitic metagabbro; MD = Mafic dyke; MGN = mafic gneiss; MGR = mafic granulite; PGN = pelitic gneiss; PGR = pelitic granulite; PM = pelitic mylonite; PS = pelitic schist; A = average; C = core; R = rim; INC = inclusion; MTX = matrix; *n* = number of analyses. Formulae calculated on the basis of 12 atoms of oxygen. Compositions expressed as oxides quoted in wt.%.

TABLE A1. CONTINUED

| Area | SHAWANAGA DOMAIN | | | | | | | | | | | |
|---|---|---|---|---|---|---|---|---|---|---|---|---|
| | LA | | | | | | | | OA | | | |
| Sample | N7F | N31A | N43B | N1D | N58A | N71B | N71B | N1C | D47A | 129B | 125 | 208B |
| Lithology | PGN | PGN | PGN | PGN | PM | PM | PM | AM | PGN | PGN | CM | AM |
| Location | R | R | R | R | R | C | R | R | R | A | R | R |
| *n* | 27 | 31 | 30 | 28 | 15 | 4 | 14 | 7 | 6 | 11 | 1 | 2 |
| $SiO_2$ | 36.92 | 37.32 | 37.14 | 38.03 | 37.95 | 37.78 | 37.57 | 38.53 | 37.25 | 36.71 | 37.89 | 38.01 |
| $Al_2O_3$ | 21.30 | 21.07 | 21.68 | 22.19 | 22.06 | 20.70 | 20.33 | 21.37 | 20.75 | 20.97 | 21.05 | 21.23 |
| FeO | 34.70 | 34.01 | 34.22 | 31.07 | 31.82 | 31.98 | 33.46 | 27.81 | 35.23 | 32.85 | 27.79 | 24.93 |
| MnO | 1.25 | 1.02 | 0.89 | 0.51 | 0.60 | 0.48 | 0.51 | 2.03 | 1.83 | 5.47 | 1.56 | 3.60 |
| MgO | 3.23 | 3.32 | 4.05 | 7.16 | 6.31 | 5.25 | 5.31 | 4.39 | 2.88 | 2.65 | 3.79 | 4.30 |
| CaO | 2.41 | 2.79 | 2.35 | 1.65 | 1.65 | 3.25 | 1.84 | 7.39 | 1.71 | 1.39 | 7.91 | 7.96 |
| Total | 99.81 | 99.53 | 100.33 | 100.61 | 100.39 | 99.44 | 99.02 | 101.52 | 99.65 | 100.04 | 99.99 | 100.03 |
| Si | 2.969 | 2.998 | 2.956 | 2.956 | 2.972 | 3.006 | 3.015 | 2.991 | 3.009 | 2.976 | 2.997 | 2.993 |
| Al | 2.018 | 1.994 | 2.032 | 2.031 | 2.034 | 1.940 | 1.921 | 1.954 | 1.974 | 2.002 | 1.961 | 1.969 |
| Fe | 2.334 | 2.286 | 2.278 | 2.019 | 2.084 | 2.129 | 2.246 | 1.806 | 2.380 | 2.227 | 1.839 | 1.642 |
| Mn | 0.085 | 0.070 | 0.060 | 0.034 | 0.040 | 0.032 | 0.035 | 0.134 | 0.125 | 0.376 | 0.105 | 0.240 |
| Mg | 0.387 | 0.398 | 0.481 | 0.829 | 0.736 | 0.621 | 0.635 | 0.508 | 0.347 | 0.320 | 0.447 | 0.505 |
| Ca | 0.208 | 0.240 | 0.200 | 0.137 | 0.139 | 0.277 | 0.158 | 0.614 | 0.148 | 0.121 | 0.670 | 0.672 |
| Sum | 8.001 | 7.986 | 8.007 | 8.006 | 8.005 | 8.005 | 8.010 | 8.007 | 7.983 | 8.022 | 8.019 | 8.021 |
| Mg# | 0.140 | 0.148 | 0.175 | 0.291 | 0.262 | 0.225 | 0.221 | 0.219 | 0.127 | 0.126 | 0.196 | 0.235 |
| Alm | 0.774 | 0.764 | 0.755 | 0.669 | 0.695 | 0.696 | 0.731 | 0.580 | 0.793 | 0.732 | 0.601 | 0.537 |
| Grs | 0.069 | 0.080 | 0.066 | 0.045 | 0.046 | 0.091 | 0.207 | 0.206 | 0.049 | 0.040 | 0.219 | 0.220 |
| Prp | 0.128 | 0.133 | 0.159 | 0.275 | 0.246 | 0.203 | 0.051 | 0.171 | 0.116 | 0.105 | 0.146 | 0.165 |
| Sps | 0.029 | 0.023 | 0.020 | 0.011 | 0.013 | 0.010 | 0.011 | 0.043 | 0.042 | 0.124 | 0.034 | 0.078 |
| Fe3+ | 0.044 | 0.000 | 0.060 | 0.062 | 0.027 | 0.050 | 0.054 | 0.068 | 0.061 | 0.015 | 0.046 | 0.041 |
| Fe2+ | 2.289 | 2.287 | 2.215 | 1.956 | 2.055 | 2.076 | 2.188 | 1.736 | 2.315 | 2.191 | 1.784 | 1.592 |

# TABLE A2. BIOTITE COMPOSITIONS USED IN TWQ ANALYSIS*

| Area | PARRY SOUND DOMAIN | | | | | | | | | |
|---|---|---|---|---|---|---|---|---|---|---|
| | IPSA | | | | BPSA | | | | | TMBA |
| | | | | | GROUP II | | GROUP I | | | |
| Sample | N122B | N125B | N130A | N131A | N75C | N76B | N59 | N73 | N138 | N205A |
| Lithology | PGR | PGR | PGR | PGR | PGN | PGN | PS | PS | PS | PGN |
| Location | MTX | MTX | MTX | MTX | MTX | MTX | MTX | MTX | MTX | MTX |
| *n* | 13 | 6 | 7 | 16 | 34 | 32 | 15 | 36 | 28 | 20 |
| $SiO_2$ | 36.47 | 37.71 | 36.59 | 38.17 | 35.54 | 35.77 | 35.76 | 35.88 | 35.36 | 35.96 |
| $TiO_2$ | 4.79 | 4.94 | 4.58 | 4.16 | 3.99 | 3.62 | 2.21 | 3.69 | 3.06 | 5.07 |
| $Al_2O_3$ | 16.12 | 15.67 | 16.36 | 15.90 | 17.76 | 18.14 | 18.92 | 19.16 | 18.78 | 16.79 |
| FeO | 12.59 | 9.72 | 12.14 | 8.05 | 18.58 | 19.30 | 18.52 | 19.46 | 19.51 | 17.09 |
| MnO | 0.01 | 0.04 | 0.02 | 0.01 | 0.02 | 0.03 | 0.04 | 0.02 | 0.01 | 0.02 |
| MgO | 15.60 | 17.18 | 15.48 | 19.15 | 9.78 | 9.46 | 10.58 | 8.51 | 8.98 | 11.24 |
| CaO | 0.02 | 0.00 | 0.00 | 0.02 | 0.02 | 0.02 | 0.02 | 0.02 | 0.01 | 0.02 |
| $Na_2O$ | 0.11 | 0.26 | 0.20 | 0.23 | 0.24 | 0.21 | 0.23 | 0.25 | 0.36 | 0.30 |
| $K_2O$ | 9.99 | 10.10 | 10.00 | 9.79 | 9.57 | 9.63 | 9.32 | 9.50 | 8.73 | 9.54 |
| Total | 95.69 | 95.63 | 95.37 | 95.50 | 95.50 | 96.16 | 95.59 | 96.49 | 94.83 | 96.02 |
| Si | 5.385 | 5.490 | 5.407 | 5.504 | 5.391 | 5.400 | 5.395 | 5.386 | 5.398 | 5.390 |
| $^{IV}Al$ | 2.615 | 2.510 | 2.593 | 2.496 | 2.609 | 2.600 | 2.605 | 2.614 | 2.607 | 2.610 |
| $^{VI}Al$ | 0.188 | 0.177 | 0.254 | 0.204 | 0.564 | 0.625 | 0.758 | 0.773 | 0.767 | 0.355 |
| Ti | 0.537 | 0.547 | 0.514 | 0.456 | 0.460 | 0.415 | 0.253 | 0.421 | 0.355 | 0.577 |
| Fe | 1.555 | 1.183 | 1.500 | 0.971 | 2.357 | 2.437 | 2.337 | 2.444 | 2.489 | 2.143 |
| Mn | 0.001 | 0.005 | 0.002 | 0.002 | 0.002 | 0.003 | 0.005 | 0.003 | 0.001 | 0.002 |
| Mg | 3.432 | 3.728 | 3.410 | 4.116 | 2.211 | 2.127 | 2.378 | 1.904 | 2.042 | 2.511 |
| Ca | 0.003 | 0.000 | 0.000 | 0.003 | 0.003 | 0.003 | 0.003 | 0.003 | 0.002 | 0.003 |
| Na | 0.032 | 0.075 | 0.058 | 0.065 | 0.070 | 0.062 | 0.069 | 0.074 | 0.108 | 0.086 |
| K | 1.882 | 1.876 | 1.885 | 1.802 | 1.852 | 1.854 | 1.794 | 1.820 | 1.699 | 1.825 |
| Sum | 15.629 | 15.591 | 15.623 | 15.620 | 15.520 | 15.526 | 15.597 | 15.442 | 15.464 | 15.501 |
| Mg# | 0.688 | 0.758 | 0.696 | 0.809 | 0.484 | 0.465 | 0.505 | 0.438 | 0.451 | 0.540 |

| Area | SHAWANAGA DOMAIN | | | | | | | | | | |
|---|---|---|---|---|---|---|---|---|---|---|---|
| | LA | | | | | | | OA | | | |
| Sample | N7F | N31A | N43B | N1D | N58A | N71B | N71B | D47A | 129B | 125 | 208B |
| Lithology | PGN | PGN | PGN | PM | PM | PM | PM | PGN | PGN | CM | AM |
| Location | MTX | MTX | MTX | MTX | MTX | INC | MTX | MTX | MTX | MTX | MTX |
| *n* | 33 | 29 | 8 | 24 | 14 | 3 | 35 | 7 | 11 | 1 | 3 |
| $SiO_2$ | 35.52 | 35.29 | 35.84 | 37.38 | 36.46 | 35.20 | 35.85 | 35.06 | 35.42 | 34.93 | 36.37 |
| $TiO_2$ | 4.26 | 3.97 | 2.78 | 4.83 | 3.94 | 4.19 | 4.32 | 3.97 | 3.86 | 4.14 | 4.10 |
| $Al_2O_3$ | 18.61 | 18.69 | 18.92 | 17.00 | 17.37 | 18.45 | 18.00 | 18.11 | 18.44 | 13.94 | 15.00 |
| FeO | 19.91 | 19.11 | 19.58 | 14.18 | 14.60 | 17.85 | 16.49 | 20.98 | 19.34 | 19.32 | 16.87 |
| MnO | 0.02 | 0.02 | 0.01 | 0.01 | 0.04 | 0.03 | 0.00 | 0.00 | 0.14 | 0.00 | 0.09 |
| MgO | 7.81 | 7.97 | 9.36 | 13.13 | 12.80 | 9.60 | 10.93 | 7.73 | 8.69 | 11.62 | 12.89 |
| CaO | 0.01 | 0.02 | 0.05 | 0.01 | 0.01 | 0.01 | 0.02 | 0.00 | 0.00 | 0.19 | 0.00 |
| $Na_2O$ | 0.29 | 0.24 | 0.35 | 0.34 | 0.08 | 0.22 | 0.17 | 0.29 | 0.04 | 0.33 | 0.09 |
| $K_2O$ | 9.37 | 9.43 | 9.11 | 9.29 | 10.70 | 9.61 | 9.72 | 9.69 | 9.78 | 8.76 | 9.62 |
| Total | 95.79 | 94.75 | 96.00 | 96.16 | 96.00 | 95.14 | 95.49 | 95.83 | 95.71 | 93.23 | 95.03 |
| Si | 5.389 | 5.398 | 5.404 | 5.488 | 5.424 | 5.340 | 5.382 | 5.370 | 5.382 | 5.476 | 5.516 |
| $^{IV}Al$ | 2.611 | 2.602 | 2.596 | 2.512 | 2.576 | 2.660 | 2.618 | 2.630 | 2.618 | 2.524 | 2.484 |
| $^{VI}Al$ | 0.714 | 0.765 | 0.764 | 0.427 | 0.468 | 0.637 | 0.564 | 0.636 | 0.682 | 0.050 | 0.195 |
| Ti | 0.491 | 0.462 | 0.319 | 0.538 | 0.445 | 0.483 | 0.493 | 0.457 | 0.441 | 0.488 | 0.468 |
| Fe | 2.527 | 2.445 | 2.469 | 1.741 | 1.818 | 2.265 | 2.071 | 2.687 | 2.458 | 2.533 | 2.140 |
| Mn | 0.003 | 0.003 | 0.001 | 0.001 | 0.005 | 0.003 | 0.000 | 0.000 | 0.018 | 0.000 | 0.012 |
| Mg | 1.766 | 1.818 | 2.104 | 2.872 | 2.838 | 2.171 | 2.445 | 1.765 | 1.969 | 2.716 | 2.914 |
| Ca | 0.002 | 0.004 | 0.008 | 0.002 | 0.001 | 0.002 | 0.003 | 0.000 | 0.000 | 0.032 | 0.000 |
| Na | 0.087 | 0.071 | 0.103 | 0.097 | 0.024 | 0.063 | 0.048 | 0.086 | 0.012 | 0.100 | 0.026 |
| K | 1.813 | 1.839 | 1.752 | 1.740 | 2.032 | 1.860 | 1.861 | 1.893 | 1.896 | 1.752 | 1.861 |
| Sum | 15.402 | 15.407 | 15.519 | 15.418 | 15.632 | 15.486 | 14.484 | 15.524 | 15.476 | 15.671 | 15.616 |
| Mg# | 0.411 | 0.426 | 0.461 | 0.622 | 0.609 | 0.490 | 0.541 | 0.396 | 0.445 | 0.517 | 0.577 |

*Formulae calculated on the basis of 22 atoms of oxygen (Fe = $Fe_{TOT}$). Compositions expressed as oxides quoted in wt.%.

## TABLE A3. PLAGIOCLASE COMPOSITIONS USED IN TWQ ANALYSIS*

| Area | PARRY SOUND DOMAIN | | | | | | | | | | | | | | |
|---|---|---|---|---|---|---|---|---|---|---|---|---|---|---|---|
| | IPSA | | | | | | | BPSA | | | | | | TMBA | |
| | | | | | | | | GROUP I | | | | GROUP II | | | |
| Sample | N122B | N125B | N130A | N131A | N144 | N171 | N192A | N75C | N76B | N74C | N153C | N59 | N73 | N138 | N205A | N204B |
| Lithology | PGR | PGR | PGR | PGR | MGN | MGR | MGN | PGN | PGN | AM | MD | PS | PS | PS | PGN | AM |
| Location | MTX | MTX | MTX | MTX | MTX | MTX | MTX | MTX | MTX | MTX | MTX | MTX | MTX | MTX | MTX | MTX |
| *n* | 11 | 2 | 4 | 24 | 13 | 7 | 7 | 17 | 22 | 8 | 19 | 25 | 35 | 20 | 26 | 2 |
| $SiO_2$ | 66.20 | 63.96 | 66.73 | 63.78 | 61.67 | 63.73 | 62.16 | 62.96 | 62.17 | 56.96 | 54.41 | 60.31 | 62.85 | 61.96 | 62.28 | 55.72 |
| $Al_2O_3$ | 21.74 | 22.15 | 21.70 | 23.49 | 23.81 | 23.29 | 23.91 | 23.80 | 24.80 | 27.12 | 29.74 | 24.85 | 24.27 | 24.52 | 24.65 | 28.58 |
| FeO | 0.05 | 0.06 | 0.05 | 0.06 | 0.12 | 0.09 | 0.07 | 0.13 | 0.06 | 0.08 | 0.14 | 0.07 | 0.12 | 0.09 | 0.05 | 0.11 |
| CaO | 2.50 | 3.42 | 1.92 | 4.25 | 5.43 | 4.53 | 5.49 | 4.88 | 5.48 | 9.35 | 11.55 | 6.76 | 4.82 | 5.92 | 5.85 | 10.80 |
| $Na_2O$ | 10.29 | 8.86 | 9.42 | 8.75 | 7.72 | 8.12 | 7.66 | 7.71 | 8.34 | 5.57 | 5.64 | 7.59 | 8.82 | 7.26 | 8.06 | 5.11 |
| $K_2O$ | 0.12 | 0.30 | 0.36 | 0.31 | 0.40 | 0.27 | 0.39 | 0.16 | 0.15 | 0.10 | 0.07 | 0.05 | 0.11 | 0.07 | 0.18 | 0.12 |
| Total | 100.89 | 98.75 | 100.16 | 100.64 | 99.16 | 100.02 | 99.70 | 99.63 | 101.00 | 99.18 | 101.55 | 99.63 | 101.07 | 99.82 | 101.07 | 100.44 |
| Si | 2.884 | 2.849 | 2.913 | 2.798 | 2.754 | 2.807 | 2.759 | 2.784 | 2.728 | 2.568 | 2.426 | 2.691 | 2.754 | 2.742 | 2.732 | 2.495 |
| Al | 1.116 | 1.162 | 1.115 | 1.213 | 1.253 | 1.208 | 1.250 | 1.240 | 1.282 | 1.440 | 1.562 | 1.306 | 1.253 | 1.278 | 1.273 | 1.507 |
| Fe | 0.002 | 0.002 | 0.002 | 0.002 | 0.005 | 0.003 | 0.003 | 0.005 | 0.002 | 0.003 | 0.005 | 0.003 | 0.005 | 0.003 | 0.002 | 0.004 |
| Ca | 0.117 | 0.164 | 0.090 | 0.200 | 0.260 | 0.214 | 0.262 | 0.231 | 0.258 | 0.452 | 0.552 | 0.326 | 0.226 | 0.281 | 0.275 | 0.518 |
| Na | 0.869 | 0.765 | 0.797 | 0.744 | 0.669 | 0.693 | 0.659 | 0.661 | 0.709 | 0.487 | 0.488 | 0.652 | 0.749 | 0.623 | 0.685 | 0.444 |
| K | 0.006 | 0.017 | 0.020 | 0.017 | 0.023 | 0.015 | 0.022 | 0.009 | 0.009 | 0.006 | 0.004 | 0.003 | 0.010 | 0.004 | 0.010 | 0.007 |
| Sum | 4.994 | 4.959 | 4.937 | 4.975 | 4.963 | 4.941 | 4.955 | 4.929 | 4.988 | 4.956 | 5.037 | 4.981 | 4.997 | 4.931 | 4.977 | 4.975 |
| Ab | 0.876 | 0.809 | 0.879 | 0.774 | 0.703 | 0.752 | 0.699 | 0.734 | 0.726 | 0.515 | 0.467 | 0.665 | 0.760 | 0.686 | 0.706 | 0.458 |
| An | 0.118 | 0.173 | 0.099 | 0.208 | 0.273 | 0.232 | 0.277 | 0.256 | 0.264 | 0.478 | 0.529 | 0.329 | 0.229 | 0.309 | 0.283 | 0.535 |
| Or | 0.006 | 0.018 | 0.022 | 0.018 | 0.024 | 0.016 | 0.024 | 0.010 | 0.010 | 0.007 | 0.004 | 0.006 | 0.011 | 0.004 | 0.011 | 0.007 |

*Formulae calculated on the basis of 8 atoms of oxygen (Fe = $Fe_{TOT}$). Compositions expressed as oxides quoted in wt.%.

TABLE A3. CONTINUED.

| Area | SHAWANAGA DOMAIN | | | | | | | | | | | |
|---|---|---|---|---|---|---|---|---|---|---|---|---|
| | LA | | | | | | | | OA | | | |
| Sample | N7F | N31A | N43B | N1D | N58A | N71B | N71B | N1C | D47A | 129B | 125 | 208B |
| Lithology | PGN | PGN | PGN | PM | PM | PM | PM | AM | PGN | PGN | CM | AM |
| Location | MTX | MTX | MTX | MTX | MTX | INC | MTX | MTX | A | A | RIM | RIM |
| *n* | 31 | 22 | 26 | 41 | 9 | 6 | 32 | 13 | 6 | 9 | 4 | 1 |
| $SiO_2$ | 61.26 | 61.37 | 61.16 | 61.54 | 61.46 | 60.85 | 62.52 | 60.15 | 62.88 | 63.29 | 60.52 | 55.89 |
| $Al_2O_3$ | 24.64 | 24.40 | 25.41 | 24.79 | 23.90 | 24.93 | 23.99 | 25.09 | 23.53 | 23.00 | 24.55 | 27.48 |
| FeO | 0.12 | 0.08 | 0.09 | 0.13 | 0.04 | 0.07 | 0.08 | 0.17 | 0.07 | 0.06 | 0.39 | 0.24 |
| CaO | 5.77 | 6.41 | 6.27 | 5.69 | 5.58 | 6.83 | 5.34 | 6.80 | 4.76 | 3.86 | 6.10 | 9.90 |
| $Na_2O$ | 8.27 | 7.45 | 8.24 | 8.48 | 8.37 | 7.52 | 8.17 | 7.29 | 8.83 | 9.23 | 7.90 | 5.62 |
| $K_2O$ | 0.18 | 0.22 | 0.06 | 0.19 | 0.17 | 0.26 | 0.09 | 0.22 | 0.23 | 0.13 | 0.20 | 0.23 |
| Total | 100.24 | 100.24 | 101.23 | 100.82 | 99.51 | 100.47 | 100.19 | 99.71 | 100.30 | 99.57 | 99.66 | 99.36 |
| Si | 2.715 | 2.725 | 2.687 | 2.713 | 2.741 | 2.695 | 2.760 | 2.684 | 2.776 | 2.806 | 2.703 | 2.529 |
| Al | 1.286 | 1.276 | 1.315 | 1.287 | 1.255 | 1.301 | 1.247 | 1.319 | 1.223 | 1.201 | 1.291 | 1.465 |
| Fe | 0.005 | 0.003 | 0.003 | 0.005 | 0.001 | 0.002 | 0.003 | 0.006 | 0.003 | 0.002 | 0.015 | 0.009 |
| Ca | 0.274 | 0.305 | 0.295 | 0.269 | 0.267 | 0.324 | 0.253 | 0.325 | 0.225 | 0.183 | 0.292 | 0.480 |
| Na | 0.711 | 0.641 | 0.702 | 0.725 | 0.724 | 0.646 | 0.699 | 0.631 | 0.756 | 0.793 | 0.684 | 0.493 |
| K | 0.010 | 0.012 | 0.003 | 0.011 | 0.010 | 0.015 | 0.005 | 0.013 | 0.013 | 0.007 | 0.011 | 0.013 |
| Sum | 5.000 | 4.962 | 5.006 | 5.009 | 4.997 | 4.983 | 4.967 | 4.977 | 4.996 | 4.992 | 4.996 | 4.989 |
| Ab | 0.715 | 0.669 | 0.702 | 0.721 | 0.723 | 0.656 | 0.730 | 0.651 | 0.761 | 0.807 | 0.693 | 0.500 |
| An | 0.275 | 0.318 | 0.295 | 0.268 | 0.267 | 0.329 | 0.264 | 0.336 | 0.226 | 0.186 | 0.296 | 0.487 |
| Or | 0.010 | 0.013 | 0.003 | 0.011 | 0.010 | 0.015 | 0.006 | 0.013 | 0.013 | 0.007 | 0.011 | 0.013 |

## TABLE A4. PYROXENE COMPOSITIONS USED FOR THERMOBAROMETRY*

| Area | PSD | | | SD |
|---|---|---|---|---|
| | IPSA | BPSA | | OA |
| Sample | N131A | N153C | N74C | 125 |
| Lithology | PGR | MD | AM | CM |
| Location | MTX | MTX | MTX | MTX |
| Mineral | OPX | OPX | CPX | CPX |
| *n* | 11 | 14 | 5 | 2 |
| $SiO_2$ | 50.81 | 51.88 | 51.35 | 52.80 |
| $TiO_2$ | 0.06 | 0.05 | 0.23 | 0.00 |
| $Al_2O_3$ | 6.32 | 2.08 | 2.68 | 1.15 |
| FeO | 16.93 | 23.56 | 10.09 | 11.06 |
| MnO | 0.24 | 0.58 | 0.17 | 0.00 |
| MgO | 25.35 | 21.90 | 11.76 | 12.70 |
| CaO | 0.11 | 0.37 | 22.51 | 21.70 |
| $Na_2O$ | 0.29 | 0.28 | 0.67 | 0.78 |
| Total | 100.11 | 100.70 | 99.45 | 100.19 |
| Si | 1.829 | 1.919 | 1.934 | 1.972 |
| $^{IV}Al$ | 0.171 | 0.081 | 0.066 | 0.028 |
| $^{VI}Al$ | 0.097 | 0.010 | 0.053 | 0.023 |
| Ti | 0.002 | 0.002 | 0.006 | 0.000 |
| Fe | 0.510 | 0.728 | 0.317 | 0.345 |
| Mn | 0.007 | 0.018 | 0.005 | 0.000 |
| Mg | 1.360 | 1.208 | 0.660 | 0.707 |
| Ca | 0.004 | 0.015 | 0.908 | 0.868 |
| Na | 0.020 | 0.020 | 0.049 | 0.057 |
| Sum | 4.000 | 4.000 | 4.000 | 4.000 |
| Wo | 0.00 | 0.00 | 44.89 | 42.21 |
| En | 68.85 | 61.43 | 34.89 | 36.81 |
| Fs | 21.56 | 33.51 | 14.48 | 17.98 |
| $Fe^{3+}$ | 0.091 | 0.088 | 0.049 | 0.062 |
| $Fe^{2+}$ | 0.419 | 0.640 | 0.268 | 0.284 |

*Formulae calculated on the basis of 6 atoms of oxygen. Compositions expressed as oxides quoted in wt.%.

## TABLE A5. AMPHIBOLE COMPOSITIONS USED IN TWQ ANALYSIS*

| Area | PARRY SOUND DOMAIN | | | | | | SHAWANAGA DOMAIN | | |
|---|---|---|---|---|---|---|---|---|---|
| | IPSA | | | BPSA | | TMBA | LA | OA | |
| Sample | N144 | N171 | N192A | N153C | N74C | N204B | N1C | 125 | 208B |
| Lithology | MGN | MGR | MGN | MD | AM | AM | AM | CM | AM |
| Location | MTX | MTX | MTX | MTX | MTX | MTX | MTX | MTX | MTX |
| *n* | 4 | 6 | 5 | 22 | 11 | 11 | 7 | 2 | 2 |
| $SiO_2$ | 40.06 | 41.50 | 40.36 | 43.50 | 42.17 | 40.51 | 42.05 | 41.88 | 41.37 |
| $TiO_2$ | 1.76 | 1.78 | 1.77 | 1.55 | 1.48 | 1.61 | 1.32 | 1.68 | 1.33 |
| $Al_2O_3$ | 12.01 | 11.43 | 11.95 | 12.43 | 12.47 | 13.38 | 12.57 | 11.84 | 13.22 |
| FeO | 22.48 | 19.79 | 22.78 | 13.32 | 17.09 | 18.10 | 18.48 | 16.68 | 16.05 |
| MnO | 0.22 | 0.25 | 0.17 | 0.09 | 0.16 | 0.11 | 0.14 | 0.00 | 0.25 |
| MgO | 6.94 | 8.29 | 5.85 | 12.85 | 10.07 | 8.65 | 8.70 | 10.28 | 10.09 |
| CaO | 11.24 | 11.38 | 11.00 | 12.03 | 11.65 | 11.50 | 11.24 | 11.20 | 11.88 |
| $Na_2O$ | 1.62 | 1.72 | 1.66 | 1.89 | 1.75 | 1.31 | 1.62 | 1.93 | 1.48 |
| $K_2O$ | 1.75 | 1.50 | 1.67 | 0.55 | 0.73 | 1.62 | 1.10 | 1.29 | 1.35 |
| Total | 98.09 | 97.63 | 97.21 | 98.20 | 97.58 | 96.79 | 97.24 | 96.78 | 97.02 |
| Si | 6.223 | 6.371 | 6.320 | 6.383 | 6.352 | 6.218 | 6.398 | 6.371 | 6.267 |
| $Al^{IV}$ | 1.777 | 1.629 | 1.680 | 1.617 | 1.648 | 1.782 | 1.602 | 1.629 | 1.733 |
| $Al^{VI}$ | 0.423 | 0.440 | 0.527 | 0.534 | 0.567 | 0.640 | 0.654 | 0.492 | 0.626 |
| Ti | 0.206 | 0.206 | 0.208 | 0.171 | 0.168 | 0.186 | 0.151 | 0.192 | 0.152 |
| Fe | 2.921 | 2.541 | 2.983 | 1.634 | 2.153 | 2.323 | 2.352 | 2.122 | 2.034 |
| Mn | 0.029 | 0.033 | 0.023 | 0.011 | 0.020 | 0.014 | 0.018 | 0.000 | 0.032 |
| Mg | 1.607 | 1.897 | 1.365 | 2.810 | 2.260 | 1.979 | 1.973 | 2.331 | 2.279 |
| Ca | 1.871 | 1.872 | 1.846 | 1.891 | 1.880 | 1.892 | 1.832 | 1.825 | 1.928 |
| Na | 0.488 | 0.512 | 0.504 | 0.538 | 0.511 | 0.390 | 0.478 | 0.570 | 0.435 |
| K | 0.347 | 0.294 | 0.334 | 0.103 | 0.140 | 0.317 | 0.214 | 0.250 | 0.261 |
| Sum | 15.890 | 15.793 | 15.789 | 15.693 | 15.700 | 15.741 | 15.671 | 15.783 | 15.746 |
| $Fe^{3+}$ | 0.404 | 0.201 | 0.184 | 0.357 | 0.366 | 0.297 | 0.255 | 0.244 | 0.207 |
| $Fe^{2+}$ | 2.491 | 2.329 | 2.792 | 1.265 | 1.770 | 2.011 | 2.084 | 1.869 | 1.658 |

*Formulae calculated on the basis of 23 oxygens. Compositions expressed as oxides quoted in wt.% $Fe^{3+}$ represents the average of calculations assuming $\Sigma$cations - (Na + K) = 15.0, and $\Sigma$cations - (Ca + Na + K) = 13.0.